

The Influence of Fic1 on Polarity and Cytokinesis in Fission Yeast

By

Anthony Michael Rossi

Dissertation

Submitted to the Faculty of the
Graduate School of Vanderbilt University
in partial fulfillment of the requirements

for the degree of

DOCTOR OF PHILOSOPHY

in

Cell and Developmental Biology

August, 11th, 2023

Nashville, Tennessee

Approved:

Alissa M. Weaver, M.D., Ph.D.

Kathleen L. Gould, Ph.D.

Todd R. Graham, Ph.D.

Katherine L. Friedman, Ph.D.

Irina Kaverina, Ph.D.

Acknowledgements

The work within this dissertation was made possible by the support of my mentors, colleagues, friends, family, and wife. I would like to thank all of them for their assistance.

I must first thank my mentor Dr. Kathy Gould. Kathy has provided both the guidance and freedom that have allowed me to develop my scientific acumen while pursuing my own scientific curiosities. Working for Kathy has afforded me opportunities to share my research with an international audience and has allowed me to acquire a breadth of scientific knowledge and skills. Kathy has engrained within me the importance of paying attention to the details, something I will carry with me throughout my scientific career.

In addition to Kathy, I would like to also thank my committee: Alissa Weaver M.D. Ph.D., Todd Graham Ph.D., Katherine Friedman Ph.D., and Irina Kaverina Ph.D. These individuals have provided insight and encouragement that have helped me complete this work. I appreciate the time they have graciously given to ensure my success through graduate school.

Members of the Gould lab have also been a tremendous help and resource for me as I have completed this work. Individuals from the past and present have made this work possible through their contributions within the field, by training me, and by providing constructive feedback. I am grateful for all they have taught me and the support they have given me.

Lastly, I would like to thank my friends and family for their relentless support and encouragement. While they may not have always understood the cause of my frustrations or elations, they have always helped me through my challenges and celebrated my successes. Thank you to my amazing and beautiful wife Molly Malinda Rossi, who has provided me with unconditional love and support as I have completed this work.

Table of Contents

List of Tables.....	v
List of Figures.....	vi
List of Abbreviations.....	viii
Introduction	1
1.1 The eukaryotic cell cycle	1
1.2 Growth polarity establishment in <i>Schizosaccharomyces pombe</i>	2
1.3 <i>Schizosaccharomyces pombe</i> as a model organism for studying cytokinesis	6
1.4 Septum formation in <i>Schizosaccharomyces pombe</i>	10
1.5 Fic1's roles in septum formation in <i>Schizosaccharomyces pombe</i>	18
Phosphoregulation of the Cytokinetic Protein Fic1 Contributes to Fission Yeast Growth Polarity Establishment.....	21
2.1 Introduction.....	21
2.2 Fic1 phosphorylation is invariant through the cell cycle	22
2.3 Fic1 phosphorylation is independent of cell tip localization	24
2.4 Fic1 is phosphorylated on two C-terminal residues.....	26
2.5 Multiple kinases modulate polarity-relevant Fic1 phosphorylation	29
2.6 Fic1 phosphorylation does not affect CR localization or interaction with known CR binding partners.....	32
2.7 Disruption of Fic1 phosphorylation impacts bipolar cell growth and promotes pseudohyphal growth	34
2.8 Materials and Methods	37
The fission yeast cytokinetic ring component Fic1 promotes septum formation	42
3.1 Introduction.....	42
3.2 Fic1 phospho-ablating mutant suppresses myo2-E1	44
3.3 <i>fic1-2A</i> cells exhibit similar CR dynamics compared to wild-type cells.....	46
3.4 <i>fic1-2A myo2-E1</i> cells can complete cytokinesis.....	47
3.5 Fic1 directly interacts with Cyk3's SH3 domain.....	49
3.6 Cyk3's SH3 domain and TLD are required for Fic1's roles in septum formation ..	54

3.7 Fic1 and Cyk3 function independently of Chs2	56
3.8 Materials and Methods	58
Conclusions and future directions	62
4.1 Conclusions	62
4.2 Future directions	63

List of Tables

Table

4.1. Proteins with SH3 domains that localize to the CR.....	63
4.2. Phosphorylation sites within Cyk3's IDR.....	69
4.3. 14-3-3 RxxS binding sites within Cyk3's IDR.....	71

List of Figures

Figure

1.1. The <i>S. pombe</i> cell cycle	2
1.2. Prolonged persistence of cytokinetic components at the new ends impairs growth polarity establishment	5
1.3. <i>S. pombe</i> utilize a cytokinetic ring to promote medial cell division.....	8
2.1. Fic1 is phosphorylated <i>in vivo</i>	23
2.2. Phosphorylation occurs on the region and subpopulation of Fic1 relevant to growth polarity.....	25
2.3. Fic1 residues T178 and S241 are phosphorylated <i>in vivo</i>	27
2.4. Identification of Fic1 phosphorylation sites and potential kinases.....	28
2.5. No single kinase associated with cell growth polarity regulates Fic1's phosphorylation state	30
2.6. Fic1 phosphorylation is regulated by multiple kinases	31
2.7. Deregulation of Fic1 phosphorylation at T178 an S241 impairs new end growth ...	33
2.8. Fic1 phospho-mutants do not alter Fic1's interactions with Cdc15 or Imp2	36
3.1. Individual or single <i>fic1</i> phosphomutants are not temperature-sensitive	44
3.2. <i>fic1-2A</i> suppresses <i>myo2-E1</i>	45
3.3. <i>fic1-2A myo2-E1</i> cells can achieve membrane ingression and cell separation at <i>myo2-E1</i> 's restrictive temperature	48
3.4. Cyk3-SH3 binds Fic1	50
3.5. P174,177 is required for <i>fic1-2A</i> 's suppression of <i>myo2-E1</i>	53
3.6. Cyk3's SH3 and transglutaminase-like domain are required for <i>fic1-2A</i> 's suppression of <i>myo2-E1</i>	55
3.7. Fic1 functions independently of Chs2	57
4.1. The K22 and K27 residues within Fic1's C2 domain are required for <i>fic1-2A</i> 's suppression of <i>myo2-E1</i>	64
4.2. Fic1 does not bind liposomes.....	65

4.3. There are no genetic interactions between *chs2Δ* and temperature-sensitive glucan synthase alleles..... 73

4.4. Deletion of *pck1* or *pck2* partially disrupts *fic1-2A*'s suppression of *myo2-E1* 75

List of Abbreviations

BF	Bright field
CB	Coomassie blue
CDK	Cyclin-dependent kinase
CIP	Cell integrity pathway
CK2	Casein kinase II
CR	Cytokinetic ring
GAP	GTPase-activating protein
GEF	Guanine nucleotide exchange factor
IDR	Intrinsically disordered region
IGL	Immunoglobulin-like
IPC	Ingression progression complex
Lat A	Latrunculin A
mCh	mCherry
MAPK	Mitogen activated protein kinase
NETO	New end take off
PAK	p21-activated kinase
PCH	<i>pombe</i> Cdc15 homology
SCPR	Search, capture, pull, and release
SIN	Septation initiation network
SPB	Spindle pole body
ssNMR	Solid state nuclear magnetic resonance
TAP	Tandem affinity-purification
Y2H	Yeast two-hybrid
YE	Yeast extract

Chapter 1

Introduction

1.1 The eukaryotic cell cycle

Cells are the basic units of life. In order to support and propagate life, cells must divide to produce more cells. This propagation requires organized phases of growth and division. The cell cycle organizes these phases into chronological processes. The prototypical cell cycle contains two phases of growth, G1 and G2, which are separated by S phase during which the genetic material is replicated. Successful replication of the genetic material allows cells to proceed to G2 before entering mitosis. During mitosis the genetic material is segregated between the two poles of the dividing cell. Successful segregation of the genetic material is followed by cytokinesis, during which the dividing cell halves are physically separated to produce two independent daughter cells.

Components and processes that regulate the cell cycle have been identified and characterized in the fission yeast *Schizosaccharomyces pombe* (Nurse et al., 1976). This single-celled rod-shaped fungus has served as an excellent model organism to study the cell cycle because *S. pombe* cells grow by elongating from their cell ends and divide by medial fission (Figure 1.1) (Mitchison, 1957). Thus, the longer the *S. pombe* cell the farther the cell has progressed through the cell cycle. When components that are essential for the passage from one stage of the cell cycle to the next are disrupted *S. pombe* cells arrest in the stage of the cell cycle immediately prior to the transition (Nurse et al., 1976). *S. pombe*'s growth pattern and genetics were leveraged to generate conditional temperature-sensitive cell division cycle alleles that identified several conserved essential proteins that regulate cell cycle progression including the cyclin-dependent kinase, Cdk1 (Simanis and Nurse, 1986). While *S. pombe* has been instrumental in elucidating the molecular mechanisms that regulate cell cycle progression, it has also been key in identifying the components and molecular

mechanisms that underly other cellular processes such as polarity establishment and cytokinesis (Balasubramanian et al., 1998; Snell and Nurse, 1994).

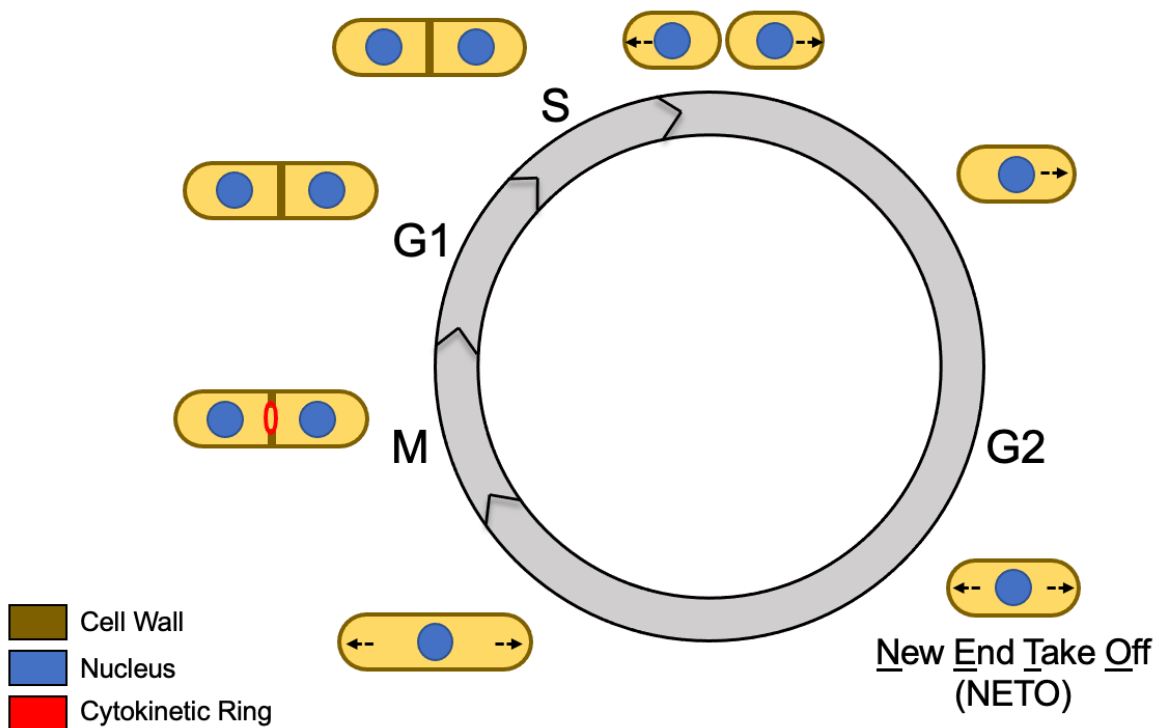


Figure 1.1. The *S. pombe* cell cycle. *S. pombe* cells grow by elongation at their cell ends in G2. Growth initially occurs from the old end, defined as the end of the cell that served as the end of the mother cell in the previous cell cycle, before growth initiates at the new end, defined as the end of the cell generated from septum digestion. This transition is referred to as NETO (new end take off). Growth ceases as the cells enter the M phase of the cell cycle. During M phase, the genetic material is segregated and the two daughter cells are physically separated by a septum. The septated daughter cells remain joined through G1 and S phase. At the end of S phase, the septum is digested and the daughter cells become independent.

1.2 Growth polarity establishment in *Schizosaccharomyces pombe*

The fission yeast *S. pombe* is an exceptional model to study growth polarity establishment. During G2, *S. pombe* cells elongate through growth at their cell ends while maintaining a constant width (Figure 1.1). *S. pombe* initially exhibit monopolar growth from the old end, the end of the cell that served as a cell tip of the mother cell in the previous division (Figure 1.1) (Mitchison and Nurse, 1985). Because *S. pombe* have a cell wall, they must simultaneously remodel their cell wall and expand their plasma membrane to prevent cell lysis during elongation. Cell wall machinery and plasma

membrane are delivered to the growing end by vesicular trafficking directed by actin cables polymerized from the growing end (Win et al., 2001).

The polymerization of actin cables requires a formin to be recruited to and activated at the growing end. This process begins with the delivery of microtubule associated polarity factors to the cell end. During G2, microtubules extend parallel to the long axis of the cell until the plus end of the microtubules encounter the cell end. Contact with the microtubules to the cell end delivers the polarity factor Tea1 and its binding partner Tea4 to the cell end (Martin et al., 2005; Mata and Nurse, 1997). The PP1 phosphatase is recruited to the cell end by Tea4 where it activates Gef1, a Cdc42 guanine nucleotide exchange factor (GEF), by removing phosphorylation from the NDR/LATS-family kinase Orb6 (Alvarez-Tabares et al., 2007; Das et al., 2015; Das et al., 2009; Kokkoris et al., 2014). Dephosphorylated Gef1 associates with the cell cortex at the cell end where it promotes local activation of the Rho family GTPase Cdc42 by promoting the exchange of GDP-Cdc42 to GTP-Cdc42 (Das et al., 2015; Das et al., 2009). This local activation of Cdc42 is enhanced by a positive feedback loop through interactions with the p21-activated kinase (PAK), Shk1 (Marcus et al., 1995; Otilie et al., 1995). Shk1 simultaneously binds GTP-Cdc42 and the scaffolding protein Scd2 (Endo et al., 2003). Scd2 directly binds Scd1, another Cdc42 GEF, which also promotes the exchange of GDP-Cdc42 to GTP-Cdc42 (Endo et al., 2003). GTP-Cdc42 can continue to associate with PAK-Scd2-Scd1 complexes to further increase GTP-Cdc42 levels at the cell end (Endo et al., 2003). Increased GTP-Cdc42 at the cell end promotes activation of Cdc42 effectors, namely the formin, For3 (Rincon et al., 2009). Upon localization and activation by Tea4 and Cdc42, For3 polymerizes F-actin from the cell end (Feierbach and Chang, 2001; Martin et al., 2005). These actin filaments form actin cables and facilitate the delivery of vesicles by the type-V myosin Myo52 to the cell end (Feierbach and Chang, 2001). This process first occurs at the old end before also occurring at the new end.

Cells undergo monopolar growth until a point in G2 where the new end, the cell end created from primary septum digestion after cytokinesis (Figure 1.1) (Mitchison and Nurse, 1985), begins to grow. The onset of bipolar growth is referred to as new end take off (NETO) and marks a rate change point during which growth increases by 35%

(Figure 1.1) (Mitchison and Nurse, 1985). NETO has previously been thought to be governed by cell size and completion of S phase (Mitchison and Nurse, 1985). However, we now understand that the activation of the calcineurin phosphatase Ppb1 by the DNA replication checkpoint kinase Cds1 during S phase is partially involved in the delay of NETO (Kume et al., 2011). Mutating Ppb1 to prevent its phosphorylation by Cds1 promotes early NETO (Kume et al., 2011). Additionally, transiently depolymerizing the F-actin in cells arrested in G1 or S phase with a pulse of Latrunculin A (Lat A) or Latrunculin B promotes bipolar actin polymerization resulting in early NETO (Kume et al., 2011; Rupes et al., 1999).

Preference for initiating growth at the old end before the new end may be partially explained by cytokinesis. Mutants with cytokinetic defects can delay or prevent NETO (Figure 1.2) (Bohnert and Gould, 2012). Inefficient cytokinesis can result in the prolonged persistence of cytokinetic components at the new of the cell (Figure 1.2) (Bohnert and Gould, 2012). These cytokinetic remnants delay NETO (Figure 1.2) (Bohnert and Gould, 2012). It is likely that wild-type cells also require time to clear the cytokinetic components from the new cell ends before actin polymerization can occur to promote NETO. These findings provide an explanation as to why new end growth occurs at a later point in G2 and links cytokinesis to polar growth establishment. These cytokinetic constraints on polarized growth were first identified by analyzing phenotypes resulting from the loss of the cytokinetic component Fic1.

Fic1 is a component of the cytokinetic ring (CR), a filamentous actin and non-muscle type-II myosin-based structure required for cytokinesis. Fic1 was identified from a yeast two-hybrid (Y2H) cDNA library screen using the C-terminus of the F-BAR protein Cdc15 as bait (Roberts-Galbraith et al., 2009). Fic1 is comprised of an N-terminal C2 domain and a proline-rich C-terminus (Roberts-Galbraith et al., 2009). A fragment from Fic1's C-terminus containing four PxxP motifs was found to interact with the C-terminal fragment of Cdc15 which included an SH3 domain (Roberts-Galbraith et al., 2009).

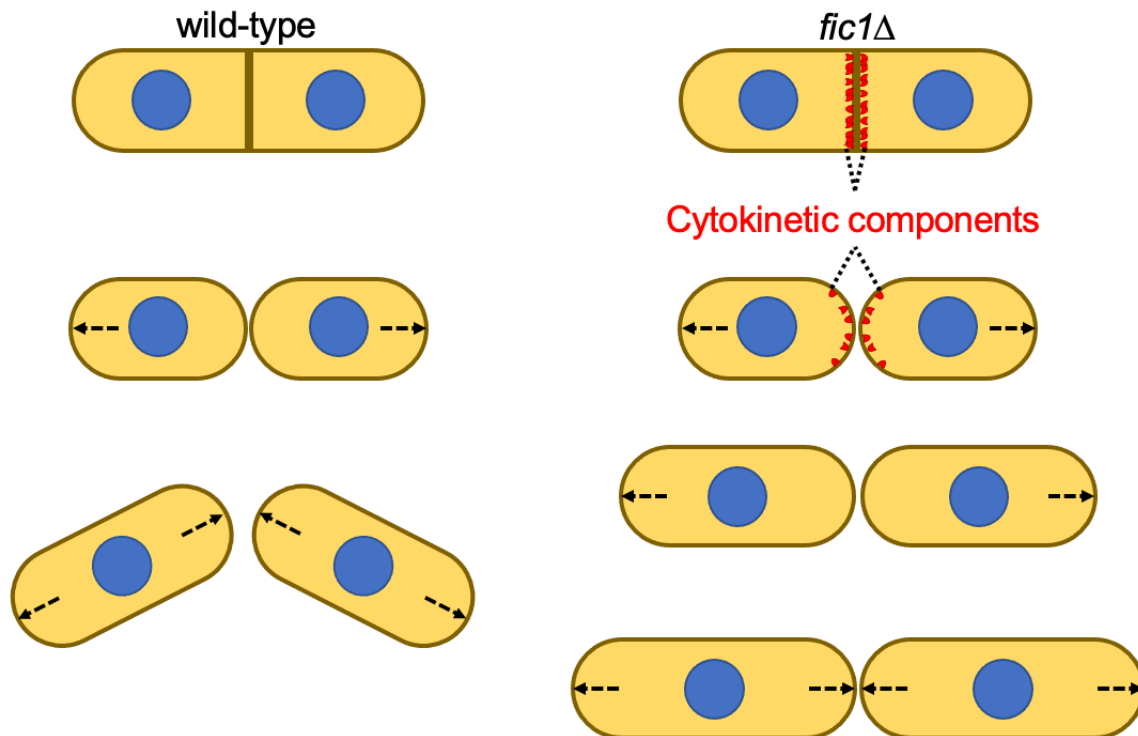


Figure 1.2. Prolonged persistence of cytokinetic components at the new ends impairs growth polarity establishment. In wild-type cells cytokinesis occurs efficiently which allows cells to undergo NETO during G2 in the subsequent cell cycle. In *fic1Δ* cells cytokinesis is inefficient which causes cytokinetic components to persist at the new ends and delays NETO during G2 in the subsequent cell cycle.

Fic1 localizes to the CR, septum, and growing interphase cell tips (Bohnert and Gould, 2012; Roberts-Galbraith et al., 2009). Fic1's C-terminus is required for its localization to the CR while the N-terminal C2 domain is required for its localization to growing interphase cell tips (Bohnert and Gould, 2012). Deletion of *fic1* causes NETO defects (Bohnert and Gould, 2012). These defects are ameliorated by expressing Fic1's C-terminus but not its C2 domain (Bohnert and Gould, 2012). Thus, Fic1's roles in polarity are not due to its activity at cell tips but rather its cytokinetic roles which ensure efficient CR constriction and disassembly (Bohnert and Gould, 2012). Defects in cytokinesis from the *fic1* deletion also influence *S. pombe*'s growth states by promoting the transition into invasive pseudohyphal growth (Bohnert and Gould, 2012).

The transition into invasive pseudohyphal growth upon the deletion of *fic1* demonstrates that disruptions to cytokinesis can influence *S. pombe*'s growth states. The exact mechanisms underlying the dimorphic switch from single cell growth to

invasive pseudohyphal growth in *fic1* Δ cells are not understood, but they are likely driven from cytokinetic defects that influence growth polarity establishment. To this point, other late cytokinetic mutants, such as *imp2* Δ , *cyk3* Δ , and *spn1* Δ cells, also exhibit invasive pseudohyphal growth (Bohnert and Gould, 2012). Like *fic1* Δ cells, these mutants exhibit NETO defects, which suggests that growth polarity establishment influences the transition into invasive pseudohyphal growth (Bohnert and Gould, 2012). Late cytokinetic mutants predominantly grow from their old end because they fail to establish growth at their new ends, likely due CR remnants occluding polarity factors from the new end. The result of this monopolar growth pattern is outward directional growth, a common feature of *S. pombe* pseudohyphal growth (Amoah-Buahin et al., 2005; Dodgson et al., 2010; Sipiczki et al., 1998). Thus, the invasive growth phenotype of late cytokinetic mutants with NETO defects aligns with what is known about pseudohyphal growth in *S. pombe*. Identifying Fic1's cytokinetic functions has been pivotal in advancing our understanding of Fic1's influence on growth polarity establishment and invasive pseudohyphal growth.

Fic1 displays multiple electrophoretic mobilities upon SDS-PAGE, which likely indicates the presence of post-translational modifications (Bohnert and Gould, 2012). It is unclear if these post-translational modifications alter Fic1's cytokinetic functions. If they do, they may also influence growth polarity establishment and the transition into invasive pseudohyphal growth. Identifying the enzymes responsible for Fic1's post-translational modifications could provide insight into a pathway that signals through Fic1. Identifying this pathway may provide additional insight into Fic1's roles in growth polarity establishment and its influence on invasive pseudohyphal growth. Identifying the specific residues these modifications target may also provide further insight as the regions and/or domains Fic1 utilizes for its cytokinetic roles. Lastly, if Fic1's post-translational modifications are cell cycle regulated we may be able to determine how Fic1's protein-protein interactions or localization are regulated.

1.3 *Schizosaccharomyces pombe* as a model organism for studying cytokinesis

Upon completing the G1, S, and G2 interphase stages of the cell cycle, cells enter mitosis during which the duplicated genetic material is segregated, and the

daughter cells are abscised. The spatial and temporal regulation of nuclear division and cytokinesis are coordinated to ensure the genetic material and the cytoplasm are properly partitioned between the dividing cell halves. Failure to regulate cytokinesis can result in aneuploidy, which can lead to cancer or even cell death (Fujiwara et al., 2005; Ganem et al., 2009; Krajcovic et al., 2011). In animal cells the plane of cellular division is selected through positive signaling from the centralspindlin complex (Alsop and Zhang, 2003; Bringmann and Hyman, 2005; Dechant and Glotzer, 2003; Werner et al., 2007). These signals ensure the plane of cell division occurs between the segregated genetic material. After the division plane is selected, a CR is assembled along cell cortex within this plane (Uehara et al., 2010; Yumura et al., 2008; Zhou and Wang, 2008). Following assembly, the CR constricts, causing the plasma membrane to ingress and the two daughter cells to be physically separated. Homology between many of the CR components is observed between a variety of eukaryotic organisms, suggesting that the underlying mechanisms of regulation are similar between these organisms (Glotzer, 2017; Gu and Oliferenko, 2015; Mangione and Gould, 2019).

S. pombe is an excellent model to study cytokinesis because both *S. pombe* and animal cells utilize a CR to achieve symmetric medial cell division (Glotzer, 2017; Gu and Oliferenko, 2015; Mangione and Gould, 2019); the pathways and proteins that regulate the *S. pombe* cell cycle are well studied; and *S. pombe* is amenable to genetic manipulation, biochemical techniques, and live-cell imaging. As *S. pombe* enter mitosis, growth ceases and the duplicated spindle pole bodies (SPB), the centrosome ortholog, separate (Ding et al., 1997; Mitchison, 1957). In contrast to the open mitosis observed in some other eukaryotic cells, *S. pombe* undergo a closed mitosis, where the nuclear envelope is maintained throughout mitosis (Sazer et al., 2014; Tanaka and Kanbe, 1986). The SPBs then embed themselves in the nuclear envelope before polymerizing intranuclear microtubules, or mitotic spindle, which segregate each SPB to opposite sides of the nuclear envelope (Ding et al., 1997). Sister chromatids adhere to microtubules polymerized from opposing SPBs through their kinetochore in metaphase and are separated from each other during anaphase A, as a result of microtubule depolymerization (Ding et al., 1997; Nabeshima et al., 1998). Anaphase B is marked by the increase in the length of the mitotic spindle, which propels the SPBs with their

associated genetic material to their respective poles (Ding et al., 1997; Nabeshima et al., 1998). The mitotic spindle is disassembled and the nuclei are abscised during telophase (Lucena et al., 2015).

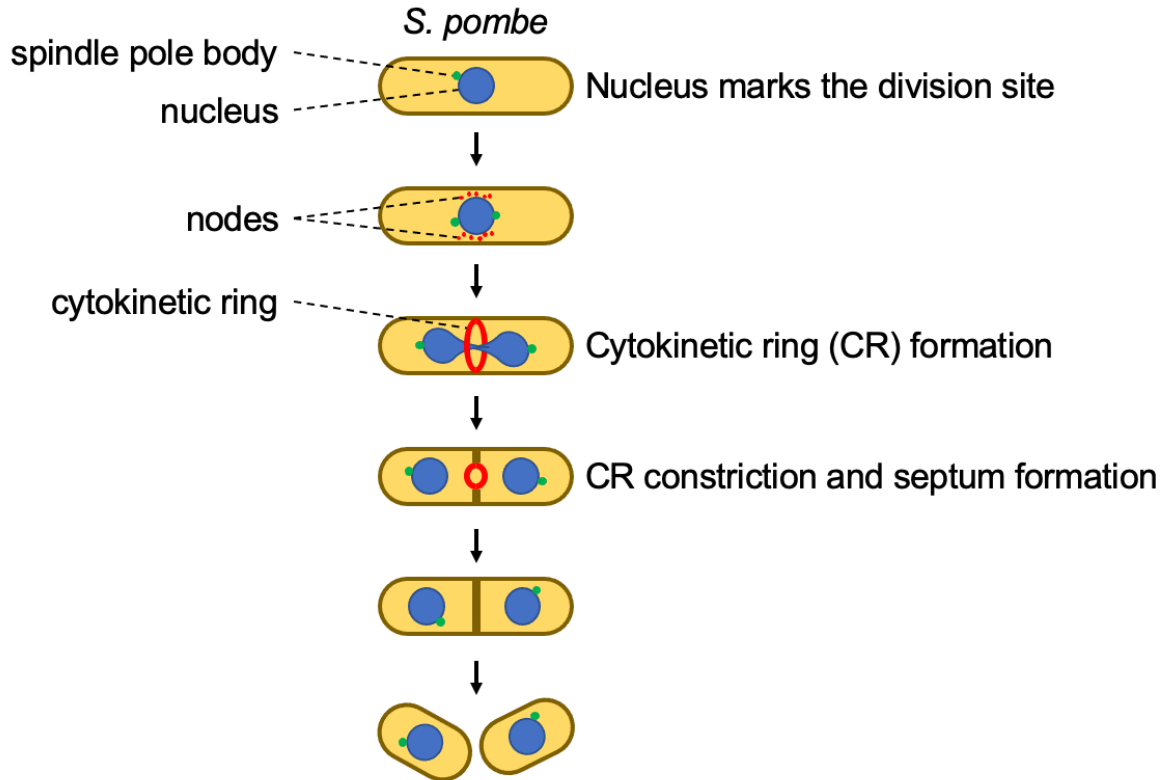


Figure 1.3. *S. pombe* utilize a cytokinetic ring to promote medial cell division. Upon mitotic commitment Mid1 is phosphorylated by Plo1 which causes Mid1 to form cytokinetic nodes on the medial cortex of the cell. These nodes recruit additional cytokinetic components that assist in assembling these nodes into a cytokinetic ring. After the genetic material is segregated the cytokinetic ring constricts and as the cytokinetic ring constricts cell wall machinery within the membrane that encompasses the cytokinetic ring initiates septum formation. Cytokinetic ring constriction and septum formation remain coordinated until the daughter cells are physically separated. The septated daughter cells remain joined until the septum is digested and the two daughter cells become independent.

S. pombe begin CR assembly upon entering mitosis. This process is guided by the position of the nucleus, which is maintained at the cell center by cytoplasmic microtubules (Figure 1.3) (Tran et al., 2001). Extensive genetic experimentation has elucidated many of the proteins involved in CR assembly. The polo kinase, Plo1, initiates CR assembly by phosphorylating the anillin-like protein Mid1 at the onset of mitosis (Almonacid et al., 2011; Bahler et al., 1998a). This phosphorylation causes Mid1

to be shuttled out of the nucleus where it then binds the medial cortex of the cell (Almonacid et al., 2011; Bahler et al., 1998a). Mid1 is relegated to the medial cortex of the cell through negative signaling by the DYRK family kinase Pom1 radiating from either cell tip (Bahler and Pringle, 1998; Celton-Morizur et al., 2006; Padte et al., 2006). Mid1 is phosphorylated on its N-terminus by the protein kinase Shk1, which promotes its association with the protein kinase Cdr2 to form cytokinetic nodes (Figure 1.3) (Magliozzi et al., 2020). After node formation, Mid1 associates with the non-muscle type-II myosin Myo2, the myosin light chain Rlc1, the IQGAP protein Rng2, the F-BAR protein Cdc15, and the formin Cdc12 (Almonacid et al., 2011; Celton-Morizur et al., 2004; Coffman et al., 2009; Laporte et al., 2011; Motegi et al., 2004; Padmanabhan et al., 2011; Wu et al., 2003; Wu et al., 2006). Recruitment of these proteins into cytokinetic nodes facilitates CR assembly through a process known as the search, capture, pull, and release (SCPR) (Figure 1.3) (Vavylonis et al., 2008; Wu et al., 2006). During CR assembly by SCPR, Cdc12 polymerizes actin filaments that span the distance between cytokinetic nodes (search). These filaments are bound by Myo2 on neighboring nodes (capture). Myo2 begins to pull on these filaments to pull the nodes closer to one another (pull), and then the actin filament is severed (release) (Vavylonis et al., 2008; Wu et al., 2006). This process continues until the nodes coalesce into a ring. This is the canonical pathway for CR assembly, but in *mid1* Δ cells CR assembly is achieved through an alternative pathway.

Assembly of the CR in *mid1* Δ cells utilizes the spot-leading cable pathway. Because cytokinetic nodes do not form in *mid1* Δ cells, this pathway relies on the formation of a single Cdc12 focus at the medial cortex of the cell, which polymerizes long actin filaments that line the circumference of the medial cortex at the site of cell division (Arai and Mabuchi, 2002; Carnahan and Gould, 2003; Kamasaki et al., 2007). Cytokinetic components, such as Myo2 and Cdc15, associate with this actin ring to assemble the CR. Assembling the CR through this pathway often results in off-center placement of the CR because CR placement is normally regulated by Mid1's medial cortex localization and inhibitory Pom1 signaling from either cell tip (Bahler and Pringle, 1998; Celton-Morizur et al., 2006; Padte et al., 2006; Sohrmann et al., 1996). Thus, in cells lacking Mid1, CR assembly can become misplaced due to the loss the Mid1 CR

placement cue. Improper regulation of CR placement can lead to cytokinesis occurring over the genetic material, leading to a “cut” phenotype during which chromosomes can be damaged by CR constriction (Hirano et al., 1986; Saka et al., 1994; Samejima et al., 1993).

The composition of the CR during assembly, maturation, and constriction is dynamic. Most notably, CR maturation requires the addition and loss of various proteins to ensure the CR is ready for constriction (Ge and Balasubramanian, 2008; Pinar et al., 2008; Ren et al., 2015; Roberts-Galbraith et al., 2009; Willet et al., 2019). The motor activity of Myo2 is required for CR constriction (Kitayama et al., 1997; May et al., 1997; Motegi et al., 1997). During constriction, Myo2 clusters pull on actin filaments causing the diameter of the CR to decrease. As the diameter decreases, excess actin is removed from the CR while the number of Myo2 molecules remains constant (Cheffings et al., 2019; Chen and Pollard, 2011; Malla et al., 2022; McDargh et al., 2023). Because of this turnover of actin, the formin Cdc12 continues to polymerize actin filaments throughout the constriction of the CR (Pelham and Chang, 2002). Unlike animal cells, CR constriction in *S. pombe* is performed in coordination with cell wall deposition to form a septum between daughter cells.

1.4 Septum formation in *Schizosaccharomyces pombe*

Organisms with a cell wall, such as *S. pombe*, utilize a structure known as a septum to partition dividing cells. *S. pombe* septa are composed of a primary septum flanked by two secondary septa (Humbel et al., 2001; Johnson et al., 1973). Septum deposition concentrically follows the constricting CR (Humbel et al., 2001; JC et al., 2018; Johnson et al., 1973; Liu et al., 2002; Ramos et al., 2019). Formation of the primary septum precedes the secondary septa. During primary septum formation the polymerization of linear- $\beta(1,3)$ glucan molecules by the glucan synthase Bgs1 provides the force necessary to overcome the high internal turgor pressure and drive membrane ingression (Cortes et al., 2007; JC et al., 2018; Liu et al., 1999; Proctor et al., 2012; Ramos et al., 2019). Because primary septum formation provides the force necessary to drive membrane ingression, the rate of CR constriction is linked to the rate of septum deposition (Ramos et al., 2019). In addition to the linear- $\beta(1,3)$ glucans formed by Bgs1,

the primary septum contains $\alpha(1,3)$ glucans synthesized by the glucan synthase Ags1 (Cortes et al., 2012; Hochstenbach et al., 1998; Katayama et al., 1999). The secondary septum consist of the two glucans synthesized by Bgs1 and Ags1 in addition to branched- $\beta(1,3)$ glucans synthesized by Bgs3 and Bgs4 and branched- $\beta(1,6)$ glucans presumably synthesized by Bgs4 (Cortes et al., 2005; Martin et al., 2003; Munoz et al., 2013; Ribas et al., 1991). If septum formation fails to produce a trilaminar structure or if the cell wall machinery and their regulatory components are disrupted, cells may fail cytokinesis (Arellano et al., 1999a; Arellano et al., 1996; Balasubramanian et al., 1998; Cortes et al., 2005; Davidson et al., 2016; Liu et al., 1999; Longo et al., 2022; Martin et al., 2003; Palani et al., 2017; Palani et al., 2018; Ramos et al., 2019; Ribas et al., 1991; Sethi et al., 2016; Tajadura et al., 2004).

The septation initiation network (SIN) is one pathway that regulates CR assembly and septum formation to prevent premature cell abscission, which could damage the genetic material. Insufficient SIN signal produces cells that progress through mitosis but fail to perform cytokinesis, resulting in multi-nucleated cells (Mitchison and Nurse, 1985). Conversely, excessive SIN signal causes cells to form multiple septa during cytokinesis (Fankhauser and Simanis, 1994; Minet et al., 1979; Ohkura et al., 1995; Schmidt et al., 1997). However, the SIN's influence on cytokinesis is best demonstrated by the ability of ectopic SIN signals to drive CR assembly and septum formation at any point in the cell cycle (Ohkura et al., 1995; Schmidt et al., 1997).

SIN signaling originates from the cytoplasmic face of the SPB. The SPB protein Ppc89 binds and localizes the SIN component scaffold protein Sid4 to the SPB (Rosenberg et al., 2006). Sid4 binds and localizes the centriolin ortholog Cdc11 to the SPB (Krapp et al., 2001; Morrell et al., 2004). Cdc11 binds the GTPase Spg1, which is maintained in its inactive GDP bound state throughout interphase by its associations with the two component GTPase-activating protein (GAP) of Spg1, Byr4-Cdc16 (Furge et al., 1998; Krapp et al., 2008). During mitosis, Spg1 binds GTP and becomes activated. The impetus for this activation is not known since no GEFs for Spg1 have been identified (Schmidt et al., 1997). GTP-Spg1 binds the STE-20 family protein kinase Cdc7 (Fankhauser and Simanis, 1994; Mehta and Gould, 2006; Schmidt et al., 1997). The formation of the Spg1-Cdc7 complex promotes the interaction between the PAK-

GC kinase Sid1 and its activator Cdc14, which is followed by the interaction between the NDR-family kinase Sid2 and its activator Mob1 (Guertin et al., 2000; Guertin and McCollum, 2001; Hou et al., 2004; Hou et al., 2000; Salimova et al., 2000). While all three kinase complex localize to the SPB, only Sid2-Mob1 also localizes to the CR in mid-late anaphase (Guertin et al., 2000; Guertin and McCollum, 2001; Hou et al., 2004; Hou et al., 2000; Mehta and Gould, 2006; Salimova et al., 2000). This allows Sid2-Mob1 to propagate the SIN signal from the SPB to downstream effectors at the site of cell division.

Sid2 targets the consensus sequence RxxS, which creates binding sites for the 14-3-3 protein Rad24 (Chen et al., 2008a; Feoktistova et al., 2012; Gupta et al., 2013; Mah et al., 2005; Yaffe et al., 1997). These interactions with Rad24 can modulate a protein's interactions and/or localization to assist in cell division. Sid2 phosphorylation promotes the association of Cdr2 and Clp1 with Rad24, which removes Cdr2 from cytokinetic nodes and promotes Clp1's cytoplasmic localization (Chen et al., 2008a; Rincon et al., 2017). Sid2 phosphorylation also evokes effects independent of Rad24. Sid2 phosphorylation of Cdc12 promotes Cdc12's ability to bundle actin filaments, which promotes CR assembly (Bohnert et al., 2013). In addition to these downstream effectors, Sid2 phosphorylated Cdc11 promotes its association with Cdc7 during anaphase (Feoktistova et al., 2012). This creates a positive-feedback loop that ensures maximum SIN activity during anaphase (Feoktistova et al., 2012). These examples highlight some of Sid2's downstream effectors that assist in promoting the SIN's function. In addition to the SIN positive-feedback loop, the SIN responds to feedback from the cell wall machinery during septum formation.

The *cps1-191* temperature-sensitive allele of the Bgs1 glucan synthase produces binucleate cells that arrest during cytokinesis because cells are unable to form a primary septum (Liu et al., 1999). CR assembly is not perturbed in *cps1-191* cells, but CR constriction cannot occur in the absence of primary septum formation by Bgs1, which normally drives drive membrane ingression (Liu et al., 1999; Proctor et al., 2012; Ramos et al., 2019). The CR persists at the medial cortex even as the cell progresses into the subsequent cell cycle because the SIN remains active (Mishra et al., 2004). This demonstrates that the SIN can alter its activation pattern in response to feedback

from the cell wall machinery. Despite these clear connections between the SIN and the cell wall machinery, the mechanisms that the SIN utilizes to regulate the cell wall machinery are uncharacterized. However, several proteins have been described to play a role in cell wall synthesis by regulating the cell wall machinery.

The essential Rho GTPase Rho1 acts as the regulatory subunit of Bgs1, Bgs3, and Bgs4 (Cortes et al., 2005; Cortes et al., 2002; Liu et al., 1999; Martin et al., 2003). GTP-Rho1 stimulates β -glucan synthase activity to promote cell wall formation and influences actin remodeling through unidentified effectors (Arellano et al., 1996; Arellano et al., 1997; Garcia et al., 2006; Nakano et al., 1997). Cells lacking Rho1 activity lyse during cytokinesis (Arellano et al., 1997). Interestingly, this phenotype is not rescued by osmotic stabilizers, which typically prevent cell lysis due to damaged or weakened cell walls (Arellano et al., 1997). This suggests Rho1's roles in cell wall formation only partially explain its cytokinetic roles and that Rho1's enigmatic roles in actin remodeling are also required for successful cell division.

Rho1 is converted to its GTP bound state by three RhoGEFs: Rgf1, Rgf2, and Rgf3 (Garcia et al., 2009; Garcia et al., 2006; Morrell-Falvey et al., 2005; Mutoh et al., 2005; Tajadura et al., 2004). Each of these RhoGEFs act on Rho1 at different locations and times during the cell cycle (Mutoh et al., 2005). While Rgf1, Rgf2, and Rgf3 localize to the site of cell division during cytokinesis, Rgf3 exclusively localizes to the site of cell division and is the only essential RhoGEF (Mutoh et al., 2005; Tajadura et al., 2004). Similar to the loss of Rho1 activity, depletion of Rgf3 causes cell lysis during cytokinesis (Tajadura et al., 2004). Conversely, overexpression of Rgf3 increases β -glucan synthase activity, resulting in an increase of β -glucans in the cell wall (Tajadura et al., 2004). Rho1 is inactivated when GTP-Rho1 is hydrolyzed to GDP-Rho1. Rho1 inactivation can be mediated by three RhoGAPs, Rga1, Rga5, and Rga8 (Calonge et al., 2003; Nakano et al., 2001). Deletion of Rga1 increases the number of actin patches and the thickness of the cell wall (Nakano et al., 2001). Thus, the regulatory subunit of the β -glucan synthases, Rho1, is an important signaling molecule that ensures proper formation of the cell wall and the septum.

While Rho1 regulates the β -glucan synthases, the Rho GTPase Rho2 regulates the α -glucan synthase Ags1 (Calonge et al., 2000). Rho2's regulation of Ags1 is not

fully understood, but it involves Pck2, a protein kinase C (Calonge et al., 2000). The RhoGEFs that convert Rho2 to its GTP bound state are unidentified, but the RhoGAPs Rga2, Rga4, Rga6, and Rga7 promote the conversion of GTP-Rho2 to GDP-Rho2 (Revilla-Guarinos et al., 2016; Soto et al., 2010; Villar-Tajadura et al., 2008). Rho2 localizes to the septum during cytokinesis and overexpression of Rho2 increases the septation index of asynchronous cells and causes a multi-septation phenotype (Hirata et al., 1998). These observations suggest that Rho2's roles in septum formation are due to its relationship with Ags1. More importantly, Rho2 and Rho1 are components of the cell integrity pathway (CIP) which regulates cell wall synthesis.

The CIP promotes cell wall synthesis in response to cell wall damage and environmental stress through a mitogen activated protein kinase (MAPK) pathway (Loewith et al., 2000; Madrid et al., 2006; Toda et al., 1996; Zaitsevskaya-Carter and Cooper, 1997). Cell wall damage is sensed by the cell wall sensors Wsc1 and Mlt2, which in turn promote Rgf1's activation of Rho1 (Cruz et al., 2013). GTP-Rho1 directly stimulates the β -glucan synthases to initiate cell wall synthesis and binds both protein kinase C homologs, Pck1 and Pck2 (Arellano et al., 1999a; Arellano et al., 1996; Sayers et al., 2000; Tajadura et al., 2004). These interactions with Pck1 and Pck2 promote the phosphorylation of Mkh1, a MAPKKK, which signals through Pek1, a MAPKK, and Pmk1, a MAPK, to effect change through Rnc1 and Nrd1, two RNA-binding proteins, Atf1, a transcription factor, Clp1, a Cdc14-like phosphatase, and Cch1–Yam8 calcium channels (Broadus and Gould, 2012; Kobayashi et al., 2013; Ma et al., 2011; Satoh et al., 2009; Sugiura et al., 2003; Takada et al., 2007). Rho2 activates Pck2 in response to environmental stressors, such as osmolarity shocks and high levels of chloride ions (Barba et al., 2008; Sanchez-Mir et al., 2014). The upstream activation of Rho2 is uncharacterized largely because Rho2's RhoGEF(s) are unknown. Pck1 and Pck2's interactions with these Rho GTPases regulate the activity of the α - and β -glucan synthases independent of the MAPK signaling cascade (Calonge et al., 2000). While Pck1 and Pck2 both regulate the CIP, Pck2 is the main regulator of CIP signaling, and Pck2's interaction with Rho2 elicits a stronger downstream response than Pck2's interaction with Rho1 (Barba et al., 2008; Sanchez-Mir et al., 2014). In addition to its

roles in regulating cell wall synthesis in response to cell wall damage and environmental stressors, the CIP plays a role in septum formation.

Cells depleted of Pck1 and Pck2 lyse during cytokinesis similar to Rho1 depleted cells, demonstrating the importance of Pck1 and Pck2's influence on cell wall synthesis during septum formation (Arellano et al., 1999b). Cells exhibit separation defects when CIP signaling is disrupted by hyperactive Pmk1 or by deleting *mek1* or *pmk1* (Madrid et al., 2017; Sugiura et al., 1999). Deleting *mkh1* does not cause cell separation defects at normal growing conditions, but high temperatures or hyperosmotic environments cause separation defects in *mkh1* Δ cells (Sengar et al., 1997). The separation defects observed from these genetic perturbations suggest that CIP signaling ensures proper septum formation and efficient cell separation. Lastly, the CIP has been shown to delay septum formation upon the presence of cell wall stress. Wild-type cells treated with blankofluor, a reagent that binds linear- β (1,3)glucans and inhibits their synthesis, delay the initiation of septum formation (Edreira et al., 2020). This delay is attributed to CIP signaling because it was not observed in *rgf1* Δ or *pmk1* Δ cells (Edreira et al., 2020). These data suggest that the CIP modulates glucan synthase activity during septum formation in response to environmental factors to ensure successful cytokinesis.

Rho1, Rho2, and the CIP broadly regulate cell wall synthesis, but additional regulatory mechanisms ensure proper function and localization of each specific β -glucan synthase. Bgs1's stability and localization are regulated by *sbg1*, an essential gene first identified as a multi-copy suppressor of *cps1-191* (Davidson et al., 2016; Sethi et al., 2016). Cell division fails in *sbg1* Δ spores because these cells lyse during cytokinesis due to improper septum formation (Davidson et al., 2016; Sethi et al., 2016). Furthermore, downregulating expression of *sbg1* in vegetative cells produces multi-septate cells with increased cell wall and septa thickness (Davidson et al., 2016). Despite these thicker septa, these cells have gaps in their primary septa (Davidson et al., 2016). These studies show that proper septum formation cannot occur in the absence of Sbg1 due to dysregulation of Bgs1's localization and function.

Much like Sbg1's interactions with Bgs1, the essential β -glucan adapter protein Smi1 assists in localizing Bgs4 to the site of cell division (Longo et al., 2022). Cells with the temperature-sensitive allele of *smi1*, *smi1-1*, have an increased septation index and

lyse at the restrictive temperature (Longo et al., 2022). These phenotypes are attributed to cell wall defects such as thin primary septa and thin lateral cell walls at the division site (Longo et al., 2022). Smi1 colocalizes with Bgs1, Bgs4, and Ags1 in cytoplasmic vesicles but only co-immunoprecipitates with Bgs4 (Longo et al., 2022). Furthermore, mislocalizing either Bgs4 or Smi1 to the mitochondria causes mislocalization of the other protein as well (Longo et al., 2022). The exact mechanisms underlying the interaction between Smi1 and Bgs4 are unknown, but it is clear that Smi1 regulates Bgs4's localization and stability, which ensures proper septum morphology.

The localization of Bgs4 and Ags1 is dependent on Bgs1. Repressed expression of *bgs1* causes Bgs4 and Ags1 to diffusely localize to the site of cell division (Ramos et al., 2019). This is in contrast to the compact ring Bgs4 and Ags1 form behind the CR in wild-type cells (Ramos et al., 2019). Reducing the amount of Bgs1 at the site of cell division alters the localization of Ags1 and Bgs4, which results in the formation of thickened septa (Ramos et al., 2019). This highlights the importance that Bgs1 and primary septum formation have on the other glucan synthases.

While Bgs4 and Ags1 are dependent on Bgs1 for proper localization, Bgs1 is not dependent on either Ags1 or Bgs4 (Ramos et al., 2019). Because of this, downregulation of Ags1 or Bgs4 activity only produces abnormalities in the morphology of the secondary septum (Cortes et al., 2012; Munoz et al., 2013). Downregulation of Ags1 or Bgs4 activity can lead to the production of thin, missing, or unanchored secondary septa (Cortes et al., 2012; Munoz et al., 2013). These disruptions to secondary septum formation can result in cell lysis during cytokinesis or cell separation (Cortes et al., 2012; Munoz et al., 2013). Proper secondary septum morphology is crucial because the secondary septa become the cell wall for each daughter cell's new ends. Disruptions to septum morphology are expected from disruptions to the glucan synthases, but cytokinetic mutants with defects in CR constriction also exhibit septation defects (Balasubramanian et al., 1998; Kovar et al., 2005; May et al., 1997; Pollard et al., 2012; Willet et al., 2018).

CR constriction and septum formation are likely linked through an unidentified protein network. Tension generated from the constriction of Myo2 regulates Bgs1's localization and activation for proper primary septum formation (Ramos et al., 2019). A

temperature-sensitive allele of Myo2, *myo2-E1*, produces cells that can assemble CRs but, due to steric hinderance in the motor domain of the mutant Myo2 protein, are unable to constrict the CRs (Balasubramanian et al., 1998; Palani et al., 2017; Palani et al., 2018). These cells become multinucleate and lyse because they cannot form a septum to complete cytokinesis (Balasubramanian et al., 1998). Bgs1 is diffusely localized to the site of cell division in *myo2-E1* cells at a semi-restrictive temperature, which leads to aberrant cell wall deposition along the cortex instead of proper septum formation (Ramos et al., 2019). Interestingly, if *myo2-E1* cells are permitted to complete at least 50% of the septum at the permissive temperature before being shifted to the restrictive temperature, they will proceed to complete proper septum formation (Proctor et al., 2012). Additionally, if wild-type cells are permitted to complete at least 50% of the septum before being treated with Lat A, which depolymerizes the F-actin of the CR, they will proceed to complete proper septum formation (Proctor et al., 2012; Ramos et al., 2019). In either case, disrupting the CR prior to completing at least 50% of the septum results in cells with septation defects. The ability for septum formation to persist upon loss of CR constriction combined with the failure to initiate in the absence of CR constriction highlights the role of CR constriction on cell wall machinery regulation.

The primary septum is important for driving membrane ingression during cytokinesis, and it is important for the separation of daughter cells. Once septum formation is complete, the two daughter cells are partitioned and will remain joined until the primary septum is digested during S phase. Primary septum digestion is performed by the Agn1 and Eng1 glucanases (Dekker et al., 2004; Martin-Cuadrado et al., 2003). Individual cells produced from this digestion proceed through G2 phase during which cell wall remodeling and cell growth occur at the cell ends. Thick and misshapen septum morphologies can prevent the Eng1 and Agn1 glucanases from accessing and digesting the primary septum, which leads to the formation of multi-septated cells (Cortes et al., 2007; Cortes et al., 2015; Dekker et al., 2004; Garcia et al., 2005; Martin-Cuadrado et al., 2003). Thus, it is imperative that the glucan synthases, signaling pathways, and cell wall machinery are all properly regulated to form a trilaminar structure with a digestible primary septum that allows for cell separation and robust secondary septa which prevents cell lysis.

1.5 Fic1's roles in septum formation in *Schizosaccharomyces pombe*

The *Saccharomyces cerevisiae* ingression protein one, Inn1, is an essential protein that is required for primary septum deposition (Sanchez-Diaz et al., 2008). Inn1 directly interacts with two other proteins, the F-BAR protein Hof1 and the cytokinetic protein Cyk3 (Nishihama et al., 2009). Together these three proteins form a complex named the ingression progression complex (IPC) (Devrekanli et al., 2012; Meitinger et al., 2010; Nishihama et al., 2009; Sanchez-Diaz et al., 2008). The IPC promotes membrane ingression by stimulating primary septum formation during cytokinesis (Devrekanli et al., 2012; Meitinger et al., 2010; Nishihama et al., 2009; Sanchez-Diaz et al., 2008). In *S. cerevisiae* the primary septum is composed of N-acetylglucosamine polymers, also known as chitin, which are generated by the chitin synthase, Chs2 (Sburlati and Cabib, 1986; Shaw et al., 1991; Silverman et al., 1988). Chs2 is stimulated by Inn1's C2 domain and Cyk3 conserved C-terminal region (Devrekanli et al., 2012; Meitinger et al., 2010; Nishihama et al., 2009). The presence of an IPC has not been established in *S. pombe*, but all of the IPC constituents have *S. pombe* orthologs.

S. pombe has two Hof1 orthologs, Cdc15, and another *pombe* Cdc15 homology (PCH) family protein, Imp2 (Demeter and Sazer, 1998; Fankhauser et al., 1995). Fic1 directly interacts with the SH3 domains of both Cdc15 and Imp2 through the canonical SH3-PxxP motif interface (Roberts-Galbraith et al., 2009). Both Cdc15 and Imp2 bind the same PxxP motif on Fic1, P254,257 (Bohnert and Gould, 2012). Disrupting this interaction by removing the SH3 domain from either Cdc15 or Imp2 or by introducing the Fic1-P257A substitution mutation evokes growth polarity establishment defects similar to those observed in *fic1* Δ cells (Bohnert and Gould, 2012). These findings suggest that the Fic1-Cdc15 and Fic1-Imp2 interactions are required for Fic1's cytokinetic functions that promote proper cell growth polarity establishment.

The *S. pombe* Cyk3 ortholog has the same namesake as its *S. cerevisiae* counterpart (Pollard et al., 2012). Cyk3 in *S. pombe* is largely uncharacterized, but like the *S. cerevisiae* ortholog, it contains an N-terminal SH3 domain linked to a transglutaminase-like domain through an intrinsically disordered region (IDR) (Pollard et al., 2012). The C-terminus of Cyk3 is conserved among fungi and is predicted to be

structured, but the structure has not been described. Fic1 and Cyk3 co-immunoprecipitate from the lysates of mitotically arrested cells, but a direct interaction between Fic1 and Cyk3 has not been reported (Bohnert and Gould, 2012). Deletion of *cyk3* leads to defects in growth polarity establishment and promotes the transition into invasive pseudohyphal growth, similarly to *fic1* Δ cells (Bohnert and Gould, 2012). Because *cyk3* Δ and *fic1* Δ cells exhibit similar phenotypes, it is possible that these two proteins work together in the same pathway similarly to Inn1 and Cyk3 in *S. cerevisiae*. Determining if Fic1 and Cyk3 directly interact would demonstrate that an IPC-like protein network is conserved in *S. pombe*.

The IPC stimulates Chs2 to promote primary septum in *S. cerevisiae*, but *S. pombe*'s primary septum is not thought to contain N-acetylglucosamine polymers (Horisberger et al., 1978; Sietsma and Wessels, 1990). Instead, the *S. pombe* primary septum is largely composed of linear- β (1,3)glucans polymerized by the Bgs1 glucan synthase (Cortes et al., 2005; Cortes et al., 2002; Cortes et al., 2007). Despite the lack of N-acetylglucosamine polymers in *S. pombe*'s primary septum and overall cell wall, *S. pombe* does have a Chs2 ortholog with the same namesake (Martin-Garcia et al., 2003; Matsuo et al., 2004). Conservation of an IPC-like protein network in *S. pombe* would lead to two questions: is the function for stimulating primary septum deposition conserved or is the interaction between the IPC-like protein network and Chs2 conserved? If the IPC-like protein network in *S. pombe* stimulates primary septum formation it would likely do so through Bgs1, not Chs2, due to *S. pombe*'s primary septum composition (Cortes et al., 2005; Cortes et al., 2002; Cortes et al., 2007). If the IPC-like protein network does promote primary septum deposition, there are likely other proteins involved in this process because *fic1* Δ *cyk3* Δ cells are viable, suggesting there are alternative pathways for promoting primary septum deposition (Ren et al., 2015). As for the possibility that components of the IPC-like protein network interact with Chs2 in *S. pombe*, deletion of *chs2* results in an increase in CR constriction time, similarly to *fic1* Δ and *cyk3* Δ cells, but phenotypes specific to *fic1* Δ and *cyk3* Δ such as growth polarity establishment defects or invasive pseudohyphal growth have not been reported in *chs2* Δ cells (Martin-Garcia et al., 2003; Matsuo et al., 2004). Determining the presence of an IPC in *S. pombe* and its cytokinetic function would elucidate Fic1's

cytokinetic roles and would allow us to determine which protein-protein interactions and functions are conserved between *S. pombe* and *S. cerevisiae*.

Chapter 2

Phosphoregulation of the Cytokinetic Protein Fic1 Contributes to Fission Yeast Growth Polarity Establishment

This chapter is adapted from “Phosphoregulation of the Cytokinetic Protein Fic1 Contributes to Fission Yeast Growth Polarity Establishment” published in the *Journal of Cell Science* doi: 10.1242/jcs.244392 and has been reproduced with the permission of my publisher and co-authors: K. Adam Bohnert, Quan-wen Jin, Jun-Song Chen, and Kathleen L. Gould

2.1 Introduction

Polarization is a common feature of eukaryotic and prokaryotic cells (Hu and Lutkenhaus, 1999; Miller and Johnson, 1994). Multicellular organisms couple polarization events in neighboring cells to drive key developmental processes (Moorhouse et al., 2015). In a single cell, polarization governs such processes as growth, motility, and fate specification (Mortimer et al., 2008; Pham et al., 2015; Ueda and Masahiro, 2018).

The fission yeast *Schizosaccharomyces pombe* is a powerful model organism for studying mechanisms by which polarization is established, maintained, and modified (Arellano et al., 1999a; Miller and Johnson, 1994; Otilie et al., 1995). *S. pombe* is a rod-shaped organism, with growth limited to its cell tips (Streiblova and Wolf, 1972). After cell division, elongation occurs first only at old ends inherited from mother cells. Then, at a later point known as new end take off (NETO), cells transition to bipolar growth by also extending at new ends established by the most recent cell division (Mitchison and Nurse, 1985).

Historically, NETO was thought to be triggered when cells reached a minimal cell size and completed S-phase (Mitchison and Nurse, 1985). However, NETO also requires proper completion of cytokinesis (Bohnert and Gould, 2012). Specifically, loss of the cytokinetic ring (CR) protein Fic1 (Roberts-Galbraith et al., 2009) leads to abnormal persistence of CR components at new ends and curbs NETO even if factors responsible for growth are properly positioned at new cell ends (Bohnert and Gould, 2012). Barriers to NETO, caused by loss of Fic1 or other late cytokinetic factors, in turn promote growth orientations that favor a dimorphic switch from a unicellular state to a more invasive, pseudohyphal form (Bohnert and Gould, 2012).

Our growing knowledge of NETO highlights the role of protein kinases at cell tips (Arellano et al., 2002; Fujita and Misumi, 2009; Grallert et al., 2013; Kettenbach et al., 2015; Kim et al., 2003; Kume et al., 2017; Kume et al., 2011; Martin et al., 2005). Cell tip kinases also target CR proteins and influence their localization and cytokinesis function (Bhattacharjee et al., 2020; Lee et al., 2018; Magliozzi et al., 2020). The interplay between the fidelity of cytokinesis and proper polarity establishment in the next cell cycle, demonstrated by the role of Fic1, may therefore be phosphoregulated.

Here, we show that Fic1 is phosphorylated at two C-terminal residues. Though Cdk1 and casein kinase II Orb5 each phosphorylate one of the sites in vitro, we found that none of the 111 *S. pombe* protein kinases are solely responsible for phosphorylation of either site. Fic1 phospho-mimetic and phospho-ablating mutations impaired *S. pombe* NETO and produced an invasive pseudohyphal phenotype, indicating phosphorylation controls its role in polarity. Our findings predict complex regulation of cytokinesis-based polarity determinants and suggest at least two different groups of kinases influence polarity by modulating Fic1 phosphostate.

2.2 Fic1 phosphorylation is invariant through the cell cycle

As shown previously (Bohnert and Gould, 2012), immunoblotting of Fic1-FLAG₃ immunoprecipitates revealed four distinct bands collapsible to one band by phosphatase treatment (Fig. 2.1A). Thus, Fic1 is a phosphoprotein, and, given the

multiple Fic1-FLAG₃ species, we conclude that Fic1 is phosphorylated at multiple residues.

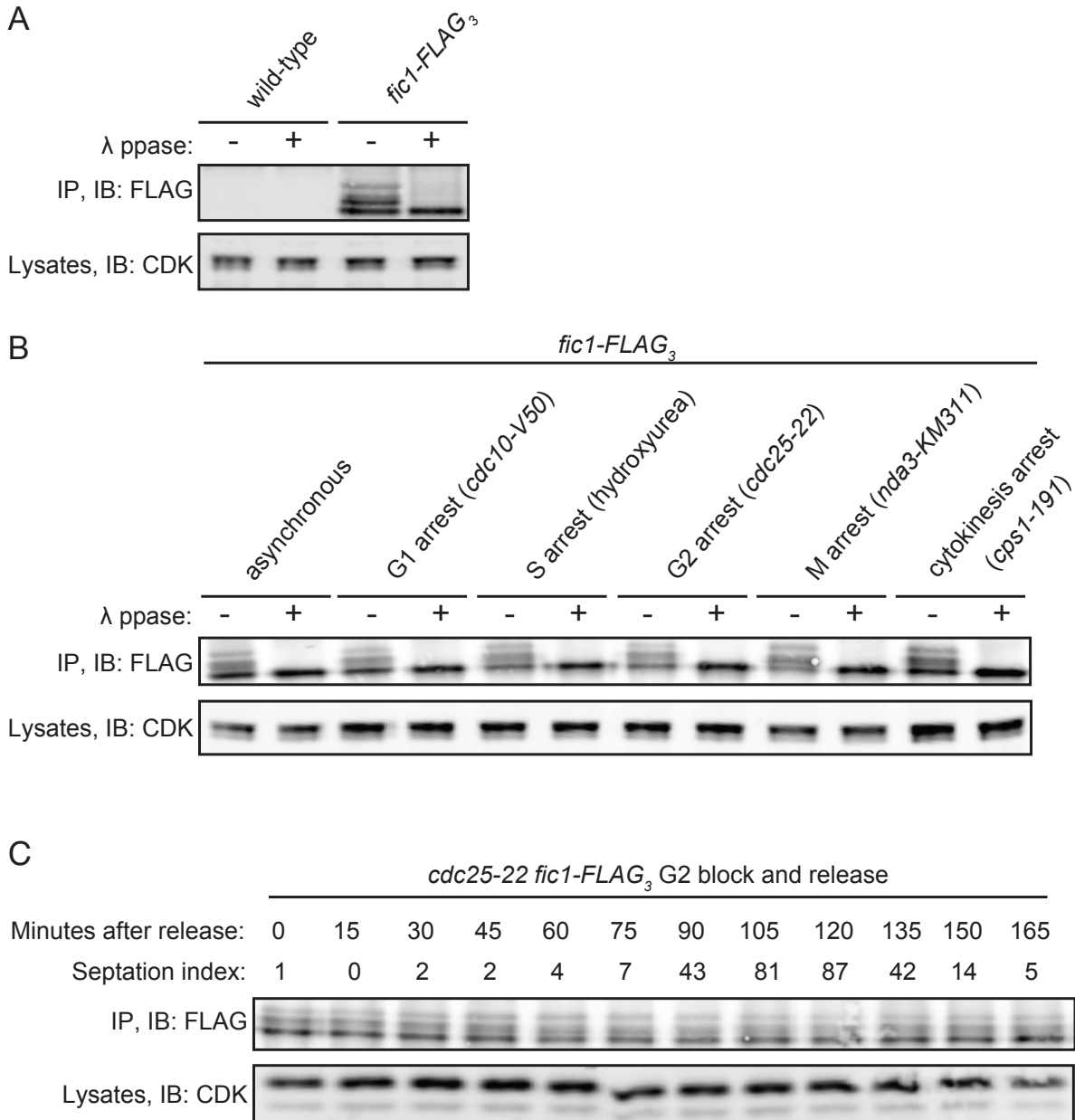


Figure 2.1. Fic1 is phosphorylated *in vivo*. A-B) Anti-FLAG immunoprecipitates from cells of indicated genotypes or from *cdc25-22 fic1-FLAG₃* cells following release from a G2 arrest (C) were treated with lambda phosphatase or vehicle and subsequently blotted with an anti-FLAG antibody. Lysate samples were blotted with anti-CDK (PSTAIRE) as a control for input into the immunoprecipitation.

To assess whether Fic1 phosphostatus is cell cycle regulated, we analyzed Fic1-FLAG₃ gel mobility in different cell cycle arrests, either through temperature-sensitive

alleles (*cdc10-V50* G1 arrest, *cdc25-22* G2 arrest, *nda3-KM311* prometaphase arrest, or *cps1-191* cytokinesis arrest) or by addition of hydroxyurea (S-phase arrest). In all cases, Fic1-FLAG₃ gel mobilities were identical (Fig. 2.1B). We corroborated this result using a *cdc25-22* block-and-release experiment, in which samples were taken following release from a G2 arrest. Fic1-FLAG₃ gel mobility shifts were identical at each time point (Fig. 2.1C), verifying that multiple phospho-species of Fic1 exist throughout the cell cycle.

2.3 Fic1 phosphorylation is independent of cell tip localization

Fic1's C-terminus (amino acids 127-end, "Fic1C" (Fig. 2.2A)) localizes to the CR but not to cell tips, and this fragment is necessary and sufficient for NETO (Bohnert and Gould, 2012). In contrast, the N-terminal C2 domain (amino acids 1-126, "Fic1N" (Fig. 2.2A)) neither localizes to the CR nor contributes to bipolar growth establishment, but is required for anchoring Fic1 to cell tips (Bohnert and Gould, 2012). Whereas Fic1N-GFP did not migrate as multiple species on SDS-PAGE (Fig. 2.2B), Fic1C-GFP showed a phosphoshift that was collapsed by phosphatase treatment (Fig. 2.2C). These results suggested that Fic1 phosphorylation might affect its function at the CR and therefore, in NETO.

If this were the case, we expected that Fic1 phosphorylation would occur even if Fic1 lost its ability to anchor at cell tips. Based on homology to *S. cerevisiae* Inn1 (Devrekanli et al., 2012; Sanchez-Diaz et al., 2008), we predicted that two lysines within the C2 domain (Fig. 2.2A) mediated cell-tip localization and we mutated them to alanines. Cell tip localization of Fic1-K22A,K27A-GFP was greatly reduced compared to Fic1-GFP (Fig. 2.2D and E). Additionally, whereas wild-type Fic1-GFP localized broadly across cell tips, Fic1-K22A,K27A-GFP localization at cell tips was restricted to puncta that also contained Cdc15-mCherry, a tip protein and Fic1 interactor (Roberts-Galbraith et al., 2009) (Fig. 2.2D and E). However, Fic1-K22A,K27A promoted proper bipolar growth (Fig. 2.2F-H), targeted to the CR (Fig. 2.2I), and was phosphorylated to the same extent as wildtype (Fig. 2.2J), consistent with the idea that Fic1 phosphorylation influences its function at the CR to modulate polarity.

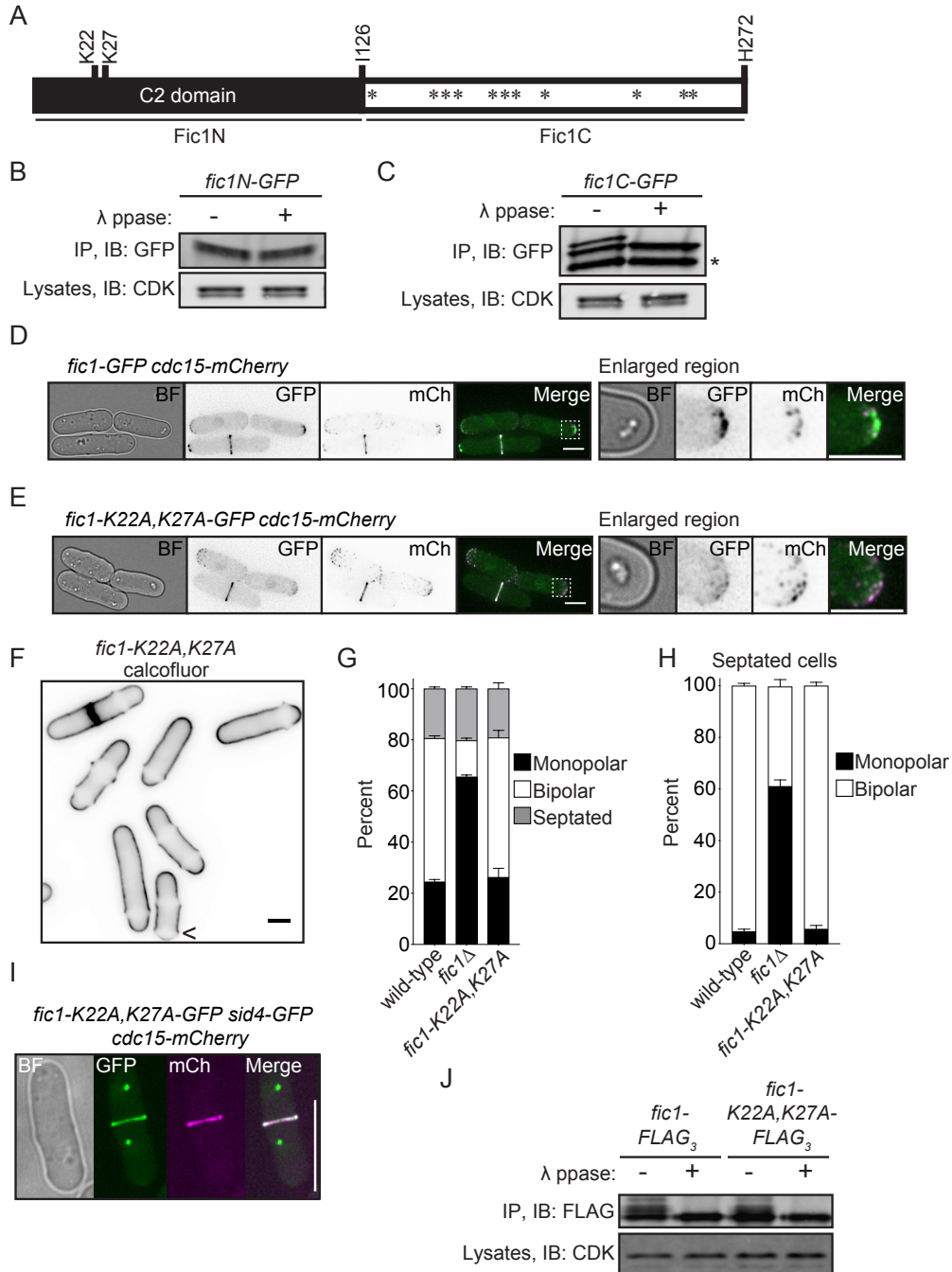


Figure 2.2. Phosphorylation occurs on the region and subpopulation of Fic1 relevant to growth polarity. A) Schematic of Fic1, drawn to scale, with residues of interest, fragments, and PxxP motifs (*) indicated. B and C) Anti-GFP immunoprecipitates from *fic1N-GFP* (B) and *fic1C-GFP* cells (C) were either treated with lambda phosphatase or vehicle and subsequently blotted with an anti-GFP antibody. Lysate samples were blotted with anti-CDK (PSTAIR) as a control for input into the immunoprecipitation. An asterisk (*) indicates degradation products. D and E) Live-cell bright field (BF), GFP, mCherry (mCh), and merged GFP/mCh images of *fic1-GFP cdc15-mCh* (D) and *fic1-K22A,K27A-GFP cdc15-mCh* (E) cells. Regions of interest

are enlarged on the right. Scale bars in (D) and (E), 5 μm . F) Live-cell image of calcofluor-stained *fic1-K22A,K27A* cells. Arrowhead indicates a monopolar cell. Scale bar, 5 μm . G) Quantification of growth polarity phenotypes for cells of the indicated genotypes. Data from three trials per genotype with $n > 200$ for each trial are presented as mean \pm SEM. H) Quantification of growth polarity phenotypes for septated cells of the indicated genotypes. Data from three trials per genotype with $n > 200$ for each trial are presented as mean \pm SEM. I) Live-cell BF, GFP, mCh, and merged GFP/mCh images of a *fic1-K22A,K27A-GFP sid4-GFP cdc15-mCh* cell during cytokinesis. Scale bar, 10 μm . J) Anti-FLAG immunoprecipitates from *fic1-FLAG₃* and *fic1-K22A,K27A-FLAG₃* cells as in Fig. 2.1.

2.4 Fic1 is phosphorylated on two C-terminal residues

Fic1 phosphorylation sites have not been identified in proteome-wide screens (Lock et al., 2019). Thus, we used mass spectrometry of tandem affinity-purified (TAP) Fic1-TAP to identify phosphorylation sites in a targeted manner. Phosphorylation of two C-terminal residues, T178 and S241, was identified (Figs 2.3A and 2.4A and B). T178 and S241 were each mutated to alanine to abolish phosphorylation, or to aspartate to potentially mimic constitutive phosphorylation. These phosphomutants were then integrated at the endogenous *fic1* locus, tagged with FLAG₃, and tested for alteration in SDS-PAGE mobility. Alanine mutations of T178 or S241 individually eliminated two of the four bands, indicating that one band, the upper band, represented dually phosphorylated protein and each intermediate band represented singly phosphorylated Fic1 (Fig. 2.4C), also confirming that these two residues are the major Fic1 phosphosites. Consistent with this interpretation, Fic1-T178A,S241A (Fic1-2A) migrated as a single band (Fig. 2.4C). In Fic1 aspartate mutants, similar gel mobility patterns were observed, except that all bands were slightly retarded in mobility (Fig. 2.4C). Thus, phosphorylation occurs individually and in combination at T178 and S241 *in vivo*.

A

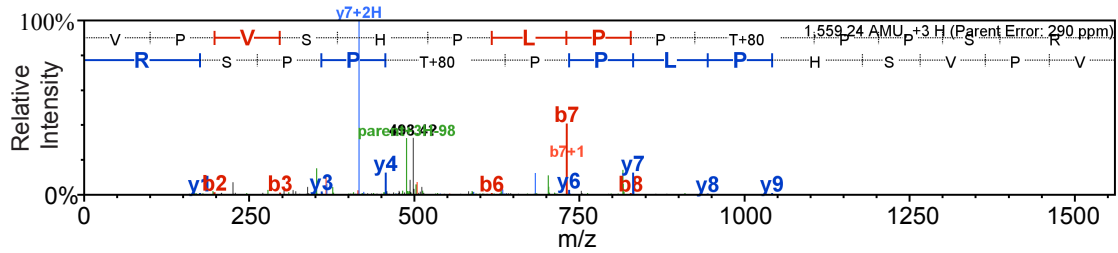
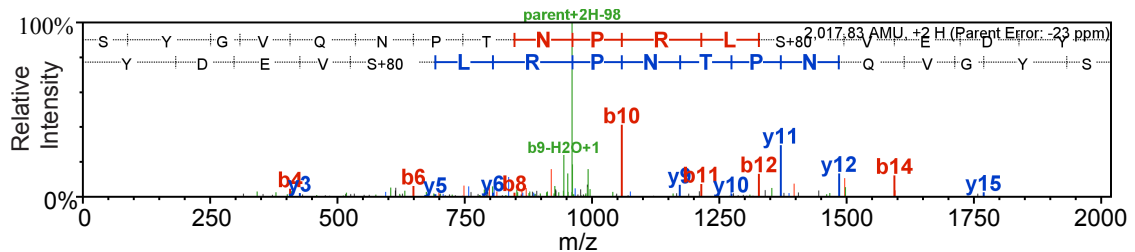
T178**S241**

Figure 2.3. Fic1 residues T178 and S241 are phosphorylated *in vivo*. A) Representative MS2 spectra of peptides with phosphorylated T178 or S241, respectively, identified from Fic1-TAP affinity purifications. The peptide sequence ladder depicts y (colored blue) and b (colored red) ions of the peptide. Green peaks indicate either neutral loss of phosphate from the parent ions or loss of water from the fragmented product ions. Black peaks represent unidentified ions.

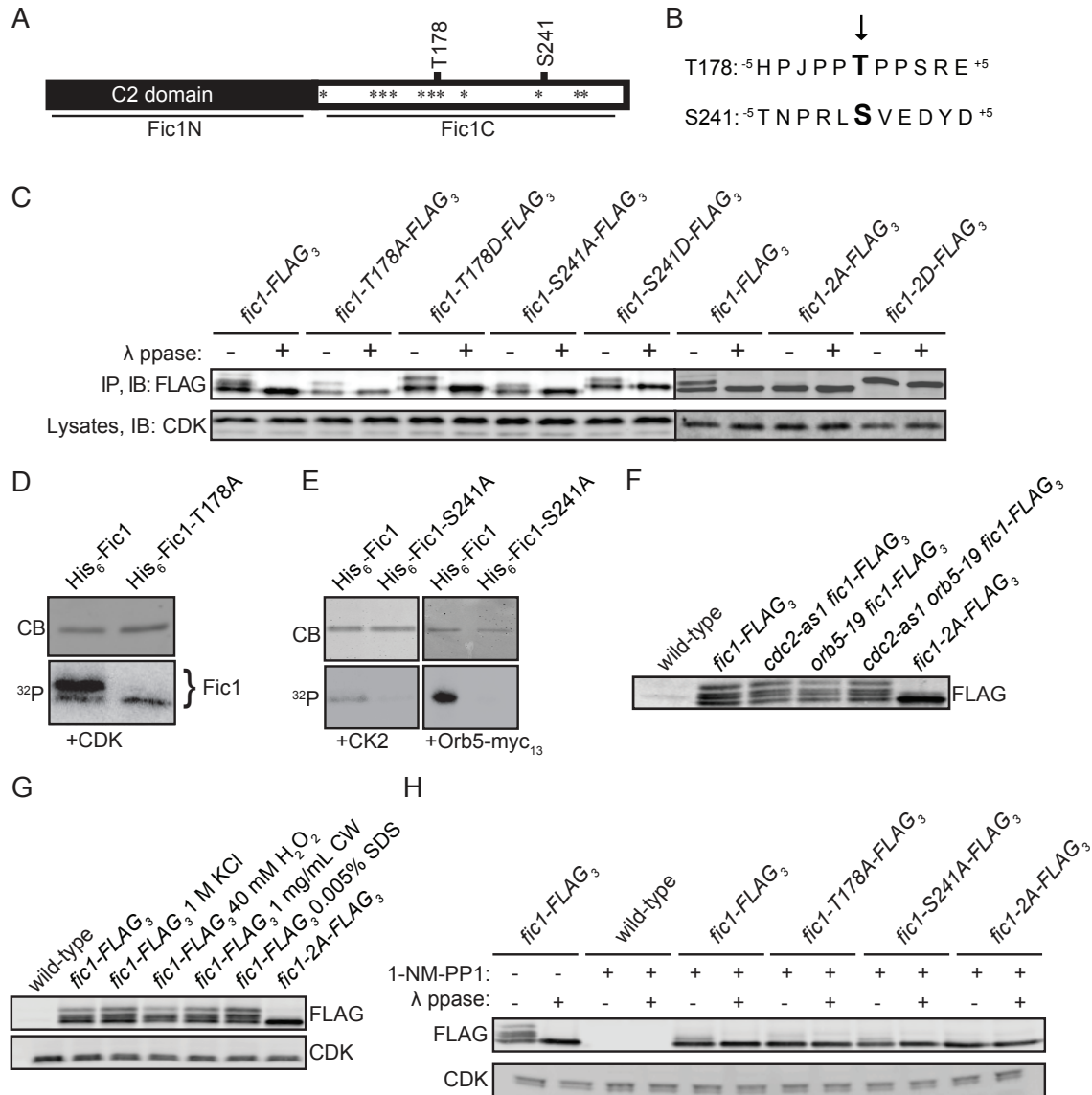


Figure 2.4. Identification of Fic1 phosphorylation sites and potential kinases. A) Schematic of Fic1. PxxP motifs (*), and phosphosites (labeled above) are indicated. B) Schematic of Fic1 phosphosites. The phosphorylated residues are in bold text and marked by an arrow. C) Anti-FLAG immunoprecipitates from asynchronous cells producing the indicated Fic1 proteins were either treated with lambda phosphatase or vehicle and subsequently blotted with an anti-FLAG antibody. Lysate samples were blotted with anti-CDK (PSTAIRE) as a control for input into the immunoprecipitation. D) CDK *in vitro* kinase assay using His₆-Fic1 and His₆-Fic1-T178A. E) CK2 *in vitro* kinase assay using His₆-Fic1 and His₆-Fic1-S241A. D and E) Protein labeled by ATP-γ-³²P was detected by autoradiography, and the gel was stained with Coomassie blue as a loading control. F) Lysates from cells of the indicated genotypes were immunoblotted with anti-FLAG antibody to assess Fic1-FLAG₃ gel mobilities. For *orb5-19* strains, cells were shifted to 36°C for 4 hours prior to lysis. For *cdc2-as1* strains, cells were treated with 1 μM of 1-NM-PP1 for 30 min prior to lysis. G) Lysates from cells of the indicated

genotypes were immunoblotted with anti-FLAG antibody to assess Fic1-FLAG₃ gel mobilities after 60 minutes in 1 M KCl, 1 mg/mL calcofluor white, or 0.005% SDS or 15 minutes in 40 mM H₂O₂. Lysates were immunoblotted with anti-CDK (PSTAIRE) as a loading control. H) Anti-FLAG immunoprecipitates from cells of indicated genotypes were treated with 50 μM of 1-NM-PP1 for 30 minutes before treatment with lambda phosphatase or vehicle and subsequently blotted with an anti-FLAG antibody. Lysate samples were blotted with anti-CDK (PSTAIRE) as a control for input into the immunoprecipitation.

2.5 Multiple kinases modulate polarity-relevant Fic1 phosphorylation

Because phosphorylation occurs in Fic1C that is important for polarity establishment, we set out to identify the kinase(s) responsible. T178 and S241 fit the consensus sequences for cyclin-dependent kinase (CDK) (S/T-P) and casein kinase II (CK2) (S-X-X-E/D), respectively (Fig. 2.4B) (Meggio et al., 1994; Nigg, 1993), and these kinases are important for polarized growth (Adams et al., 1990; McCusker et al., 2007; Rethinaswamy et al., 1998; Shimada et al., 2000; Snell and Nurse, 1994). *In vitro* kinase assays using Cdk1-cyclinB, *S. pombe* CK2 (Orb5), or human CK2 with His₆-Fic1, His₆-Fic1-T178A, and/or His₆-Fic1-S241A revealed that they can phosphorylate the sites that fit their consensus sequence (Fig. 2.4D and E). His₆-Fic1-T178A phosphorylation by Cdk1 was significantly reduced compared to His₆-Fic1, demonstrating that *in vitro* Cdk1 primarily targets T178 (Fig. 2.4D). To test if Cdk1 and Orb5 phosphorylate Fic1 *in vivo*, we assayed Fic1 phosphostatus in analog-sensitive and temperature-sensitive mutants of these kinases. Fic1's phosphostate was unaltered in these single and double mutants (Fig. 2.4F). Thus, Cdk1 and Orb5 are not solely responsible for Fic1 phosphorylation *in vivo*.

We next took an unbiased approach to try to identify the kinase(s) responsible for Fic1 phosphorylation. Starting with polarity kinases, then extending to all kinases, we screened gene deletions of individual non-essential kinases, temperature or analogue-sensitive mutants of essential protein kinase genes, and combination mutants of paralogs (e.g. *pck1-as pck2-as*) for changes to Fic1's phosphostate (Bimbo et al., 2005; Chen et al., 2014; Cipak et al., 2011; Gregan et al., 2007; Kim et al., 2010). In the course of this screening, we determined that several kinase deletion strains in Bioneer V3 (Kim et al., 2010) contained not only a targeted deletion allele but also the wild-type kinase gene. Thus, we constructed new deletion mutants of *atg1*, *hal4*, *lsk1*, *mak2*,

mek1, *sty1*, *ppk24*, *ppk34*, and *wis1*. By immunoblotting, we did not detect loss of either Fic1 phosphorylation event in any of the 111 single or 11 combination kinase mutants tested (Figs. 2.5 and 2.6), indicating that multiple kinases can phosphorylate Fic1.

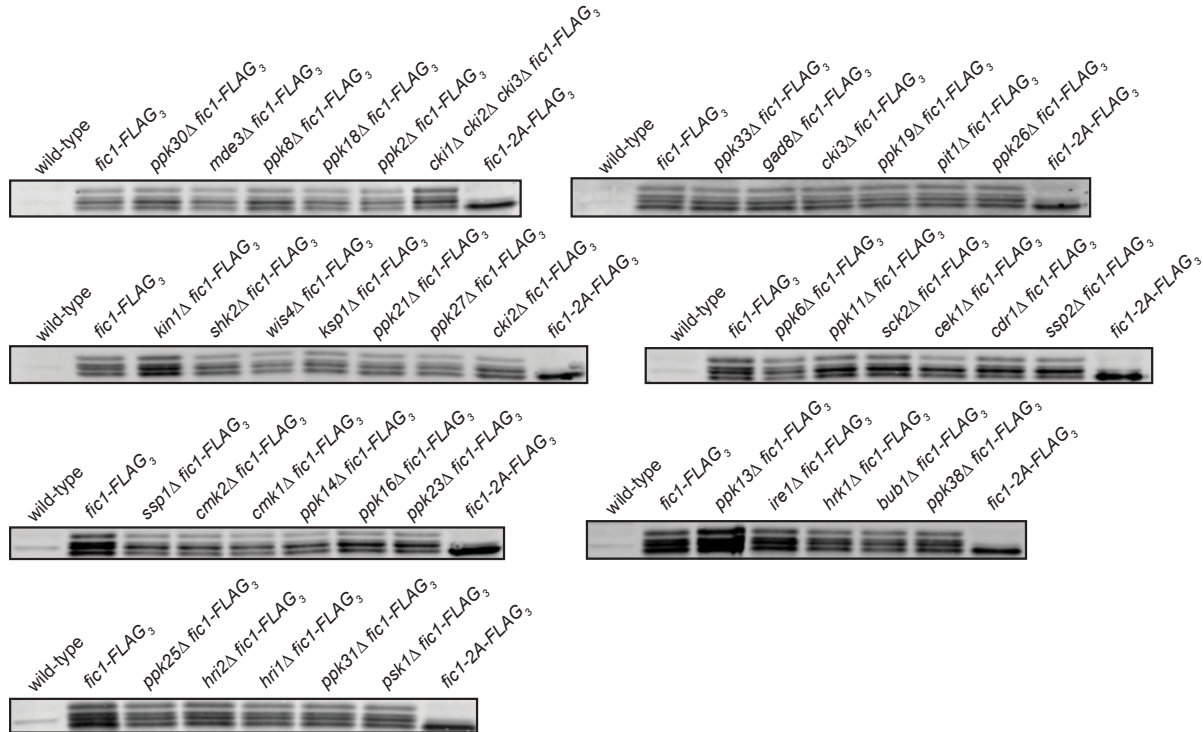


Figure 2.5. No single kinase associated with cell growth polarity regulates Fic1's phosphorylation state. Lysates from asynchronous cells of the indicated strains producing Fic1-FLAG₃ were immunoblotted for FLAG. In each panel, an untagged strain, a tagged strain with no kinase deletions, and Fic1-2A-FLAG₃ served as controls.

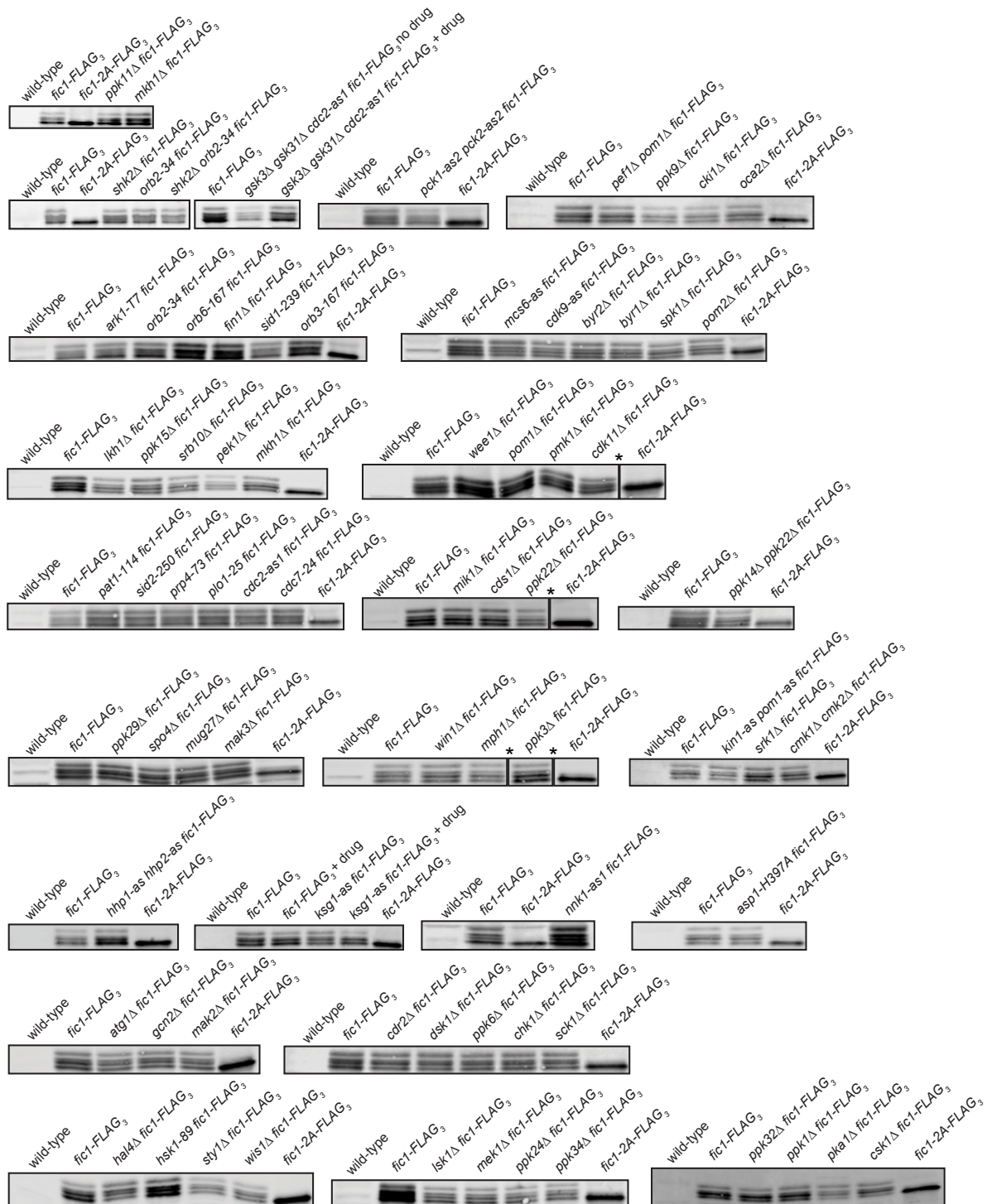


Figure 2.6. Fic1 phosphorylation is regulated by multiple kinases. Lysates from asynchronous cells of the indicated strains producing Fic1-FLAG₃ were immunoblotted for FLAG. In each panel, an untagged strain, a tagged strain with no kinase deletions, and Fic1-2A-FLAG₃ served as controls. For temperature-sensitive kinase strains, cells were shifted to 36°C from 2 to 4 hours prior to lysis. For analog-sensitive strains, cells

were treated with either 1-NM-PP1 (1 μ M *cdc2-as1*, 25 μ M *hhp1-as*, 25 μ M *hhp2-as*), 3-BrB-PP1 (30 μ M *pck1-as2*, 30 μ M *pck2-as2*, 30 μ M *mcs6-as*), or 3-MB-PP1 (40 μ M *cdk9-as*, 30 μ M *ksg1-as*, 15 μ M *kin1-as*, 15 μ M *pom1-as*) for 30 min prior to lysis. Four asterisks (*) indicate where 4 lanes were cropped out of gel images.

We next tried to identify pathways regulating Fic1 phosphostate. To this end, we treated cells with osmotic, oxidative, cell wall integrity, and plasma membrane stressors (Cadou et al., 2010; Chen et al., 2008b; Madrid et al., 2006; Robertson and Hagan, 2008). None of the stressors tested evoked a change in Fic1's phosphostate (Fig. 2.4G). However, phosphorylation at S241 but not T178 was lost after treatment with a high dose of 1-NM-PP1 (Fig. 2.4H). 1-NM-PP1 is an inhibitor designed to preferentially target kinases with space-creating mutations in their ATP-binding pocket. However, some kinase families such as Src, CDK, and CAMKII, are sensitive to high levels of 1-NM-PP1 (Bishop et al., 2000). Loss of phosphorylation at S241 but not T178 suggests that distinct groups of kinases phosphorylate each site, one of which can be inhibited by high levels of 1-NM-PP1. Collectively, these data establish that Fic1 phosphoregulation involves multiple kinases that are apparently coordinated to keep the ratios of Fic1 phosphorylation events similar throughout the cell cycle and under different physiological conditions.

2.6 Fic1 phosphorylation does not affect CR localization or interaction with known CR binding partners

To assess whether disrupting Fic1's phosphorylation state altered its localization, we analyzed the fluorescence intensities of mNeonGreen tagged Fic1 variants at the CR and cell tips. We observed no differences between Fic1 and the Fic1 phosphomutants (Fig. 2.7A and B). Next, we performed time-lapse imaging to determine if Fic1 CR recruitment timing relative to spindle pole body (SPB) separation differed for either phosphomutant. Fic1, Fic1-2A, and Fic1-2D were recruited to the CR with similar timing (Fig. 2.7C).

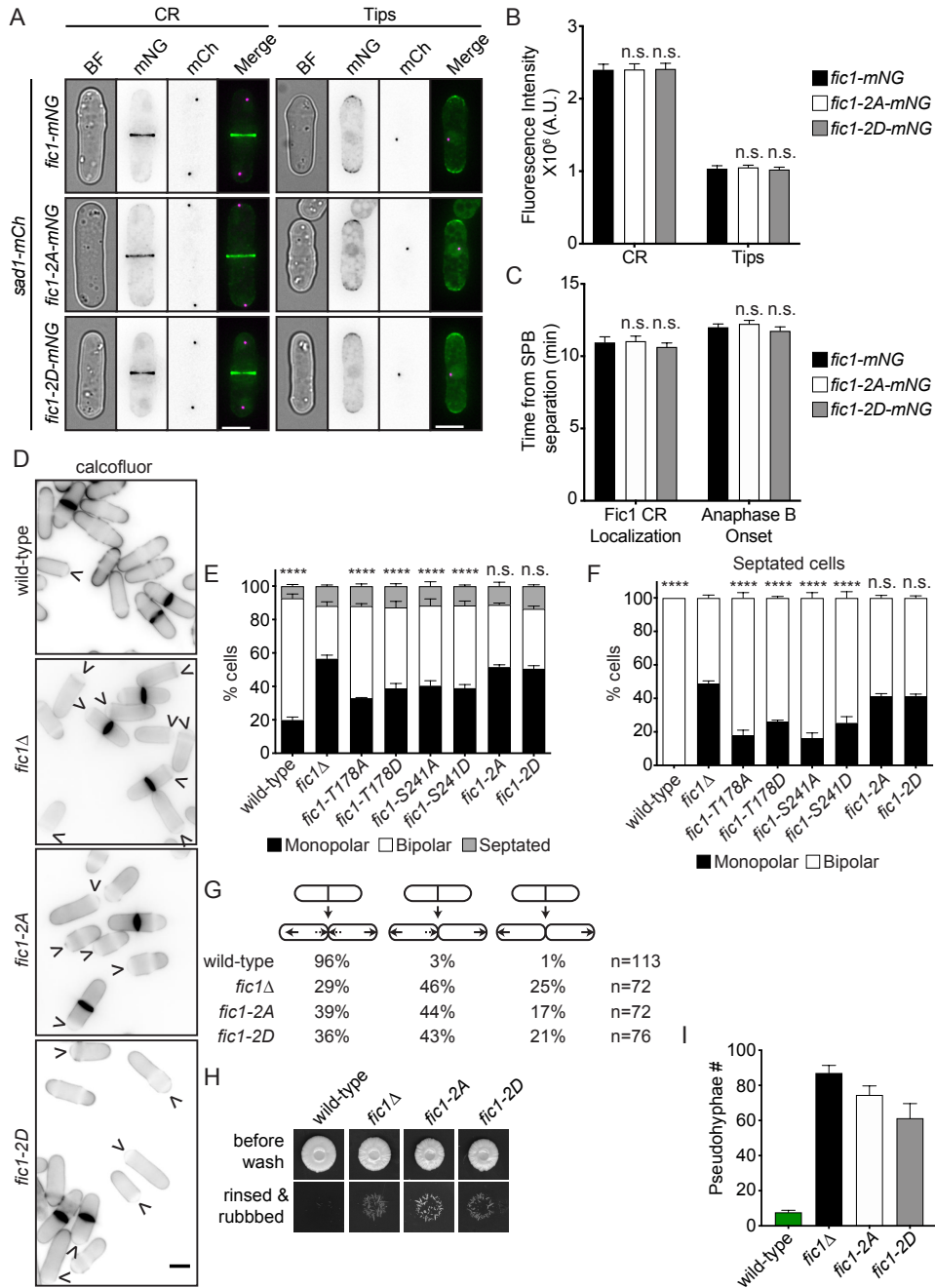


Figure 2.7. Deregulation of Fic1 phosphorylation at T178 and S241 impairs new end growth. A) BF, GFP, mCh, and merged GFP/mCh images of cells of indicated genotypes during cytokinesis and interphase. Scale bars, 5 μ m. B) Quantification of fluorescence intensities of CR and cell tips for cells of indicated genotypes. Data from three trials per genotype with $n=15$ for each trial are presented as mean \pm SEM. C) Quantification from time-lapse imaging for cells of indicated genotypes. Data from two trials $n=25$ are presented as mean \pm SEM. B) and C) Analyzed by ANOVA. D) Live-cell images of calcofluor-stained cells of the indicated genotypes. Arrowheads indicate monopolar cells. E) and F) Quantification of growth polarity phenotypes for cells (E) and

septated cells (F) of the indicated genotypes. Data from three trials per genotype with $n > 200$ for each trial are presented as mean \pm SEM. E) and F) The percent of monopolar cells between *fic1* Δ and each other genotype was analyzed by ANOVA Dunnett's multiple-comparisons test. **** $P < 0.0001$, n.s., not significant. G) Quantification of growth patterns for cells of the indicated genotypes. H) Invasive growth assays for strains of the indicated genotypes on 2% agar. Cells were spotted on rich medium and incubated for 20 days at 29°C (top panel). Colonies were then rinsed under a stream of water and rubbed off (bottom panel). I) Quantification of pseudohyphae for cells of the indicated genotypes, with $n \geq 3$ spots counted for each genotype.

Fic1 localizes to the CR via its interaction with the SH3 domains of the F-BAR proteins, Cdc15 and Imp2 (Roberts-Galbraith et al., 2009; Ren et al., 2015). Because one Fic1 phosphosite (S241) is proximal to the P254-P257 PxxP motif required for these SH3 domain interactions (Bohnert and Gould, 2012), we tested if phosphorylation interferes with Cdc15 and Imp2 binding. Consistent with normal CR recruitment, both Fic1 phosphomutants co-immunoprecipitated with Cdc15 and Imp2 (Fig. 2.8A), indicating that deregulation of Fic1 phosphorylation does not grossly alter these known interactions.

2.7 Disruption of Fic1 phosphorylation impacts bipolar cell growth and promotes pseudohyphal growth

To assess the relevance of Fic1 phosphorylation to NETO, we analyzed the growth polarity of the phosphomutants (Fig. 2.7D). *fic1-2A* and *fic1-2D* had similar levels of monopolar cells as *fic1* Δ , while each individual phosphomutant displayed levels intermediate between *wildtype* and *fic1* Δ (Fig. 2.7D-F). Also, as expected given that wild-type cells commonly initiate NETO by late interphase, nearly all *fic1*⁺ cells arrested in late G2 exhibited bipolar growth (Fig. 2.8B and C). In contrast, a high percentage of *cdc25-22 fic1-2A* and *cdc25-22 fic1-2D* were still monopolar like *cdc25-22 fic1* Δ (Fig. 2.8B and C). Using time-lapse DIC imaging, we confirmed that the polarized growth defects in *fic1* Δ , *fic1-2A*, and *fic1-2D* were specific to new ends (Figs 2.7G and 2.8D). Although the phosphomutants did not support proper NETO, they retain some function because they are not synthetically lethal with *pxl1* Δ , *ppb1* Δ , or *sid2-250* like *fic1* Δ (Bohnert and Gould, 2012) (Fig. 2.8E), possibly because they can still associate with Cdc15 and Imp2 (Fig. 2.8A). Considering our results together, we hypothesize that

phosphorylation affects Fic1's interaction with an unknown factor(s) at the CR that influences its CR function.

Inability to support proper NETO is exhibited by *S. pombe* and *S. japonicus* cells that have undergone the dimorphic switch from single-celled to pseudohyphal growth (Dodgson et al., 2010; Sipiczki et al., 1998), and *fic1* Δ cells show increased invasive pseudohyphal growth compared to wild-type (Figs 2.7H and I, and 2.8F) (Bohnert and Gould, 2012). Consistent with *fic1* phosphomutants possessing growth polarity defects akin to *fic1* Δ , *fic1-2A* and *fic1-2D* formed pseudohyphal structures invading the agar (Figs 2.7H and 2.8F and G). Also, each individual Fic1 aspartate mutant was more invasive than wild-type (Fig. 2.8F). Thus, the dimorphic switch from single-celled to pseudohyphal form may involve Fic1 phosphoregulation.

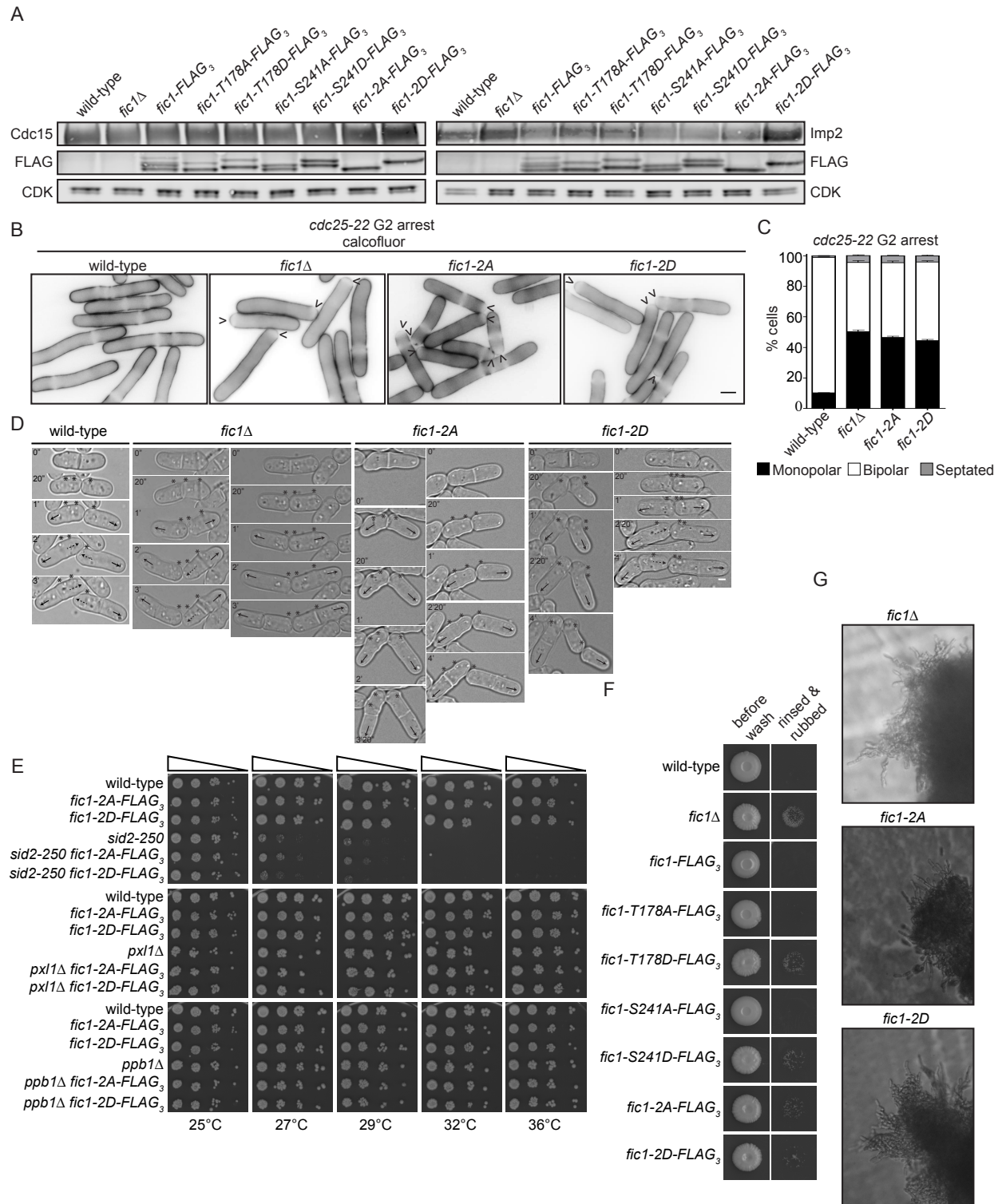


Figure 2.8. Fic1 phospho-mutants do not alter Fic1's interactions with Cdc15 or Imp2 A) Anti-Cdc15 or anti-Imp2 immunoprecipitates from cells of indicated genotypes were blotted with an anti-FLAG, anti-Cdc15, or anti-Imp2 antibody. Lysate samples were blotted with anti-CDK (PSTAIRE) as a control for input into the immunoprecipitations. B) Live-cell images of G2-arrested, calcofluor-stained cells of the

indicated genotypes. Arrowheads indicate monopolar cells. Scale bar, 5 μm . C) Quantification of growth polarity phenotypes for G2-arrested cells of the indicated genotypes. Data from three trials per genotypes and $n > 200$ for each trial are presented as mean \pm SEM. D) Live-cell DIC movies of cells of the indicated genotypes. Solid arrows denote old end growth, whereas dashed arrows indicate new end growth. Birth scars are marked by asterisks. Time points are noted. Scale bar, 2 μm . E) Serial 1:10 dilutions of the indicated genotypes were spotted onto rich medium and incubated at the indicated temperatures. F) Invasive growth assays for strains of the indicated genotypes on 2% agar. Cells were spotted on rich medium and incubated for 20 days at 29°C (left panel). Colonies were then rinsed under a stream of water and rubbed off (right panel). G) Images of pseudohyphae for the genotypes indicated.

In conclusion, though phosphorylation serves diverse roles during eukaryotic cytokinesis (Bohnert and Gould, 2011), it has been unclear whether CR protein phosphorylation impacts cellular processes other than cell division. In this study, we found that Fic1 phosphorylation influences polarity and the transition to hyphal growth. Our findings support the ideas that (1) regulating CR function can directly impact the dimorphic switch; and (2) modulation of kinase and/or phosphatase signaling may be sufficient for this switch. As extensive phosphosignaling occurs during hyphal growth (Sudbery, 2011), integration of multiple cues likely guarantees the robustness of this transition.

2.8 Materials and Methods

Yeast methods

S. pombe strains (Table S1) were grown in yeast extract (YE) media or Edinburgh minimal media with relevant supplements. Genes were tagged at the 3' end of their ORFs with sequences encoding GFP:kan^R, HA₃:hyg^R, FLAG₃:kan^R, or FLAG₃:hyg^R using pFA6 cassettes as previously described (Bahler et al., 1998b; Wach et al., 1994). A lithium acetate method (Keeney and Boeke, 1994) was used in *S. pombe* tagging transformations, and integration of tags was verified using whole-cell PCR and/or microscopy. Introduction of tagged loci into other genetic backgrounds was accomplished using standard *S. pombe* mating, sporulation, and tetrad dissection techniques. For arresting *cdc25-22* and *cps1-191*, cells were grown at 25°C and then shifted to 36°C for 3 h. *nda3-KM311* arrest was achieved by growing cells at 32°C and

then shifting to 18°C for 6.5 h. For blocking of *cdc10-V50*, cells were grown at 25°C and then shifted to 36°C for 4 h. S-phase arrest was achieved by treating cells with 12 mM hydroxyurea for 4 h at 32°C.

Mutants and truncations of *fic1* were expressed from the endogenous *fic1*⁺ locus. To make these strains, a pIRT2 vector was used in which *fic1*⁺ gDNA with 5' and 3' flanks was inserted between BamHI and PstI sites of pIRT2 (Bohnert and Gould, 2012). Mutations were then introduced via site-directed mutagenesis and confirmed by DNA sequencing. *fic1*Δ was transformed with these pIRT2-*fic1* constructs, and stable integrants resistant to 1.5 g/L 5-fluoroorotic acid (5-FOA) were isolated and confirmed by whole-cell PCR, DNA sequencing, and immunoblotting.

To construct analog-sensitive protein kinase strains, the coding sequences with 5' and 3' flanks of *pck1*⁺, *pck2*⁺ and *nnk1*⁺ were PCR amplified from *S. pombe* genomic DNA using PrimeSTAR GXL DNA polymerase (Takara) and ligated into the pCR-Blunt II-TOPO® vector (Invitrogen). The resulting inserts were verified by sequencing. The gate-keeper residues in Pck1 and Pck2 kinases were identified as M744 and M763, respectively, and in Nnk1 kinase as M537 (Gregan et al., 2007). These residues were mutated to glycine or alanine using mutagenic oligonucleotide primers and QuikChange II site-directed mutagenesis kit (Stratagene). The desired mutations were verified by sequencing. Next the *pck1*- and *pck2*-containing plasmids were linearized and transformed into *pck1::ura4*⁺ and *pck2::ura4*⁺ cells, respectively, and the plasmids containing *nnk1*-as mutations were transformed into *nnk1::ura4*⁺-*HA₃-TAP:kan^R* *P_{nmt41}*-*GBP-mCherry-nnk1-leu1*⁺, using a lithium acetate method (Keeney and Boeke, 1994). Transformants were selected based on resistance to 5-FOA and then confirmed first by colony PCR and then by DNA sequencing. Next, the allele *P_{nmt41}*-*GBP-mCherry-nnk1-leu1*⁺ was crossed out to obtain *nnk1(M537G)-HA₃-TAP:kan^R* and *nnk1(M537A)-HA₃-TAP:kan^R*.

For serial-dilution growth assays, cells were grown in liquid YE at 32°C, three serial 1:10 dilutions starting at 4 x 10⁶ were created, 2 μL of each dilution was spotted on YE agar and cells were grown at the indicated temperatures for 3-5 d.

Protein methods

Cells were lysed by bead disruption in NP40 lysis buffer in denaturing conditions as previously described (Gould et al., 1991), except with the addition of 0.5 mM diisopropyl fluorophosphate (Sigma-Aldrich). Immunoblot analysis of cell lysates and immunoprecipitates was performed using anti-FLAG (M2; Sigma-Aldrich) or anti-PSTAIRE Cdc2 (Sigma-Aldrich) antibodies or serums raised against GST-Cdc15 (VU326) (Roberts-Galbraith et al., 2009) or His₆-Imp2 (VU483) (McDonald et al., 2016) as previously described (Bohnert et al., 2009). For gel shifts, denatured samples were treated with lambda-phosphatase (New England Biolabs) in 25 mM HEPES-NaOH (pH 7.4), 150 mM NaCl, and 1 mM MnCl₂ and incubated for 30 min at 30°C with shaking.

In vitro kinase assays with kinase-active Cdk1 were performed as described by (Yoon et al., 2006) using a kinase buffer consisting of 50 mM Tris-HCl, pH 7.4, 10 mM MgCl₂, and 2 mM DTT supplemented with 10 μM cold ATP and 5 μCi γ-[³²P]ATP. Reactions contained 100 ng of kinase-active Cdk1 and 1 μg of recombinant His₆-Fic1, His₆-Fic1-T178A, or His₆-Fic1-S241A. The addition of sample buffer and boiling terminated the reactions. Samples of each reaction were separated by SDS-PAGE and visualized by Coomassie blue staining and autoradiography.

Microscopy

Live-cell images of *S. pombe* were acquired using one of the following: (1) a spinning disc confocal microscope (Ultraview LCI, PerkinElmer) equipped with a 100× NA 1.40 PlanApo oil immersion objective, a 488-nm argon ion laser (GFP), a 594-nm helium neon laser (mCherry), a charge-coupled device camera (Orca-ER, Hamamatsu Phototronics), and Metamorph 7.1 software (MDS Analytical Technologies and Molecular Devices) or (2) a personal DeltaVision microscope system (Applied Precision) that includes an Olympus IX71 microscope, 60× NA 1.42 PlanApo and 100× NA 1.40 UPlanSApo objectives, a Photometrics CoolSnap HQ2 camera, and softWoRx imaging software. All cells were in log phase growth before temperature-sensitive shifts and/or live imaging.

For calcofluor staining, cells were washed in PBS and then resuspended in PBS containing 5 μg/mL calcofluor. After incubation on ice for 30 min, cells were washed three times in PBS and images were acquired. Using the proximity of birth scars to cell ends, growth/morphology was scored as one of the following: monopolar (i.e., growth on

one end), bipolar (i.e., growth on both ends), monopolar and septated, bipolar and septated, or multiseptated. For cells just completing division, daughter cells were scored as monopolar as long as ingression of the mother cell had progressed to such a degree that birth scars could be easily identified at new ends. All cells stained with calcofluor were grown to log phase at 25°C, except that *cdc25-22* mutants were grown overnight at 25°C and then shifted to 36°C for 3 h before staining.

Intensity measurements were made with ImageJ software (Schindelin et al., 2012) using non-deconvolved summed Z projections of the images. For all intensity measurements, the background was subtracted by creating a region of interest (ROI) in the same image in an area clear of cells. The background raw intensity was divided by the area of the background, which was multiplied by the area of the ROI. This number was subtracted from the raw integrated intensity of that ROI. To account for autofluorescence, cells lacking fluorescent tags but otherwise of isogenic backgrounds, were imaged and fluorescence intensity per pixel was quantified from summed Z projections of the images by subtracting the background intensity from the measured raw integrated intensity of the ROI before dividing the raw integrated intensity of the ROI by the area of that ROI. This autofluorescence per pixel measurement was multiplied by the area of the ROI from fluorescent cells before subtracting this value from the raw integrated intensity of that ROI. Representative images are max intensity Z projections.

Time-lapse imaging was performed using an ONIX microfluidics perfusion system (CellASIC ONIX; EMD Millipore). A suspension of 50 μ l of 40×10^6 cells/ml YE was loaded into Y04C plates for 5 s at 8 psi. YE media was flowed through the chamber at 5 psi throughout imaging.

Images of yeast cells and pseudohyphae on YE agar plates were acquired by focusing a camera (PowerShot SD750; Canon) through a microscope (Universal; Carl Zeiss) equipped with a 20X NA 0.32 objective.

Invasive growth assays

To assay pseudohyphal invasion into 2% agar, 5 μ l containing a total of 10^5 cells were spotted on 2% YE agar and incubated at 29°C for 20 days. Colonies were subsequently placed under a steady stream of water and surface growth was wiped off

using a paper towel, as described previously (Pohlmann and Fleig, 2010; Prevorovsky et al., 2009).

Chapter 3

The fission yeast cytokinetic ring component Fic1 promotes septum formation

This chapter is adapted from “The fission yeast cytokinetic ring component Fic1 promotes septum formation” published in *Biology Open* doi: 10.1242/bio.059957 and has been reproduced with the permission of my publisher and co-authors: K. Adam Bohnert and Kathleen L. Gould

3.1 Introduction

Cytokinesis is the final process in the cell cycle which creates two independent daughter cells. Many eukaryotic organisms use an actin-myosin structure known as the cytokinetic ring (CR) to mark the plane of cell division and to drive membrane ingression (reviewed in (Cheffings et al., 2016; Mangione and Gould, 2019)). In organisms with cell walls, such as *Schizosaccharomyces pombe* and *Saccharomyces cerevisiae*, the CR alone is insufficient for cytokinesis (Jochova et al., 1991; Munoz et al., 2013; Proctor et al., 2012; Ramos et al., 2019; Schmidt et al., 2002). These organisms require the formation of a septum coupled to CR constriction to drive cell abscission (Cortes et al., 2007; Cortes et al., 2015; Jochova et al., 1991; Proctor et al., 2012; Schmidt et al., 2002).

Yeast septa are trilaminar structures composed of a primary septum flanked by secondary septa (Humbel et al., 2001; Wloka and Bi, 2012). In *S. pombe* and *S. cerevisiae*, CR constriction promotes septation perpendicular to the cell cortex (Cortes et al., 2002; Cortes et al., 2007; Johnson et al., 1973; Roncero et al., 2016; Schmidt et al., 2002). In *S. cerevisiae* the chitin synthase Chs2 polymerizes N-acetylglucosamine to form the primary septum (Sburlati and Cabib, 1986; Shaw et al., 1991; Silverman et al., 1988). In contrast, in *S. pombe* it is the glucan synthases Bgs1 and Ags1 that

polymerize linear- β (1,3)glucans and α (1,3)glucans, respectively, to form the primary septum (Cortes et al., 2002; Cortes et al., 2007; Cortes et al., 2015; Cortes et al., 2012).

S. cerevisiae Chs2 and septum formation are stimulated by a protein complex within the CR named the ingression progression complex (IPC), comprised of the ingression protein Inn1, the F-BAR protein Hof1, and Cyk3 (Devrekanli et al., 2012; Nishihama et al., 2009; Sanchez-Diaz et al., 2008). Analogous proteins exist in *S. pombe*. Specifically, *S. pombe* Fic1, Cdc15/Imp2, and Cyk3 are the orthologs of Inn1, Hof1, and Cyk3, respectively (Demeter and Sazer, 1998; Fankhauser et al., 1995; Pollard et al., 2012; Roberts-Galbraith et al., 2009). Fic1 was identified in a yeast-two hybrid screen using the SH3 domains of Cdc15 as bait and directly interacts with Cdc15 and Imp2 (Ren et al., 2015; Roberts-Galbraith et al., 2009). *S. pombe* Cyk3 was identified based on sequence similarity to *S. cerevisiae* Cyk3 and has been found to co-immunoprecipitate with Fic1 (Bohnert and Gould, 2012; Roberts-Galbraith et al., 2009). However, it is unknown if these *S. pombe* proteins cooperate to promote primary septum formation similarly to the IPC.

We previously found that Fic1 is phosphorylated on two sites by multiple kinases (Bohnert et al., 2020). Preventing phosphorylation at these sites produces defects in the establishment of normal cell polarity. Here, we pursued the observation that the *fic1* phospho-ablating mutant, *fic1-2A*, also suppressed the *myo2-E1* temperature-sensitive allele of the essential type-II myosin Myo2 (Balasubramanian et al., 1998; Kitayama et al., 1997). The inability of *myo2-E1* cells to form a functional CR to guide septum formation prevents cytokinesis and leads to cell death (Balasubramanian et al., 1998). Time-lapse microscopy showed that *fic1-2A* suppressed *myo2-E1* by promoting septum formation and daughter cell abscission and that cells lacking *fic1* exhibited significant delays in septation. We determined that the ability of *fic1-2A* to suppress *myo2-E1* required its interactions with Cyk3, Cdc15, and/or Imp2 but not Chs2. This work revealed that *S. pombe*'s IPC analogs interact to promote septum formation through a mechanism that is functionally divergent from the IPC in *S. cerevisiae*

3.2 Fic1 phospho-ablating mutant suppresses *myo2-E1*

To determine if Fic1's phosphorylation state impacts cytokinesis, we took a genetic approach and probed interactions between *fic1* phosphomutants and deletions or temperature-sensitive alleles of genes involved in actin dynamics (*cdc12*), septum formation (*sid2*, *bgs1*, and *bgs4*), and CR constriction (*cdc4* and *myo2*) (Fig. 3.1A).

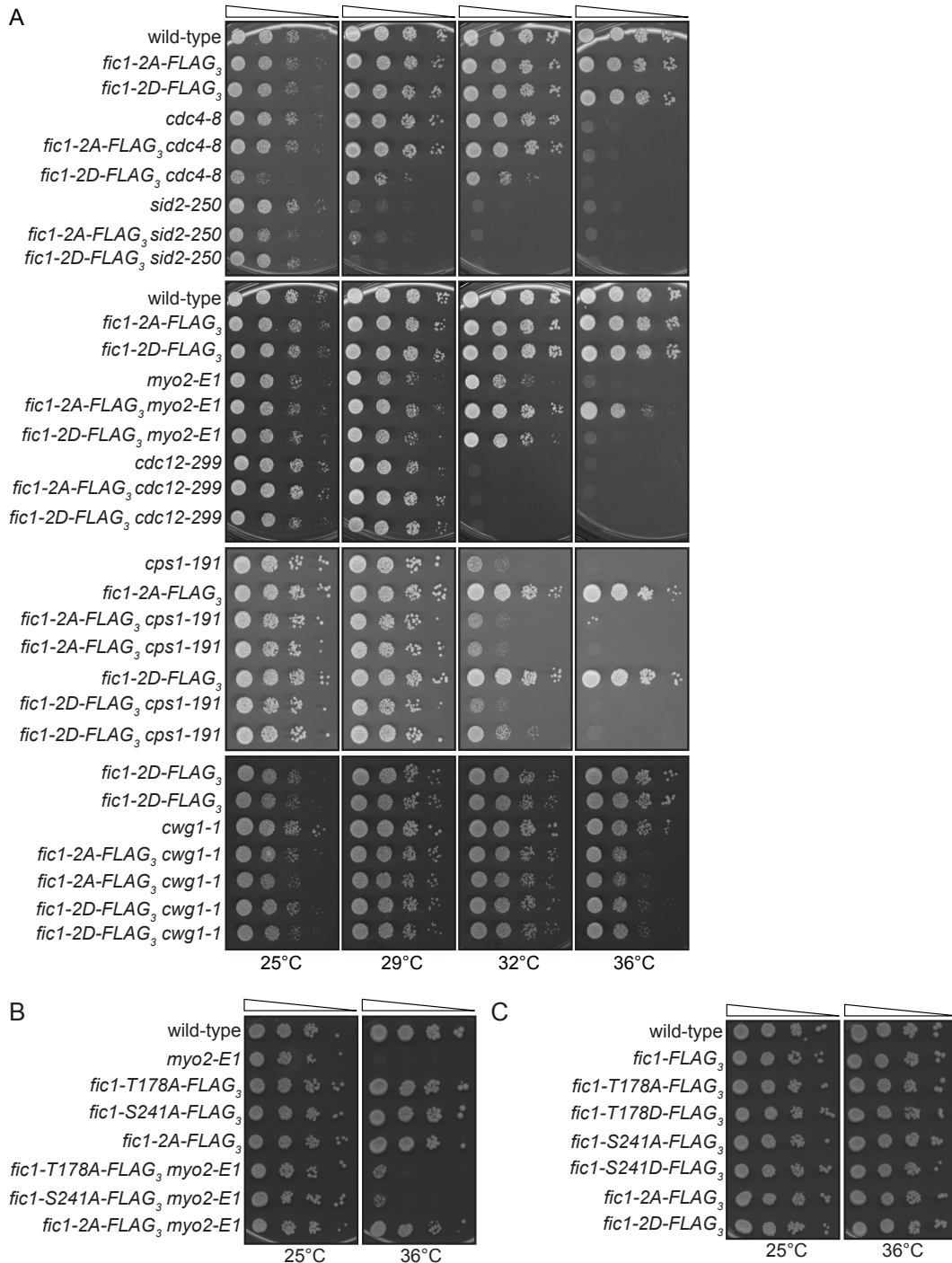


Figure 3.1. Individual or single *fic1* phosphomutants are not temperature-sensitive. A-C) Ten-fold serial dilutions of the indicated strains were spotted on YE agar media and incubated at the indicated temperatures for 3-5 days.

From this screen we observed one significant interaction: *fic1*'s phospho-ablating mutant, *fic1-2A*, suppressed *myo2-E1* (Fig. 3.2A and B and 3.1A). *myo2-E1* is a temperature-sensitive allele of the essential type-II myosin, *myo2*, that inhibits Myo2's activity and produces non-constricting CRs at the restrictive temperature (Balasubramanian et al., 1998; Palani et al., 2017; Palani et al., 2018).

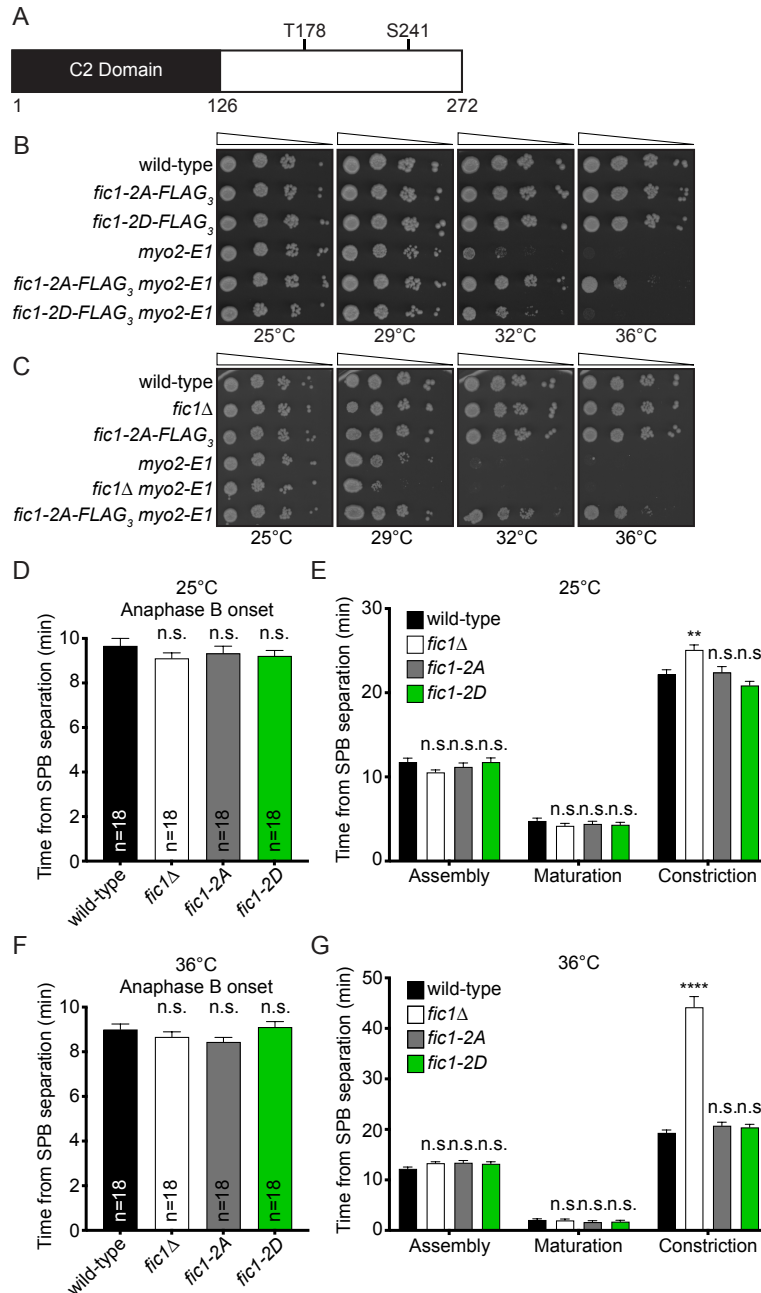


Figure 3.2. *fic1-2A* suppresses *myo2-E1*. A) Schematic of Fic1 with domain boundaries and phosphorylation sites indicated. Drawn to scale. B and C) Ten-fold serial dilutions of the indicated strains were spotted on YE agar media and incubated at the indicated temperatures for 3-5 days. D-G) Quantification of timing of anaphase B (D and F) and CR assembly, maturation, and constriction (E and G) for each strain at the indicated temperatures. n=number of cells analyzed. Data presented as mean \pm S.E.M. **** $p \leq 0.0001$, ** $p \leq 0.01$, n.s., not significant, one-way ANOVA.

Without CR constriction, cell wall accumulates at the division site but does not form a septum (Balasubramanian et al., 1998; Palani et al., 2017; Palani et al., 2018; Ramos et al., 2019). Interestingly, *fic1* Δ did not suppress *myo2-E1* and no genetic interaction was observed between *fic1-2D* and *myo2-E1* (Fig. 3.2B and C), which suggests *fic1-2A* is a gain-of-function allele but whether this gain in function is due to alterations to Fic1's phosphorylation state is unclear. The individual phospho-ablating *fic1* mutants only partially suppressed *myo2-E1* and none of the *fic1* phosphomutants were temperature sensitive (Fig. 3.1B and C). We then pursued the underlying mechanisms behind *myo2-E1*'s suppression to gain insight into the cytokinetic roles of Fic1, a CR protein of enigmatic function.

3.3 *fic1-2A* cells exhibit similar CR dynamics compared to wild-type cells

We postulated that *myo2-E1* suppression by *fic1-2A* could be achieved by altering CR dynamics. *fic1-2A* could provide additional time for proper glucan synthase localization by prolonging CR maturation and/or constriction. Glucan synthases are trafficked to the site of cell division and localize diffusely on the cortex (Cortes et al., 2002; Hoya et al., 2017; Katayama et al., 1999; Mulvihill et al., 2006; Ramos et al., 2019). As the CR constricts the glucan synthases coalesce into a ring concentric with the CR, Bgs1 is activated, and primary septum formation begins (Ramos et al., 2019). By providing additional time for glucan synthase ring formation by prolonging CR maturation and/or constriction *fic1-2A* could effectively promote septum formation. Alternatively, *fic1-2A* could increase the rate of CR constriction which could allow *fic1-2A* to suppress *myo2-E1* by restoring the contractile function of the CR and septum formation.

To test these possibilities, we performed live-cell time-lapse imaging at 25°C and 36°C of wild-type, *fic1* Δ , *fic1-2A*, and *fic1-2D* cells containing a CR marker, *rlc1-mNG*, to

monitor CR dynamics and a spindle pole body (SPB) marker, *sid4-GFP*, to monitor mitotic progression (Chang and Gould, 2000; Naqvi et al., 2000). The timing of anaphase B onset was similar between all strains at both temperatures (Fig. 3.2D,F), as was the timing of CR assembly and CR maturation (Fig. 3.2E,G). The timing of CR constriction was similar between wild-type, *fic1-2A*, and *fic1-2D* cells at both temperatures indicating that Fic1 phosphostate does not appreciably affect CR dynamics (Fig. 3.2E,G). However, *fic1Δ* took longer, an average of 25.1 ± 0.6 and 44.2 ± 2.1 minutes at 25°C and 36°C, respectively whereas wild-type cells took 22.2 ± 0.5 and 19.3 ± 0.6 minutes at 25°C and 36°C, respectively (Fig. 3.2E,G). Delayed CR constriction in *fic1Δ* but not *fic1-2A* suggests that prolonging CR constriction is not how *fic1-2A* suppresses *myo2-E1*. Rather, because the rate of CR constriction is linked to the rate of septum deposition (Proctor et al., 2012; Ramos et al., 2019), the delay in CR constriction of *fic1Δ* suggests that Fic1 promotes septation and that the *fic1-2A* allele may enhance this function.

3.4 *fic1-2A myo2-E1* cells can complete cytokinesis

We next probed this possibility for Fic1 function that would be analogous to Inn1 in *S. cerevisiae* (Sanchez-Diaz et al., 2008). We performed time-lapse imaging at 36°C with wild-type, *fic1-2A*, *myo2-E1*, and *fic1-2A myo2-E1* cells expressing the membrane marker LactC2-GFP, to monitor membrane ingression, and the SPB marker Sad1-GFP, to monitor mitotic progression (Curto et al., 2014; Hagan and Yanagida, 1995). The kinetics of septation were measured by timing membrane ingression and daughter cell abscission beginning from SPB separation at the onset of mitosis. The timing of anaphase B onset was similar between all genotypes (Fig. 3.3A and B). The initiation of membrane ingression was similar between wild-type and *fic1-2A* cells, averaging 14.9 ± 0.4 and 16.2 ± 0.3 minutes, respectively (Fig. 3.3A,C). However, both *myo2-E1* and *fic1-2A myo2-E1* cells exhibited delays in the initiation of membrane ingression compared to wild-type, averaging 28.4 ± 1.0 and 28.8 ± 1.9 minutes, respectively (Fig. 3.3A,C). Daughter cell separation was completed at similar times in the wild-type and *fic1-2A* cells, averaging 40.6 ± 0.6 and 43.1 ± 0.6 minutes, respectively (Fig. 3.3A,D). None of the *myo2-E1* daughter cells separated but 7 out of the 22 imaged *fic1-2A*

myo2-E1 daughter cells took an average time of 117.9 ± 20.2 minutes to separate (Fig. 3.3A,D). The ability of some *fic1-2A myo2-E1* cells to complete membrane ingression and abscission is consistent with idea that Fic1-2A enhances septum formation.

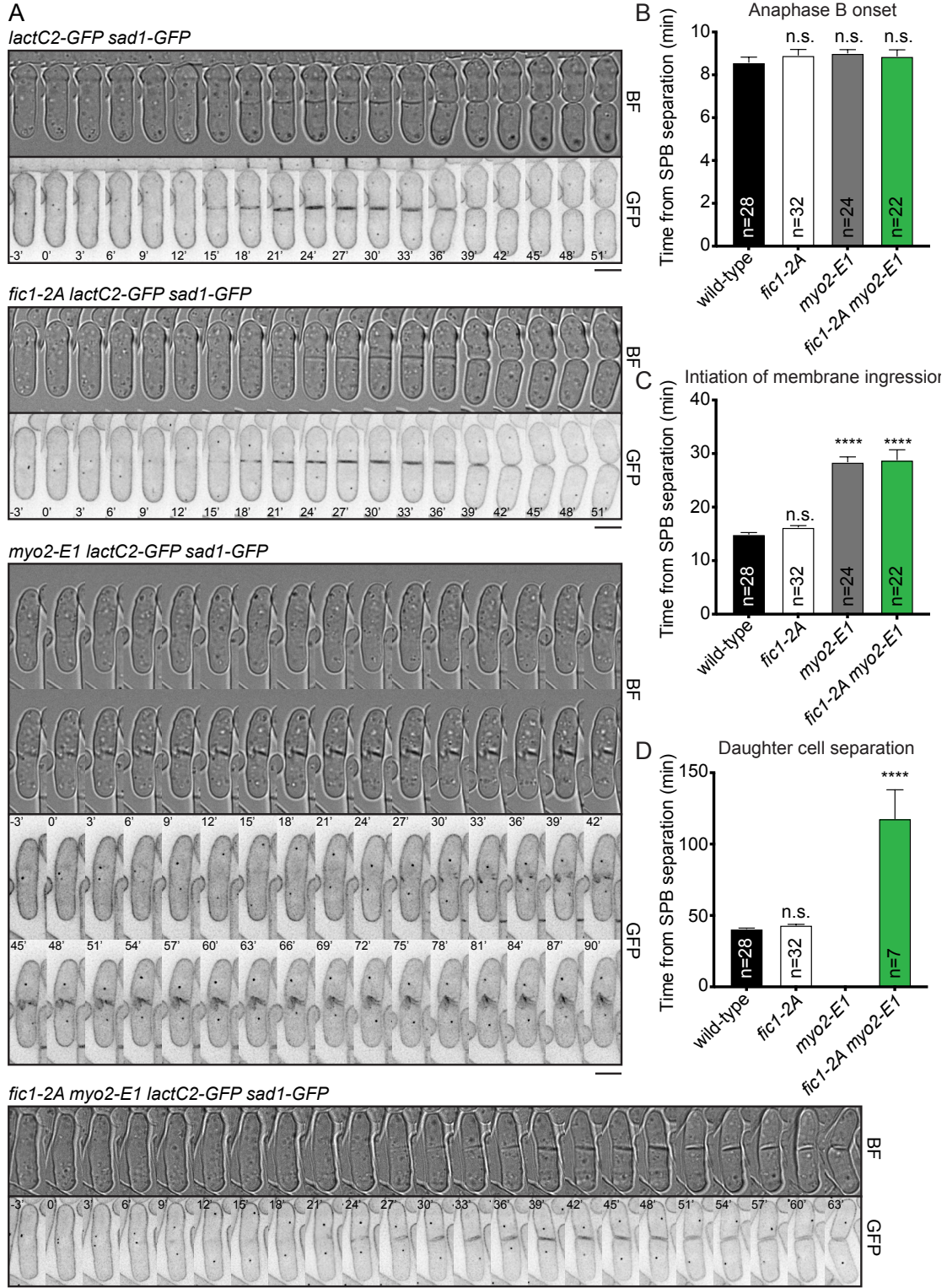


Figure 3.3. *fic1-2A myo2-E1* cells can achieve membrane ingression and cell separation at *myo2-E1*'s restrictive temperature. A) Representative images of live-cell time-lapse movies from the indicated strains at 36°C. Images were acquired every 3 minutes. Scale bar = 5 μ m. B-D) Quantification of timing of anaphase B (B), initiation of membrane ingression (C), and completion of daughter cell separation (D) for each strain. Anaphase B onset was defined as the period from the separation of the SPBs to the initiation of SPB segregation towards opposite cell poles. CR assembly was defined as the period from the separation of the SPBs to the coalescence of cytokinetic nodes into a ring. CR maturation was defined as the period from the completion CR assembly to the initiation of CR contraction. CR constriction was defined as the period from CR contraction to the disappearance of the *rlc1-mNG* from the site of division. n, number of cells analyzed. Data presented as mean \pm S.E.M. **** $p \leq 0.0001$, n.s., not significant, one-way ANOVA.

3.5 Fic1 directly interacts with Cyk3's SH3 domain

Because the involvement of Fic1 in promoting septation was reminiscent of the role of *S. cerevisiae*'s IPC (Devrekanli et al., 2012; Nishihama et al., 2009; Sanchez-Diaz et al., 2008), we asked whether Fic1's interactions with Cdc15 and Imp2 were required for *myo2-E1* suppression. Fic1 binds the SH3 domains of the F-BAR proteins Cdc15 and Imp2 (Roberts-Galbraith et al., 2009) through the P254,257 PxxP motif and the *fic1-P257A* mutation, which disrupts Fic1's interactions with Cdc15 and Imp2 (Bohnert and Gould, 2012), prevented *fic1-2A*'s suppression of *myo2-E1* (Fig. 3.4A and B). These data suggest that Fic1's interaction with Cdc15 and Imp2 are required for *fic1-2A*'s suppression of *myo2-E1* and thus, Fic1's role in promoting septum formation.

We next asked if *S. pombe* Cyk3 was required for *fic1-2A*'s suppression of *myo2-E1*. Indeed, *cyk3* Δ prevented *fic1-2A* from suppressing *myo2-E1* (Fig. 3.4C). We then aimed to determine if Cyk3 bound Fic1 through an SH3-PxxP interface, similarly to Cyk3 and Inn1 in *S. cerevisiae* (Nishihama et al., 2009) (Fig. 3.4D). To test this, we generated recombinant Cyk3-SH3-GST and as a negative control, Cyk3-SH3-W43S-GST. Based on SH3 domain homology, the W43S substitution is predicted to disrupt Cyk3-SH3's ability to bind PxxP motifs (Saksela and Permi, 2012). Immobilized Cyk3-SH3-GST purified Fic1-FLAG₃ from lysates of *S. pombe* arrested by *cps1-191*, a temperature-sensitive allele of *bgs1* which allows CRs to form but prevents primary septum deposition (Liu et al., 1999), but Cyk3-W43S-SH3-GST did not (Fig. 3.4E). Finally, we found that Fic1-MBP directly bound Cyk3-SH3-GST indicating that Cyk3-SH3 directly binds Fic1 (Fig. 3.4F).

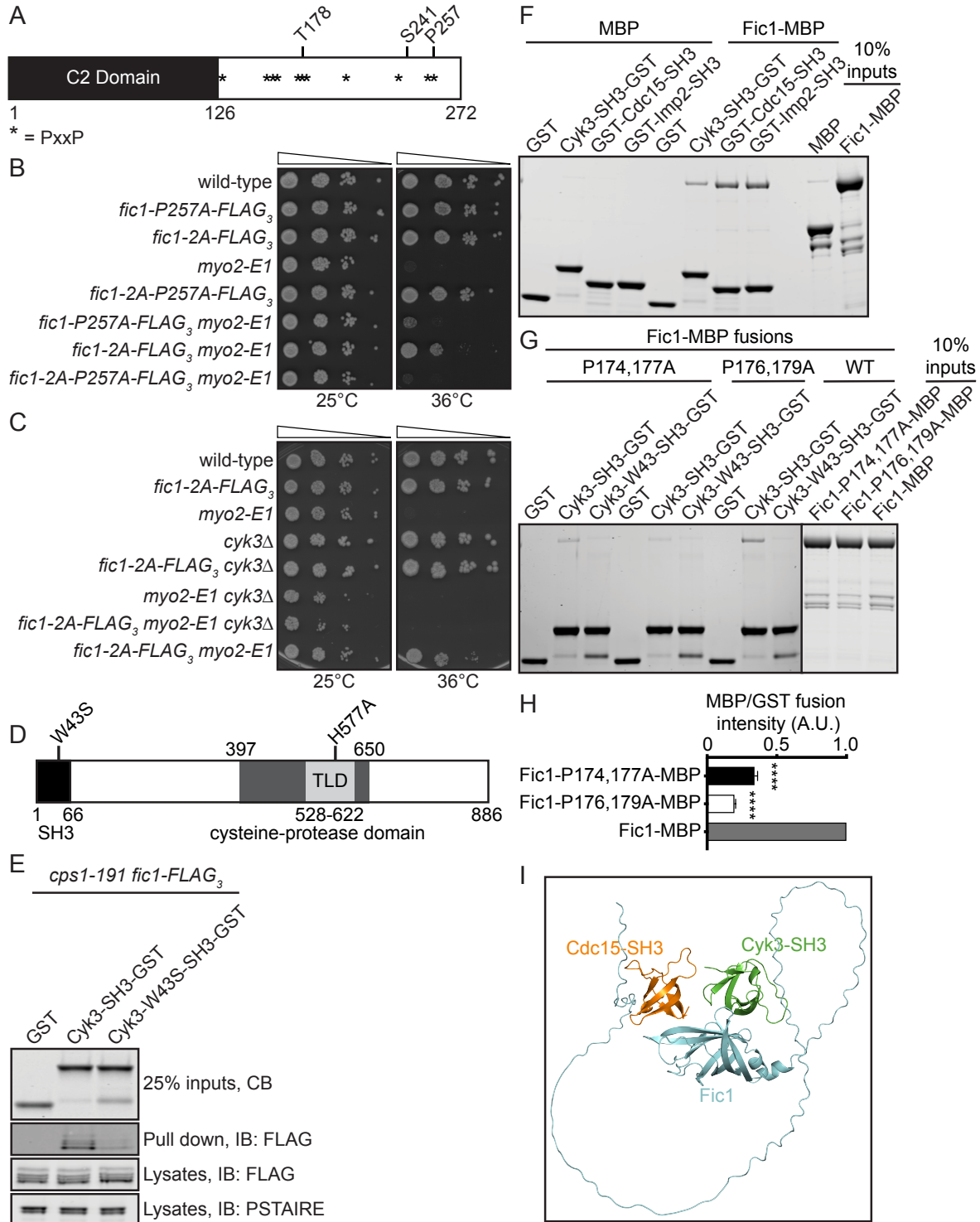


Figure 3.4. Cyk3-SH3 binds Fic1. A) Schematic of Fic1 with domain boundaries and phosphorylation sites indicated with amino acids numbers and PxxP motifs by asterisks. Drawn to scale. B and C) Ten-fold serial dilutions of the indicated strains were spotted on YE agar media and incubated at the indicated temperatures for 3-5 days. D) Schematic of Cyk3 drawn to scale. Domains and their boundaries and mutations within the domains indicated. E) A portion of protein lysates from *cps1-191 fic1-FLAG₃* cells

was subjected to immunoblotting with FLAG anti-CDK (PSTAIRE) antibodies. The remainder of the lysates was incubated with the indicated bead-bound GST recombinant proteins, of which a portion was detected by Coomassie blue (CB) staining. Fic1 bound to the beads after washing was detected with anti-FLAG immunoblotting. Cells were shifted to 36°C for 3 hours prior to lysis. F and G) Coomassie blue stained SDS-PAGE gel of *in vitro* binding assays using the indicated recombinant proteins. H) Quantification of the amount of soluble protein captured by bead-bound proteins, normalized to the amount of bead-bound protein. Data presented as mean \pm S.E.M. **** $p \leq 0.0001$, one-way ANOVA. I) Molecular modeling predictions of interactions between Fic1 in cyan, Cyk3-SH3(aa1-66) in green, and Cdc15-SH3(aa867-927) in orange.

To verify that at least one of Fic1's 11 PxxP motifs was necessary for interaction with Cyk3's SH3 domain, we generated recombinant Fic1-MBP with every PxxP motif mutated to AxxA, referred to as Fic1-11AxxA-MBP. As predicted, Fic1-11AxxA-MBP did not bind Cyk3-SH3-GST or Cyk3-W43S-SH3-GST (Fig. 3.5A). To identify which PxxP motif was required for the interaction, we generated Fic1-MBP fusion proteins with each individual AxxA mutation. Fic1-P174,177A-MBP and Fic1-P176,179A-MBP exhibited reduced binding to Cyk3-SH3-GST compared to Fic1-MBP (Fig. 3.4G and H). Because these are distinct from the PxxP motif involved in binding Cdc15 and Imp2, Fic1 might be able to bind Cyk3 and Cdc15 or Imp2 simultaneously (Bohnert and Gould, 2012) to form an analog of the IPC. Indeed, molecular modeling using ColabFold predicted that Fic1 could simultaneously bind the SH3 domains of Cdc15 and Cyk3 (Fig. 3.4I and 3.5B) (Jumper et al., 2021; Mirdita et al., 2022).

Because the Fic1-2A mutant eliminates phosphorylation on T178, we wondered whether disrupting the prolines required for Cyk3 binding around T178 might alter Fic1's phosphorylation status. We were especially cognizant of this possibility because T178 can be phosphorylated *in vitro* by CDK, a proline-directed kinase (Bohnert et al., 2020). To examine whether these proline mutations affected Fic1 phosphorylation *in vivo*, we analyzed the gel mobilities of Fic1-P174,177A and Fic1-P176,179A. Fic1-FLAG₃ migrates as four bands. The top band represents dual phosphorylation at T178 and S241, the two intermediate bands are singly phosphorylated at T178 or S241, and the fastest migrating form is not phosphorylated (Bohnert et al., 2020). As predicted, Fic1-P176,179A formed only two bands, consistent with a loss of T178 phosphorylation (Fig. 3.5C) (Bohnert et al., 2020). Interestingly, Fic1-P174,177A displayed the wild-type

pattern of phosphorylation suggesting that it could be used to selectively test the role of Cyk3 binding to Fic1 in the suppression of *myo2-E1* (Fig. 3.5C). We found that *fic1-2A-P174,177A* did not suppress *myo2-E1* (Fig. 3.5D) and similarly, inactivation of the Cyk3-SH3 domain by the *cyk3-W43S* allele disrupted *fic1-2A*'s suppression of *myo2-E1* (Fig. 3.6A). Taken together, these results suggest Cyk3 is required for Fic1's roles in septum formation.

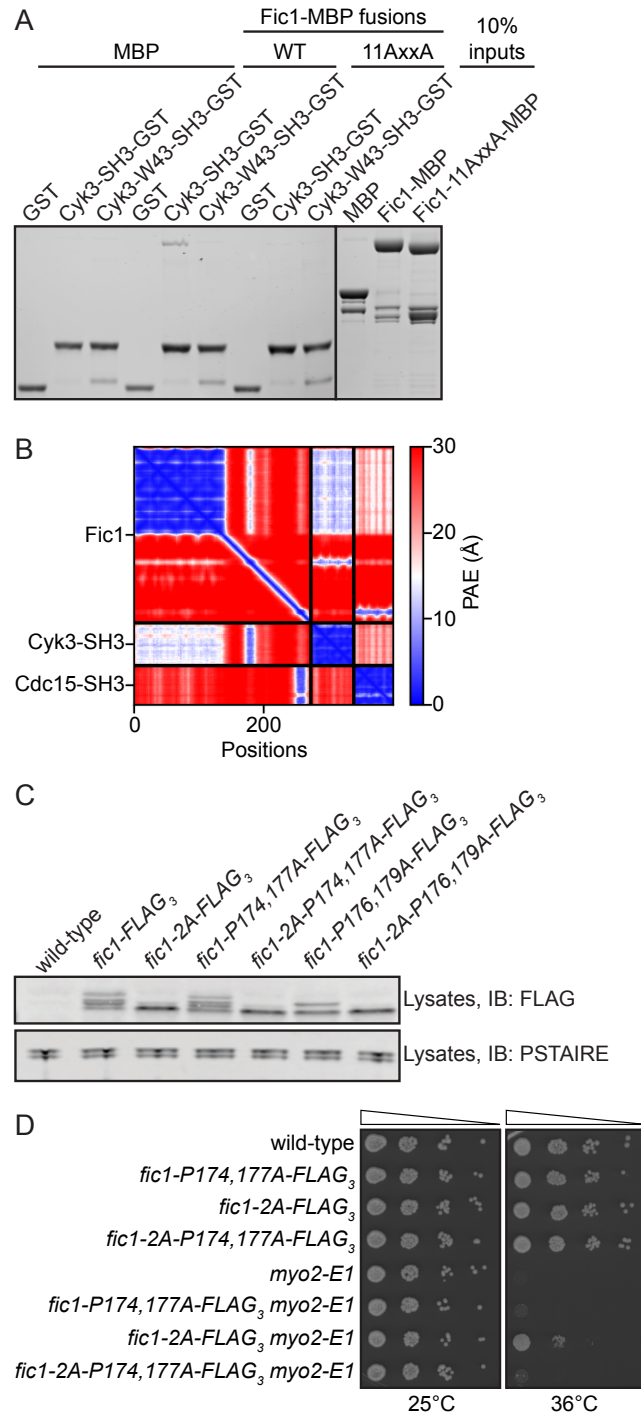


Figure 3.5. P174,177 is required for *fic1-2A*'s suppression of *myo2-E1*. A) Coomassie-stained SDS-PAGE of *in vitro* binding assays using the indicated recombinant proteins. B) The predicted aligned error (PAE) map from the molecular modeling between Fic1, Cyk3-SH3, and Cdc15-SH3. C) Lysates from cells of the indicated genotypes were immunoblotted with anti-FLAG antibody to assess Fic1-FLAG₃ gel mobilities and anti-CDK (PSTAIRE) antibody as a loading control. D) Ten-fold serial dilutions of the indicated strains were spotted on YE agar media and incubated at the indicated temperatures for 3-5 days.

3.6 Cyk3's SH3 domain and TLD are required for Fic1's roles in septum formation

In addition to its SH3 domain, Cyk3 has a central transglutaminase-like domain (TLD) within a larger cysteine protease-like domain (CPD), which has been implicated in Cyk3 function but not thought to have enzymatic activity (Fig. 3.4D) (Pollard et al., 2012). To determine if Cyk3's TLD is required for *fic1-2A*'s suppression of *myo2-E1*, we inactivated the TLD through the previously established H577A mutation (Pollard et al., 2012) and found that this mutation also disrupted *fic1-2A*'s suppression of *myo2-E1* (Fig. 3.6B). To ensure that *cyk3-W43S* and *cyk3-H577A* were not disrupting *fic1-2A*'s suppression by destabilizing Cyk3 or by preventing Cyk3's localization to the CR, we measured the fluorescence intensity of GFP fusion proteins Cyk3-W43S and Cyk3-H577A. We found that both alleles had similar CR and whole cell fluorescence as Cyk3-GFP (Fig. 3.6C-E), demonstrating these alleles were stably expressed and localized normally. Additionally, we found that both Cyk3-W43S and Cyk3-H577A co-immunoprecipitated with Cdc15 from prometaphase arrested cells as Cyk3 does (Fig. 3.6F) (Bohnert and Gould, 2012; Roberts-Galbraith et al., 2010).

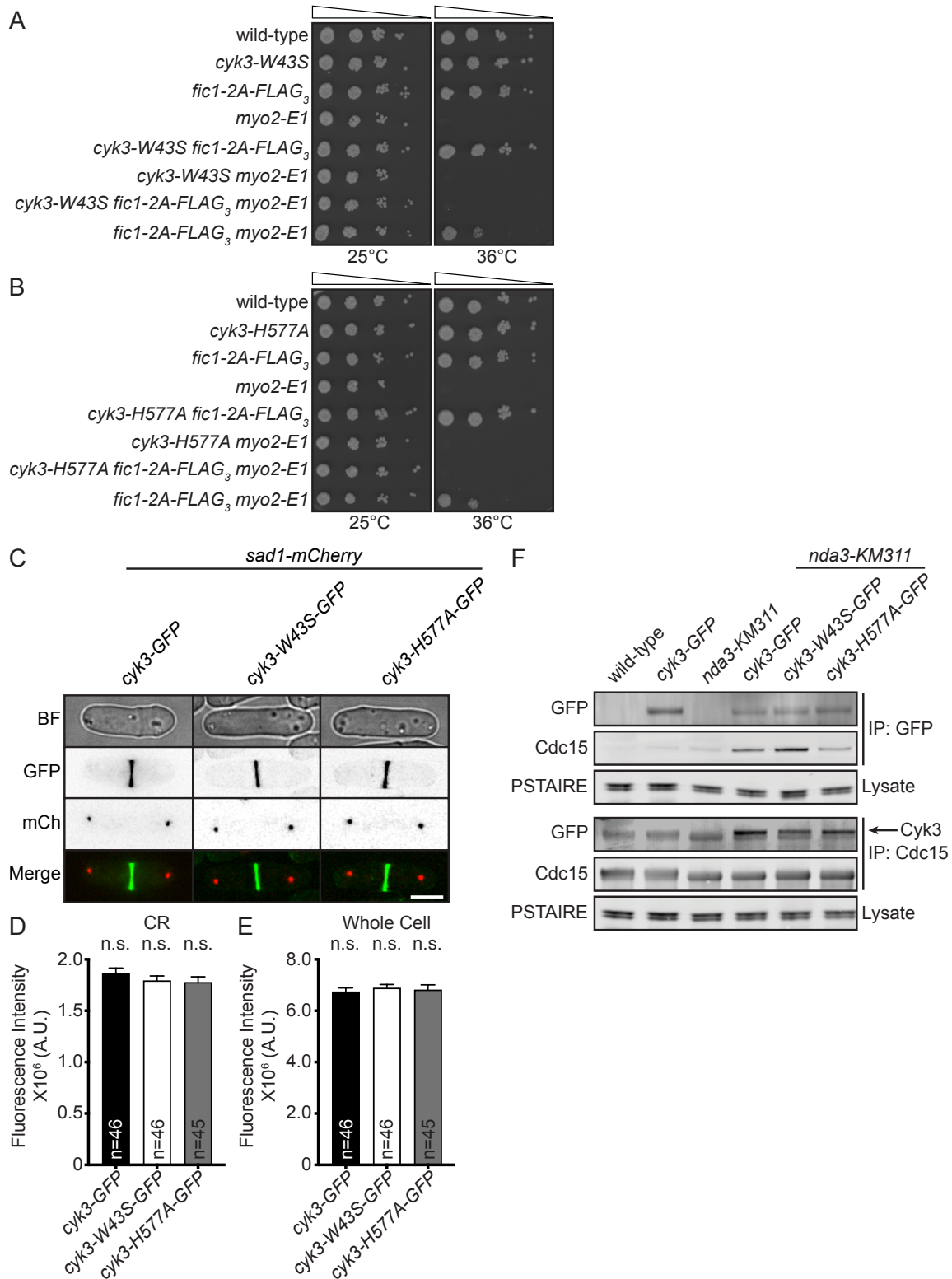


Figure 3.6. Cyk3's SH3 and transglutaminase-like domain are required for *fic1-2A*'s suppression of *myo2-E1*. A and B) Ten-fold serial dilutions of the indicated strains were spotted on YE agar media and incubated at the indicated temperatures for 3-5 days. C) Live-cell bright field (BF), GFP, mCherry (mCh) and merged GFP/mCh

images of cells of indicated genotypes during cytokinesis. Scale bar: 5 μ m. D and E) Quantification of CR (D) and whole cell (E) fluorescence intensities for cells of indicated genotypes. Data from three trials per genotype presented as mean \pm S.E.M. n.s., not significant, one-way ANOVA. F) Anti-GFP or anti-Cdc15 immunoprecipitates from cells of indicated genotypes were blotted with an anti-GFP or anti-Cdc15 antibody. Lysate samples were blotted with anti-CDK (PSTAIRE) as an input control for the immunoprecipitations. Arrow indicates Cyk3-GFP protein band.

3.7 Fic1 and Cyk3 function independently of Chs2

S. cerevisiae Cyk3's TLD stimulates Chs2 (Foltman et al., 2016; Nishihama et al., 2009). While *S. pombe*'s septum lacks chitin, *S. pombe* does have an orthologous protein to *S. cerevisiae*'s Chs2 with the same name but lacking catalytic activity (Horisberger et al., 1978; Martin-Garcia et al., 2003; Matsuo et al., 2004; Sietsma and Wessels, 1990). *S. pombe* Chs2 possibly influences septum formation indirectly because, like *fic1* Δ and *cyk3* Δ cells, *chs2* Δ cells display delays in CR constriction (Martin-Garcia and Valdivieso, 2006). In the cases of *fic1* Δ and *cyk3* Δ , CR constriction delays correlate with a postponement in the onset of bipolar growth, also known as new end take off (NETO), and a transition to invasive pseudophyphal growth (Bohnert and Gould, 2012). If Chs2 acts downstream of Fic1 and Cyk3 we would expect that *chs2* Δ cells to also exhibit NETO defects and invasive pseudophyphal growth. We analyzed bipolar growth establishment in *chs2* Δ , *fic1* Δ , *cyk3* Δ , and combination *fic1* Δ *chs2* Δ , *cyk3* Δ *chs2* Δ , and *fic1* Δ *cyk3* Δ *chs2* Δ mutants and found that interphase cells of each indicated genotype had an increase in cells growing from only one end (monopolar) compared to wild-type (Fig. 3.7A). However, *chs2* Δ cells did not exhibit polarity defects at the time of septation or invasive pseudohyphal growth (Fig. 3.7B and C). Further, deletion of *chs2* did not disrupt *fic1-2A*'s suppression of *myo2-E1* and surprisingly, *chs2* Δ independently suppressed *myo2-E1* (Fig. 3.7D). These data together indicate that Chs2 does not act downstream of Fic1 and Cyk3 in septation. In accord, ColabFold did not predict an interaction between Cyk3's CPD and Chs2 in *S. pombe* and even the predicted interaction between Cyk3's CPD and Chs2 in *S. cerevisiae* was weak (Fig. 3.7E-H) (Jumper et al., 2021; Mirdita et al., 2022).

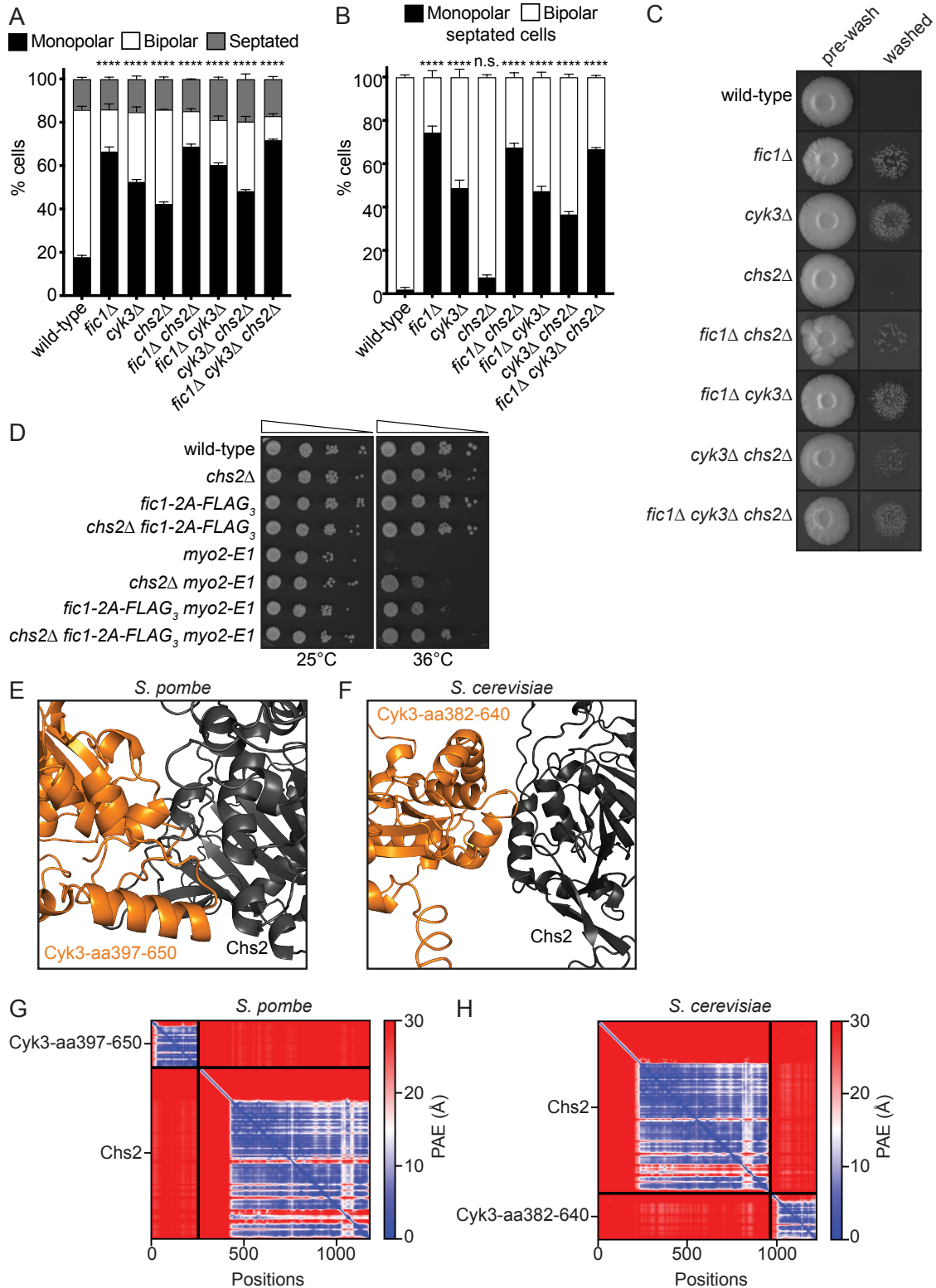


Figure 3.7. Fic1 functions independently of Chs2. A and B) Quantification of growth polarity phenotypes for interphase (A) and septated cells (B) of the indicated genotypes. Data from three trials per genotype with $n > 300$ cells for each trial are presented as mean \pm S.E.M. The percentage of monopolar cells between wild-type and other

genotypes was compared. ****P<0.0001, n.s., not significant, two-way ANOVA with Dunnett's multiple-comparisons test. C) Invasive growth assays of the indicated genotypes on 2% agar. Cells were spotted on YE agar media and incubated for 20 days at 29°C (top row, “pre-wash”). Colonies were then rinsed under a stream of water and rubbed off (bottom row, “washed”). D) Ten-fold serial dilutions of the indicated strains were spotted on YE agar media and incubated at the indicated temperatures for 3-5 days. E and F) Molecular modeling predictions of the interaction between Cyk3-aa397-650 in orange and Chs2 in grey in *S. pombe* (E) and Cyk3-aa382-640 in orange and Chs2 in grey in *S. cerevisiae* (F). G and H) The predicted aligned error (PAE) map from the molecular modeling of the indicated proteins in *S. pombe* (G) and *S. cerevisiae* (H).

In conclusion, our results suggest that mutating the two Fic1 phosphorylation sites to alanine enhances Fic1's normal role in septation to allow *myo2-E1* suppression. Whether this is due to preventing Fic1 phosphorylation or changing Fic1 structure remains to be determined. However, Fic1's interactions with Cyk3, Cdc15 and/or Imp2 are required for this function and molecular modeling suggests Fic1 could simultaneously bind the SH3 domains of Cyk3 and Cdc15/Imp2 to form a complex similar to the *S. cerevisiae* IPC. Despite similar interactions to *S. cerevisiae*'s IPC, these proteins promote septum formation independent of Chs2 and it will be interesting to determine how they influence this critical aspect of fission yeast cell division.

3.8 Materials and Methods

Yeast methods

Schizosaccharomyces pombe strains utilized in this study (Supplemental Table S1) were cultured in yeast extract (YE) media (Moreno et al., 1991). Glutamate media was used for crosses (Moreno et al., 1991). *fic1*, *cyk3*, *sid4*, *rlc1*, and *sad1* were tagged endogenously at the 3' end of their open reading frames (ORFs) with *FLAG₃:kan^R*, *GFP:kan^R*, *mNG:hyg^R*, *V5₃:hyg^R*, and/or *mCherry:nat^R* using pFA6 cassettes as previously described (Bahler et al., 1998b). G418 (100 µg/ml; Sigma-Aldrich, St. Louis, MO), Hygromycin B (125 µg/mL; Invitrogen, Waltham, MA), and Nourseothricin (125 µg/mL; Gold Biotechnology St. Louis, MO) in YE media was used for selecting *kan^R*, *hyg^R*, and *nat^R* cells respectively. *mNG*, a YFP derivative from the lancelet *Branchiostoma lanceolatum*, was selected for imaging experiments because of its superior brightness (Shaner et al., 2013; Willet et al., 2015). A lithium acetate transformation method (Keeney and Boeke, 1994) was used for introducing tagging

sequences, and endogenous integration of tags were verified by whole-cell PCR and/or microscopy. Introduction of tagged loci into other genetic backgrounds was accomplished using standard *S. pombe* mating, sporulation, and tetrad-dissection techniques. Fusion proteins were expressed from their endogenous locus under control of their native promoter unless otherwise indicated. For serial-dilution growth assays, cells were cultured in liquid YE at 25°C in a shaking incubator, four 1:10 serial dilutions starting at 1.5×10^6 cells/mL were made, 2 μ L of each dilution was spotted on YE agar, and cells were grown at the specified temperatures for 3-5 days. All spot assays were performed in triplicate and representative images are shown.

Mutants of *fic1* were expressed from the endogenous loci. To make *fic1* mutations, *fic1*⁺ gDNA with 500 bp 5' and 3' flanks was inserted between BamHI and PstI sites of pIRT2 (Bohnert and Gould, 2012) and site-directed mutagenesis was used to introduce the desired mutations, which were confirmed by DNA sequencing. *fic1::ura*⁺ was transformed with these pIRT2-*fic1* constructs, and stable integrants resistant to 1.5 g/L 5-fluoroorotic acid (5-FOA) (Fisher Scientific, Hampton, NH) were isolated. The correct insertion site and mutations were confirmed by whole-cell PCR and DNA sequencing.

cyk3 strains were made in a similar manner but pIRT2-*cyk3* (W43S, H577A, W43S,H577A) mutant plasmids were constructed from *cyk3* cDNA with 500 bp 5' and 3' flanks to allow these *cyk3* alleles to be verified by whole-cell PCR once integrated.

Invasive growth assays

To assay pseudohyphal invasive growth, 5 μ L containing a total of 10^5 cells were spotted on 2% YE agar and incubated at 29°C for 20 days. Colonies were subsequently placed under a steady stream of water and surface growth was wiped off using a paper towel, as described previously (Pohlmann and Fleig, 2010; Prevorovsky et al., 2009).

Microscopy

Live-cell imaging of *S. pombe* cells were acquired using one of the following: (1) a personal DeltaVision microscope system (Leica Microsystems, Wetzlar, Germany) that includes an Olympus IX71 microscope, 60 \times NA 1.42 PlanApo and 100 \times NA 1.40 UPlanSApo objectives, a pco.edge 4.2 sCMOS camera, and softWoRx imaging software or (2) a Zeiss Axio Observer inverted epifluorescence microscope with Zeiss

63X Oil (1.46 NA), a Axiocam 503 monochrome camera (Zeiss), and captured using Zeiss ZEN 3.0 (Blue edition) software. All cells were in log phase growth before temperature-sensitive shifts and/or live imaging. Time-lapse imaging was performed using an ONIX microfluidics perfusion system (CellASIC ONIX; EMD Millipore, Burlington, MA). A suspension of 50 μ L of 40×10^6 cells/ml YE was loaded into Y04C plates for 5 s at 8 psi. YE media was flowed through the chamber at 5 psi throughout imaging.

Anaphase B onset was defined as the period from the separation of the SPBs to the initiation of SPB segregation towards opposite cell poles. CR assembly was defined as the period from the separation of the SPBs to the coalescence of the cytokinetic nodes into a clearly defined ring. CR maturation was defined as the period from the completion CR assembly to the initiation of CR contraction. CR constriction was defined as the period from CR contraction to the disappearance of the *rlc1-mNG* from the site of division.

Intensity measurements were made from non-deconvolved summed Z-projections of the images processed through ImageJ software (Schneider et al., 2012). For all intensity measurements, the background was subtracted by selecting a region of interest (ROI) in the same image in an area free of cells. The background raw intensity was divided by the area of the background, which was multiplied by the area of the measured object. This number was then subtracted from the intensity measurement of that object. Max intensity Z projections are shown in representative images.

To visualize birth scars by Calcofluor staining, cells were washed in PBS and then resuspended in PBS containing 5 μ g/mL Calcofluor and allowed to incubate on ice for 30 minutes. Cells were then washed three times in PBS and images were acquired. Using the proximity of birth scars to cell ends, growth/morphology was categorized as one of the following: monopolar (i.e. growth on one end), bipolar (i.e. growth on both ends), monopolar and septated, or bipolar and septated. All cells stained with Calcofluor were grown to log phase at 25°C.

Protein Methods

Cells were lysed by bead disruption in NP-40 buffer in denaturing conditions as previously described (Gould et al., 1991). Immunoblot analysis of cell lysates and

immunoprecipitates was performed using anti-FLAG (M2; Sigma-Aldrich, St. Louis, MO), anti-PSTAIR Cdc2 (Sigma-Aldrich, St. Louis, MO), anti-GFP (Roche, Indianapolis, IN), or anti-GFP (VUIC9H4) antibodies or serums raised against GST-Cdc15 (amino acids 1–405; VU326; Cocalico Biologicals, Stevens, PA) as previously described (Bohnert et al., 2009). Cyk3-SH3-GST (aa1-66), Fic1-MBP, GST-Cdc15-SH3 (aa867-927), and GST-Imp2-SH3 (aa608-670) recombinant proteins and their variants were purified from *E. coli* using standard biochemistry techniques. *in vitro* binding assays were performed in 20 mM Tris (pH 7.4) and 150 mM NaCl and allowed to incubated at 4°C for 1 hour while nutating. The beads were washed 3 times with reaction buffer before performing SDS-PAGE and Coomassie staining. Affinity purifications using bead bound Cyk3-SH3-GST recombinant proteins and *S. pombe* lysate were performed by lysing cells in Cyk3 lysis buffer (50 mM Tris (pH 7.5), 150 mM NaCl, 1 mM EDTA, 50 mM NaF, 0.5% NP-40, 0.1% SDS, 1 mM DTT, 1 mM PMSF, 1.3 mM Benzamidine, and cOmplete protease inhibitors (Roche, Indianapolis, IN). *S. pombe* lysates and Cyk3-SH3-GST recombinant proteins were incubated at 4°C for 1 hour while nutating. The bead bound recombinant proteins were washed 3 times in the lysate buffer before SDS-PAGE and immunoblotting or Coomassie staining.

Chapter 4

Conclusions and future directions

4.1 Conclusions

The CR component Fic1 is required for proper CR constriction and growth polarity establishment. However, our mechanistic understanding of how Fic1 contributes to these processes is incomplete. The work described in this dissertation advances our understanding of Fic1 by revealing that Fic1 is a phospho-protein whose phosphorylation state influences growth polarity establishment and that Fic1 promotes septum formation through its interactions with Cdc15, Imp2, and Cyk3.

In Chapter 2, I discussed the evidence that Fic1 is a phospho-protein whose phosphorylation state is regulated by multiple kinases from at least two distinct groups. Additionally, I found that deregulating Fic1's phosphorylation state disrupts growth polarity establishment and promotes the transition from single cell to invasive pseudohyphal growth (Bohnert et al., 2020).

In Chapter 3, I discussed insights into Fic1's cytokinetic role by revealing that the Fic1 phospho-ablating mutating, *fic1-2A*, is a gain-of-function allele that suppresses *myo2-E1* by promoting septum formation. Fic1's role in septum formation was dependent on its interactions with Cdc15 and Imp2 as well as a newly characterized interaction with Cyk3. Molecular modeling suggested that Fic1 could simultaneously bind Cdc15 and Cyk3 similarly to Inn1's interactions with Hof1 and Cyk3 in *S. cerevisiae*. While Fic1's interactions were reminiscent of the IPC in *S. cerevisiae*, which promotes septum formation through Chs2, these analog proteins proved to be functionally divergent as they promoted septum formation independent of Chs2 in *S. pombe*.

4.2 Future directions

In this work I have identified and characterized a direct interaction between PxxP motifs within Fic1's C-terminus and Cyk3's SH3 domain. Together, this interaction and Fic1's interactions with the SH3 domains of Cdc15 and Imp2 ascribes a function to three of the eleven PxxP motifs within Fic1's C-terminus. Because Fic1's C-terminus is required for Fic1's CR localization and Fic1's CR localization is not perturbed when its interactions with Cdc15, Imp2, and Cyk3 are simultaneously disrupted, additional SH3 domains may bind Fic1's C-terminus and assist in localizing it to the CR (Bohnert and Gould, 2012). A search for protein coding genes containing SH3 domains through the *S. pombe* database, PomBase, reported 21 proteins containing at least one SH3 domain (Harris et al., 2022). After eliminating proteins that do not localize to the CR as well as the three known Fic1 interactors from this list, six proteins remain that would be good candidates to study as potential Fic1 interactors (Table 4.1).

Table 4.1. Proteins with SH3 domains that localize to the CR.

Protein name	Description
Mug137	BAR adaptor protein, human endophilin A3-like
Pob1	Boi family protein
Scd2	Cdc42 GTPase complex scaffold subunit Scd2
Shd1	cytoskeletal protein binding protein Sla1 family, Shd1
Bzz1	F-BAR domain protein Bzz1
Myo1	myosin type I

Each of the corresponding genes to these identified proteins could be deleted in the *fic1-P257A-mNG cyk3Δ* genetic background to determine if any one of these proteins are involved in Fic1's CR localization. If a protein is found to assist in Fic1's CR localization, then deleting the corresponding gene in the *fic1-2A myo2-E1* genetic background would determine if this protein is also required for Fic1's role in septum formation. Even if none of these proteins are involved in localizing Fic1 to the CR, they could interact with Fic1 and be required for Fic1's role in septum formation. Deleting each of the six genes in the *fic1-2A myo2-E1* genetic background may identify additional components required for Fic1's role in septum formation. These proteins could be analyzed for physical associations with Fic1 through Y2H and co-immunoprecipitations experiments. Direct interactions between Fic1 and the proteins of

interest could be determined through *in vitro* binding assays with purified recombinant proteins. Additional *in vitro* binding assays with the Fic1 AxxA mutant proteins could then be used to determine the specific PxxP motif that interaction utilized, as was done with Cyk3's SH3 domain in this work.

The function of Fic1's C2 domain is largely uncharacterized. Our lab has determined that the Fic1-C2-GFP fusion protein does not localize to the CR (Bohnert and Gould, 2012). Inn1's C2 domain also does not localize to the CR without its C-terminal tail, but fusing the C2 domain to Hof1 to localize it to the CR allows it to carry out Inn1's essential function of promoting septum formation (Sanchez-Diaz et al., 2008). Inn1's C2 domain promotes septum formation through an interaction with Chs2 facilitated, in part, by two lysine residues within loops 1 and 3 the C2 domain (Sanchez-Diaz et al., 2008). Disrupting homologous lysine residues, K22,27, within Fic1's C2 domain partially disrupts Fic1's localization to growing cell tips (Bohnert et al., 2020). To determine if these residues within Fic1's C2 domain are required for Fic1's role in septum formation, I generated a *fic1-K22,27A myo2-E1* strain. The K22,27A substitution mutations disrupted *fic1-2A's* suppression of *myo2-E1* (Fig. 4.1). This finding suggests that Fic1's C2 domain is required for Fic1's role septum formation.

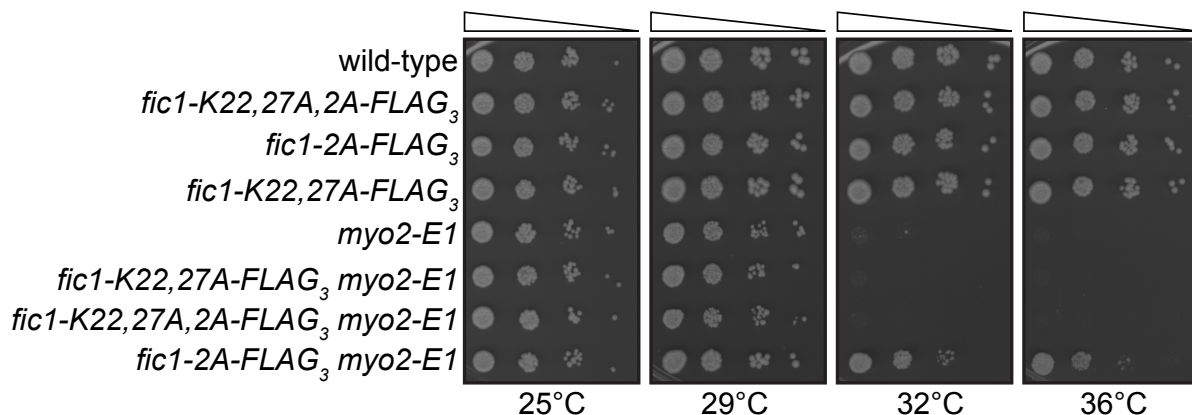


Figure 4.1. The K22 and K27 residues within Fic1's C2 domain are required for *fic1-2A's* suppression of *myo2-E1*. Ten-fold serial dilutions of the indicated strains were spotted on YE agar media and incubated at the indicated temperatures for 3-5 days.

The ability of C2 domains to bind lipid membranes in a Ca²⁺ dependent manner is well characterized (Bazzi and Nelsestuen, 1987; Bazzi and Nelsestuen, 1990; Brose et al., 1995; Sutton et al., 1995; Sutton and Sprang, 1998). Despite this, Inn1's C2

domain does not bind lipid membranes. Due to the homology between Fic1 and Inn1, it would be unexpected for Fic1's C2 domain to bind lipid membranes (Sanchez-Diaz et al., 2008), however, as this work has shown, Fic1 and Inn1 appear to be functionally divergent proteins. To determine if Fic1 binds lipid membranes, I performed liposome co-pelleting assays with Folch fraction liposomes, Fic1, and Opy1 in the presence and absence of Ca²⁺. Opy1 is a protein that binds phosphatidylinositol (4,5)-bisphosphate and served as a control (Snider et al., 2020). Fic1 did not co-pellet with the Folch fraction liposomes in either condition, suggesting that Fic1 does not bind lipids (Fig. 4.2).

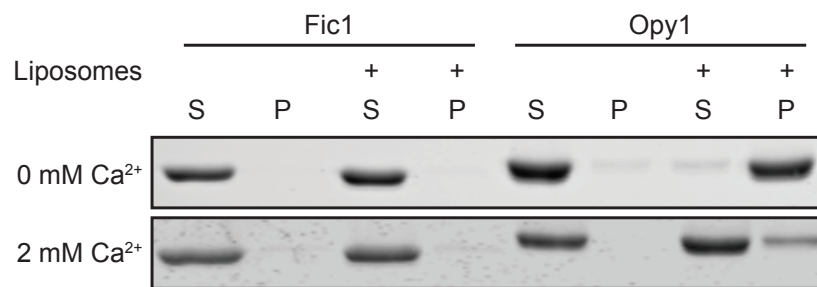


Figure 4.2. Fic1 does not bind liposomes. Co-pelleting assay with Folch fraction liposomes and 10 µg of full length Fic1 or Opy1 with and without Ca²⁺. Samples were visualized by Coomassie blue staining after SDS-PAGE. S, supernatant; P, pellet.

Because Fic1's C2 domain is required for *fic1-2A*'s suppression of *myo2-E1*, but Fic1 does not bind lipid membranes, it is possible that Fic1's C2 domain supports protein-protein interactions (Figs 4.1 and 4.2). Chs2 would be the logical candidate for an interacting partner for Fic1's C2 domain, but, as this work shows, Fic1's roles in septum formation do not require Chs2. Thus, Fic1's C2 domain likely interacts with other proteins. Unlike the canonical SH3-PxxP interaction, the protein-protein interactions facilitated by C2 domains can utilize several different binding interfaces within the C2 domain (Benes et al., 2005; Fukuda et al., 2001; Irino et al., 2005; Lopez-Lluch et al., 2001; Meuillet et al., 2004; Shao et al., 1997; Smallwood et al., 2005). Therefore, it is not possible to generate a potential list of Fic1 C2 domain interactors by searching *S. pombe*'s proteome for particular motifs. Because of this, an unbiased approach should be taken to identify proteins that interact with Fic1's C2 domain. Our lab has previously analyzed tandem affinity-purifications of Fic1 in asynchronous cells, and in both, *cps1-191* and *nda3-KM311* arrested cells by mass spectrometry. These

experiments validated Fic1's interactions with Cdc15 and Imp2, but proteins that interact with Fic1's C2 domain may be obscured within this dataset because the entire Fic1 protein was used as bait. To identify proteins that interact with Fic1's C2 domain, this approach could be modified to use Fic1's C2 domain as bait for the affinity purification. Because Fic1's C2 domain does not localize to the CR by itself, the C2 domain could be produced recombinantly and bound to beads. This immobilized Fic1-C2 domain could be incubated with *S. pombe* lysates arrested in cytokinesis by *cps1-191*, and potential interactors would then be identified by mass spectrometry. This approach is similar to the one used in Chapter 3

to demonstrate an indirect interaction between Fic1 and Cyk3's SH3 domain (Figure 3.4), while having the advantage of being unbiased due analysis by mass spectrometry instead of Western blotting.

Another unbiased approach that could be implemented to identify interactors with Fic1's C2 domain is a Y2H cDNA library screen. This screen would best be performed with a membrane-based Y2H system, which adapts the split-ubiquitin protein complementation assay in the Y2H system (Lentze and Auerbach, 2008). The advantage of this approach is that it is amenable to detecting interactions between the bait and transmembrane or membrane associated proteins. Fic1's interactions with transmembrane proteins are particularly interesting because several components of the cell wall machinery are transmembrane proteins, and it is possible that Fic1's role in septum formation is achieved through direct interactions with these proteins.

This work has determined that Fic1 has a role in promoting septum formation and this role requires Fic1's interactions with the SH3 domains of Cdc15, Imp2, and Cyk3 at the CR. However, there may be additional interactions between Fic1's C-terminus and unidentified SH3 domains because Fic1 remains at the CR when the interactions between Fic1 and all of its known SH3 domain interactions are simultaneously disrupted (Bohnert and Gould, 2012). Additionally, while Fic1's C2 domain is required for Fic1's role in septum formation, it is unclear how it contributes to this process because it does not bind membranes, and any protein-protein interactions it may support are undefined. The previously discussed experiments establish a framework that could be applied to

continue to identify proteins that interact with Fic1's C-terminus or its C2 domain, providing additional insight into the downstream effectors Fic1 utilizes to promote septum formation.

Cyk3's TLD is required for Fic1's role in septum formation, and experiments presented within Chapter 3 determined that Cyk3's TLD does not utilize Chs2 to promote septum formation (Figure 3.7), which differs from the interaction between Cyk3's TLD and Chs2 in *S. cerevisiae* (Foltman et al., 2016). Thus, Cyk3's TLD must interact with other downstream effector(s) to promote septum formation. Affinity purifications analyzed by mass spectrometry or a membrane-based Y2H screen using Cyk3's TLD (amino acids 397-650) as bait could be performed to identify these downstream effector(s) (Lentze and Auerbach, 2008). Because it was previously determined that the Cyk3-H577A mutation disrupts Fic1's role in septum formation, Cyk3-TLD-H577A could be utilized as a control to remove non-specific interactions from the datasets generated from these proposed approaches. While Cyk3's TLD is required for Fic1's role in septum formation, other regions of Cyk3 are understudied and may be involved in promoting septum formation as well.

Cyk3 is highly phosphorylated throughout its IDR (amino acids 67-396) (Carpy et al., 2014; Chen et al., 2013; Halova et al., 2021; Kettenbach et al., 2015; Koch et al., 2011; Lee et al., 2018; Mak et al., 2021; Swaffer et al., 2016; Swaffer et al., 2018; Tay et al., 2019). Within this region, 38 phosphorylation sites have been identified from at least two independent studies (Table 4.2). *In vitro* kinase assays analyzed by mass spectrometry determined that Pom1 targets 18 of these sites and Kin1, another polarity kinase, targets a single site (Lee et al., 2018). Inactivating analog-sensitive alleles of *pom1* and *kin1* disrupted Cyk3's recruitment to the CR during mitosis from the cell tips (Lee et al., 2018). However, this study did not determine if any of these 19 phosphorylation sites were specifically responsible for disrupting Cyk3's recruitment to the CR or if they are additive in their effects. In addition to the 19 of the sites that were identified from the Pom1 and Kin1 study, several of the sites were identified from studies of Cdk1 (Swaffer et al., 2016; Swaffer et al., 2018). While Cyk3's phosphorylation by Cdk1 has not been validated by *in vitro* kinase assays, some of these sites are likely *bona fide* Cdk1 phosphorylation sites.

To further characterize the effects of Cyk3's phosphorylation on its localization, phospho-peptide mapping could be performed to validate the Kin1, Pom1, and Cdk1 phosphorylation sites which could then be used to generate *cyk3* phospho-mutant alleles. Observing the localization of each Cyk3-mNeonGreen fusion of these phospho-mutant alleles could determine which phosphorylation sites and their respective kinases regulate Cyk3's localization. These phospho-mutant alleles could then be studied during cytokinesis to determine if Cyk3 phosphorylation regulates CR dynamics and septum formation. Cyk3's phosphorylation may also be implicated in regulating its protein-protein interactions. This could occur through conformational changes of the Cyk3 protein by phosphorylation of its IDR, similarly to conformational changes that occur from phosphorylation of Cdc15's IDR (Roberts-Galbraith et al., 2010).

Table 4.2. Phosphorylation sites within Cyk3's IDR.

Phosphorylation Sites	Kinase	Phosphorylation Sites	Kinase
T106	Pom1	S209	
S112		S213	Kin1
S125		T260	
S131		S261	
S137	Pom1	S267	Pom1
S140	Pom1	S271	Pom1
S141	Pom1	S280	Pom1
S143		S283	Pom1
S147		S284	Pom1
S149		S300	
S153	Pom1	S310	Pom1
S154	Pom1	T311	Pom1
S156	Pom1	T332	Pom1
S163		T333	
T169		S337	Pom1
S174		T338	Pom1
T185		S341	
S187	Pom1	S390	
S207		T393	

It is possible that Cyk3's IDR allows Cyk3 to undergo phase separation and phosphorylation of the IDR modulates its phase separation properties. Phosphorylation of Cdc15's IDR prevents its ability to phase separate which interferes with the ability of Cdc15 to form plasma membrane-bound condensates and assemble the CR (Bhattacharjee et al., 2023). Perhaps inactivating Kin1 and Pom1 prevents phosphorylation of Cyk3's IDR that is necessary for allowing it to phase separate, resulting in its inability to properly localize to the CR (Lee et al., 2018). It would be interesting to determine if Cyk3's IDR promotes phase separation and, if it does, if

phosphorylation of the IDR alters its ability to phase separate as this property may be required for Cyk3's cytokinetic function.

While phosphorylation of Cyk3's IDR influences its ability to localize to the CR, Cyk3's interactions with CR components that recruit Cyk3 to the CR are undefined. As data within Chapter 3 have shown, disrupting Cyk3's interaction with Fic1 through the *cyk3-W43S* allele does not prevent its localization to the CR (Figure 3.6). Thus, Cyk3's interaction with Fic1 is not solely responsible for Cyk3's recruitment to the CR. Further, Cyk3-W43S-GFP and Cyk3-H577A-GFP both co-immunoprecipitate with Cdc15 similarly to Cyk3-GFP. Thus, Cyk3's SH3 domain and TLD are not required for its association with Cdc15.

While we do not know if the association between Cyk3 and Cdc15 is direct, Cyk3 contains three PxxP motifs within its IDR that could serve as ligands for Cdc15's SH3 domain, P232,235, P370,373, and P388,391. Constructing a *cyk3-3AxxA* allele in which all of these PxxP motifs are mutated to AxxA could be used to determine if these PxxP motifs are required for Cyk3's localization to the CR. Individual AxxA mutations of each PxxP motif could then be used to identify the specific motif responsible for Cyk3's CR localization. To determine if these PxxP motifs are involved in Cyk3's CR localization, the AxxA mutations may need to be generated in the *cyk3-W43S* background to prevent Fic1 from localizing Cyk3 to the CR. Regardless of whether these motifs are required for Cyk3's CR localization, *in vitro* binding assays with Cdc15's SH3 domain and a Cyk3's IDR could be performed to determine if these proteins directly interact. These experiments should also be conducted with Imp2's SH3 domain as it has been shown to be functionally redundant with Cdc15's SH3 domain (Roberts-Galbraith et al., 2009). Lastly, performing these binding assays with phosphorylated Cyk3 IDR could reveal if phosphorylation of Cyk3's IDR modulates its interaction with Cdc15 and Imp2's SH3 domains.

Table 4.3. 14-3-3 RxxS binding sites within Cyk3's IDR.

Cyk3 IDR 14-3-3 RxxS Binding Sites
R85
R150
R210
R273
R277
R297
R307
R359
R364
R387

If Cyk3 and Cdc15 do not directly interact, then additional protein(s) are mediating their physical association. As discussed in Chapter 1, the 14-3-3 protein Rad24 binds to RxxS ligands phosphorylated by Sid2, and this interaction with Rad24 can alter a protein's localization (Chen et al., 2008a; Rincon et al., 2017). Cyk3 contains ten RxxS motifs within its IDR which may serve as binding sites for the Rad24 and/or Rad25 paralogs (Table 4.3) (Ford et al., 1994). Indeed, mass spectrometry analysis of Cyk3-TAPs from prometaphase arrested cells identified that both Rad24 and Rad25 co-purified with Cyk3 (Roberts-Galbraith et al., 2010). The role of Cyk3's interactions with these proteins is undefined, but they could alter Cyk3's association with Cdc15 and CR localization by modulating its protein-protein interactions. 14-3-3 protein dimers can simultaneously bind two different proteins (Brasemann and McCormick, 1995). This would allow Cyk3 to form a complex with another cytokinetic component through Rad24 and/or Rad25. Cdc15 is a potential 14-3-3-mediated Cyk3 interactor as Cdc15 co-immunoprecipitates with Rad24 (Roberts-Galbraith et al., 2010), and directly binds Rad24 *in vitro* (unpublished data). Thus, it would be interesting to first validate Cyk3's interactions with Rad24 and/or Rad25 with *in vitro* binding assays and, if these interactions are substantiated, determine if Rad24 and/or Rad25 are required for Cyk3's co-immunoprecipitation with Cdc15 and Cyk3's localization to the CR. Additionally,

these RxxS sites may be phosphorylated by Sid2 which, if demonstrated by *in vitro* kinase assays, would identify Cyk3 as a downstream effector of the SIN.

Another uncharacterized region of Cyk3 is its C-terminus. Molecular modeling using AlphaFold2 revealed that Cyk3's C-terminus (amino acids 651-886) contains two structured regions, amino acids 651-778 and amino acids 779-886 (Jumper et al., 2021; Varadi et al., 2022). Analyzing each of these predicted structured regions with the DALI distance matrix alignment server revealed that each region exhibited an immunoglobulin-like (IGL) domain fold (Holm, 2022). Because IGL domains can support a wide range of protein-protein interactions, these IGL domains may be required for Cyk3's recruitment to the CR (de Vos et al., 1992; Holmgren et al., 1992; Samson et al., 2018; Slonim et al., 1992). A GFP fusion protein containing both IGL domains could be exogenously expressed from a plasmid in *S. pombe* to determine if the IGL domains localize to the CR on their own. If they localized to the CR, the proteins they interact with could be identified using an unbiased experimental approach, such as affinity purification analyzed by mass spectrometry or a Y2H experiment. Hits from these experiments could be followed up on through an eisosome co-tethering experiment (Yu et al., 2021). This system would localize Cyk3's IGL domains to furrows within the *S. pombe* membrane by fusing it to the eisosome BAR protein, Pil1, and a fluorescent protein which would generate a Pil1-mCh-Cyk3-IGL fusion protein (Yu et al., 2021). The hits identified from affinity purifications of Y2H would be fused to mNG and cells would be imaged. Proteins that colocalize with the Pil1-mCh-Cyk3-IGL fusion protein would be submitted to co-immunoprecipitation experiments with Cyk3 before performing *in vitro* binding assays with the IGL domains and the proteins of interest. Genes of the proteins that interact with Cyk3's IGL domains could then be deleted in *fic1-2A myo2-E1* cells if these proteins are involved in Fic1's role in septum formation.

While this work has determined that Cyk3 interacts with Fic1 through its SH3 domain, many questions about Cyk3 remain. These proposed studies are aimed at validating and characterizing Cyk3's phosphorylation sites as well as determining the function of Cyk3's TLD, IDR, and IGL domains. Results from these studies could provide additional insight into this enigmatic protein while advancing our understanding of the molecular mechanisms that promote septum formation.

In this work I studied Chs2 as a potential downstream effector of Fic1 and Cyk3. While data suggests that Chs2 is not downstream of Fic1, we did determine that the deletion of *chs2* suppressed *myo2-E1*. This observation was unexpected and generated many questions about Chs2's function. To determine if Chs2 influenced septum formation through regulating or interacting with the glucan synthases, I generated *chs2Δ cps1-191*, *chs2Δ cwg1-1*, and *chs2Δ mok1-664* strains. I observed no genetic interaction between these alleles (Fig. 4.3). These data suggest that Chs2's role in septum formation does not directly involve the glucan synthases.

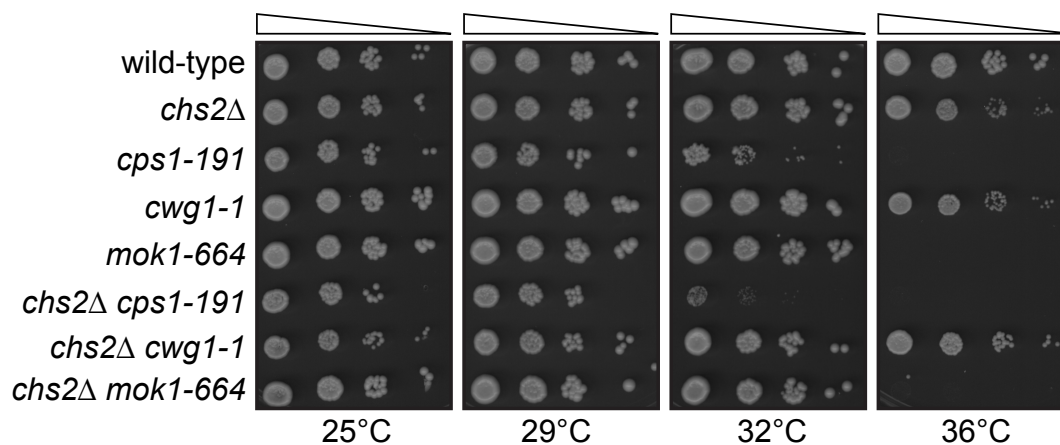


Figure 4.3. There are no genetic interactions between *chs2Δ* and temperature-sensitive glucan synthase alleles. Ten-fold serial dilutions of the indicated strains were spotted on YE agar media and incubated at the indicated temperatures for 3-5 days.

Chs2 is a transmembrane protein that localizes to mature CRs and co-immunoprecipitates with the non-essential type-II myosin Myp2 during cytokinesis (Martin-Garcia and Valdivieso, 2006). Deletion of both *chs2* and *myp2* produced cells with misshapen CRs as well as CRs that failed to constrict before disassembling (Martin-Garcia and Valdivieso, 2006). In *chs2Δ* cells the CR became detached from the membrane during CR constriction which led to asymmetrical closure (Martin-Garcia and Valdivieso, 2006). These data demonstrate that Chs2 ensures proper adhesion of the CR to the membrane during constriction and suggest that Chs2 may function as a CR-membrane anchor.

To further understand how Chs2 anchors the CR, interactions between Chs2's cytosolic face and CR components will need to be identified. It will also be helpful to characterize the binding interface between Chs2 and Myp2 to determine if that

interaction is direct. Unbiased approaches as previously discussed, such as affinity purification analyzed by mass spectrometry or a membrane-based Y2H cDNA library screen, could be used to identify proteins that interact with Chs2. These approaches could be supported by additional screens for genetic interactions with *chs2* Δ . Lastly, the use of solid state nuclear magnetic resonance (ssNMR) could be useful in determining if the *S. pombe* cell wall and septum is actually void of chitin. ssNMR is a suitable approach for characterizing the composition of the cell wall of *S. pombe* because it has previously identified chitin and $\alpha(1,3)$ glucan polymers within the cell wall of the of the pathogenic fungus *Aspergillus fumigatus* (Kang et al., 2018). Identifying chitin in the septum of *S. pombe* would suggest that Chs2 is enzymatically active which would force the field to reconsider Chs2's role in septum formation.

The observation that *chs2* Δ suppressed *myo2-E1* is interesting, but the molecular mechanisms underlying this interaction are undefined. Future studies aimed at characterizing the association between Chs2 and Myp2; identifying additional Chs2 interactors; and analyzing the composition of the cell wall could provide insights into the function of Chs2 and better define the composition of *S. pombe*'s cell wall.

The CIP allows *S. pombe* to withstand damage to the cell wall and respond to environmental stressors such as osmotic shock and high levels of chloride ions (Barba et al., 2008; Sanchez-Mir et al., 2014). While it is clear that these functions are necessary for *S. pombe*'s viability, many of the components of the CIP are undefined. During this work, analog-sensitive alleles of *pck1* and *pck2*, two CIP kinases, were generated to complete the kinase screen aimed at identifying the kinases responsible for Fic1 phosphorylation (Bohnert et al., 2020). Pck1 and Pck2 were not found to be responsible for phosphorylating Fic1, but the *pck1* and *pck2* analog-sensitive alleles could be useful in elucidating the molecular mechanisms of the CIP.

As discussed in Chapter 1, Pck1 and Pck2 both activate the CIP MAPK cascade, but Pck2 appears to elicit a stronger response than Pck1 (Barba et al., 2008; Sanchez-Mir et al., 2014). The stronger response from Pck2 suggests that Pck1 and Pck2 have some unique downstream substrates. Despite the evidence that these two homologous kinases are not completely redundant, no studies have leveraged chemical genetics

and phospho-proteomics to attempt to unveil Pck1 and Pck2's unique substrates that could explain why they evoke different CIP responses.

Inhibiting *pck1-as*, *pck2-as*, and *pck1-as pck2-as* strains with ATP-analog for a short interval of time will reduce the phosphorylation of substrates of the inhibited kinases. Phospho-proteomics by mass spectrometry could detect these changes in phosphorylation (Li et al., 2020). Substrates differentially targeted by Pck1 and Pck2 could be further studied to confirm that the candidates are directly phosphorylated by Pck1 or Pck2 before generating phospho-mutants of the substrates for endogenous expression in *S. pombe*. Ideally the phosphorylation-state of some of these substrates will evoke changes in CIP signaling, which would further our understanding of the different roles of Pck1 and Pck2 in this process. Data from this experiment could also link the CIP to other cell wall synthesis pathways which would assist in generating a more comprehensive understanding of cell wall metabolism.

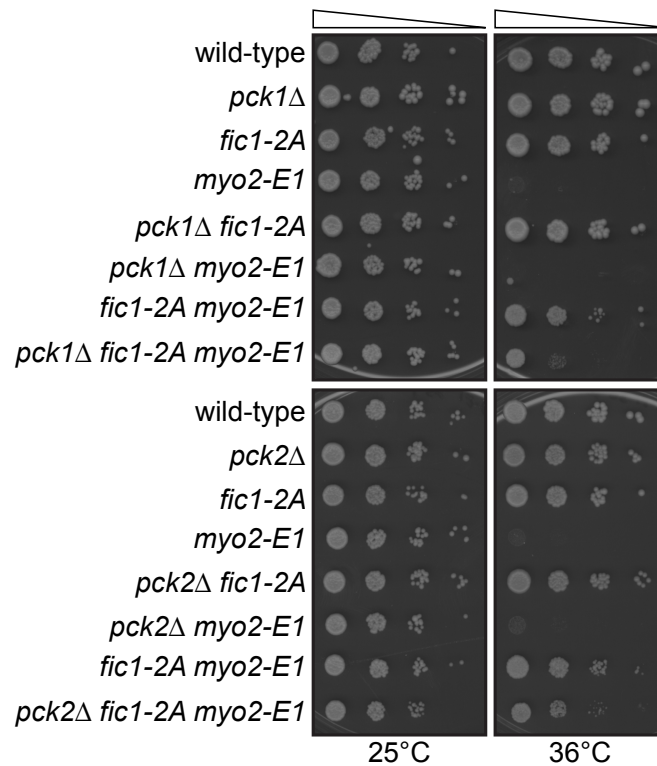


Figure 4.4. Deletion of *pck1* or *pck2* partially disrupts *fic1-2A*'s suppression of *myo2-E1*. Ten-fold serial dilutions of the indicated strains were spotted on YE agar media and incubated at the indicated temperatures for 3-5 days.

Pck1 and Pck2 did not appear to regulate Fic1's phosphorylation-state, but because Pck1 and Pck2 are implicated in cell wall synthesis, I probed for genetic interactions between *fic1-2A* and *pck1* Δ or *pck2* Δ . Deleting either *pck1* or *pck2* partially disrupted *fic1-2A*'s suppression of *myo2-E1* (Fig. 4.4). These data highlight the importance of Pck1 and Pck2 on cell wall synthesis and suggest that Fic1, Pck1, and Pck2 may converge on common downstream effectors.

Further characterization of the CIP pathway by utilizing *pck1-as* and *pck2-as* alleles in a phospho-proteomics approach could generate a rich data set with several interesting substrates to study. Identifying these substrates and characterizing their role in cell wall synthesis may provide insight into how Pck1 and Pck2 differentially regulate the CIP. Additionally, because *pck1* Δ and *pck2* Δ genetically interact with *fic1-2A*, it is possible that some of these substrates may be involved in Fic1's role in septum formation. This proposed approach would improve our understanding about the roles of Pck1 and Pck2 in the CIP and could identify additional CIP components.

References

Adams, A. E., Johnson, D. I., Longnecker, R. M., Sloat, B. F. and Pringle, J. R. (1990). CDC42 and CDC43, two additional genes involved in budding and the establishment of cell polarity in the yeast *Saccharomyces cerevisiae*. *J Cell Biol* **111**, 131-42.

Almonacid, M., Celton-Morizur, S., Jakubowski, J. L., Dingli, F., Loew, D., Mayeux, A., Chen, J. S., Gould, K. L., Clifford, D. M. and Paoletti, A. (2011). Temporal control of contractile ring assembly by Plo1 regulation of myosin II recruitment by Mid1/anillin. *Curr Biol* **21**, 473-9.

Alsop, G. B. and Zhang, D. (2003). Microtubules are the only structural constituent of the spindle apparatus required for induction of cell cleavage. *J Cell Biol* **162**, 383-90.

Alvarez-Tabares, I., Grallert, A., Ortiz, J. M. and Hagan, I. M. (2007). *Schizosaccharomyces pombe* protein phosphatase 1 in mitosis, endocytosis and a partnership with Wsh3/Tea4 to control polarised growth. *J Cell Sci* **120**, 3589-601.

Amoah-Buahin, E., Bone, N. and Armstrong, J. (2005). Hyphal Growth in the Fission Yeast *Schizosaccharomyces pombe*. *Eukaryot Cell* **4**, 1287-97.

Arai, R. and Mabuchi, I. (2002). F-actin ring formation and the role of F-actin cables in the fission yeast *Schizosaccharomyces pombe*. *J Cell Sci* **115**, 887-98.

Arellano, M., Coll, P. M. and Perez, P. (1999a). RHO GTPases in the control of cell morphology, cell polarity, and actin localization in fission yeast. *Microsc Res Tech* **47**, 51-60.

Arellano, M., Duran, A. and Perez, P. (1996). Rho 1 GTPase activates the (1-3)beta-D-glucan synthase and is involved in *Schizosaccharomyces pombe* morphogenesis. *EMBO J* **15**, 4584-91.

Arellano, M., Duran, A. and Perez, P. (1997). Localisation of the *Schizosaccharomyces pombe* rho1p GTPase and its involvement in the organisation of the actin cytoskeleton. *J Cell Sci* **110 (Pt 20)**, 2547-55.

Arellano, M., Niccoli, T. and Nurse, P. (2002). Tea3p is a cell end marker activating polarized growth in *Schizosaccharomyces pombe*. *Current biology: CB* **12**, 751-756.

Arellano, M., Valdivieso, M. H., Calonge, T. M., Coll, P. M., Duran, A. and Perez, P. (1999b). *Schizosaccharomyces pombe* protein kinase C homologues, pck1p and pck2p, are targets of rho1p and rho2p and differentially regulate cell integrity. *J Cell Sci* **112 (Pt 20)**, 3569-78.

Bahler, J. and Pringle, J. R. (1998). Pom1p, a fission yeast protein kinase that provides positional information for both polarized growth and cytokinesis. *Genes Dev* **12**, 1356-70.

Bahler, J., Steever, A. B., Wheatley, S., Wang, Y., Pringle, J. R., Gould, K. L. and McCollum, D. (1998a). Role of polo kinase and Mid1p in determining the site of cell division in fission yeast. *J Cell Biol* **143**, 1603-16.

Bahler, J., Wu, J. Q., Longtine, M. S., Shah, N. G., McKenzie, A., 3rd, Steever, A. B., Wach, A., Philippsen, P. and Pringle, J. R. (1998b). Heterologous modules for efficient and versatile PCR-based gene targeting in *Schizosaccharomyces pombe*. *Yeast* **14**, 943-51.

Balasubramanian, M. K., McCollum, D., Chang, L., Wong, K. C., Naqvi, N. I., He, X., Sazer, S. and Gould, K. L. (1998). Isolation and characterization of new fission yeast cytokinesis mutants. *Genetics* **149**, 1265-75.

Barba, G., Soto, T., Madrid, M., Nunez, A., Vicente, J., Gacto, M., Cansado, J. and Yeast Physiology, G. (2008). Activation of the cell integrity pathway is channelled through diverse signalling elements in fission yeast. *Cell Signal* **20**, 748-57.

Bazzi, M. D. and Nelsestuen, G. L. (1987). Association of protein kinase C with phospholipid vesicles. *Biochemistry* **26**, 115-22.

Bazzi, M. D. and Nelsestuen, G. L. (1990). Protein kinase C interaction with calcium: a phospholipid-dependent process. *Biochemistry* **29**, 7624-30.

Benes, C. H., Wu, N., Elia, A. E., Dharia, T., Cantley, L. C. and Soltoff, S. P. (2005). The C2 domain of PKCdelta is a phosphotyrosine binding domain. *Cell* **121**, 271-80.

Bhattacharjee, R., Hall, A. R., Mangione, M. C., Igarashi, M. G., Roberts-Galbraith, R. H., Chen, J. S., Vavylonis, D. and Gould, K. L. (2023). Multiple polarity kinases inhibit phase separation of F-BAR protein Cdc15 and antagonize cytokinetic ring assembly in fission yeast. *Elife* **12**.

Bhattacharjee, R., Mangione, M. C., Wos, M., Chen, J. S., Snider, C. E., Roberts-Galbraith, R. H., McDonald, N. A., Presti, L. L., Martin, S. G. and Gould, K. L. (2020). DYRK kinase Pom1 drives F-BAR protein Cdc15 from the membrane to promote medial division. *Mol Biol Cell* **31**, 917-929.

Bimbo, A., Jia, Y., Poh, S. L., Karuturi, R. K., den Elzen, N., Peng, X., Zheng, L., O'Connell, M., Liu, E. T., Balasubramanian, M. K. et al. (2005). Systematic deletion analysis of fission yeast protein kinases. *Eukaryot Cell* **4**, 799-813.

Bishop, A. C., Ubersax, J. A., Petsch, D. T., Matheos, D. P., Gray, N. S., Blethrow, J., Shimizu, E., Tsien, J. Z., Schultz, P. G., Rose, M. D. et al. (2000). A chemical switch for inhibitor-sensitive alleles of any protein kinase. *Nature* **407**, 395-401.

Bohnert, K. A., Chen, J. S., Clifford, D. M., Vander Kooi, C. W. and Gould, K. L. (2009). A Link between aurora kinase and Clp1/Cdc14 regulation uncovered by the identification of a fission yeast borealin-like protein. *Mol Biol Cell* **20**, 3646-59.

Bohnert, K. A. and Gould, K. L. (2011). On the cutting edge: post-translational modifications in cytokinesis. *Trends Cell Biol* **21**, 283-92.

Bohnert, K. A. and Gould, K. L. (2012). Cytokinesis-based constraints on polarized cell growth in fission yeast. *PLoS Genet* **8**, e1003004.

Bohnert, K. A., Grzegorzewska, A. P., Willet, A. H., Vander Kooi, C. W., Kovar, D. R. and Gould, K. L. (2013). SIN-dependent phosphoinhibition of formin multimerization controls fission yeast cytokinesis. *Genes Dev* **27**, 2164-77.

Bohnert, K. A., Rossi, A. M., Jin, Q. W., Chen, J. S. and Gould, K. L. (2020). Phosphoregulation of the cytokinetic protein Fic1 contributes to fission yeast growth polarity establishment. *J Cell Sci* **133**.

Braselmann, S. and McCormick, F. (1995). Bcr and Raf form a complex in vivo via 14-3-3 proteins. *EMBO J* **14**, 4839-48.

Bringmann, H. and Hyman, A. A. (2005). A cytokinesis furrow is positioned by two consecutive signals. *Nature* **436**, 731-4.

Broadus, M. R. and Gould, K. L. (2012). Multiple protein kinases influence the redistribution of fission yeast Clp1/Cdc14 phosphatase upon genotoxic stress. *Mol Biol Cell* **23**, 4118-28.

Brose, N., Hofmann, K., Hata, Y. and Sudhof, T. C. (1995). Mammalian homologues of *Caenorhabditis elegans* unc-13 gene define novel family of C2-domain proteins. *J Biol Chem* **270**, 25273-80.

Cadou, A., Couturier, A., Le Goff, C., Soto, T., Miklos, I., Sipiczki, M., Xie, L., Paulson, J. R., Cansado, J. and Le Goff, X. (2010). Kin1 is a plasma membrane-associated kinase that regulates the cell surface in fission yeast. *Mol Microbiol* **77**, 1186-202.

Calonge, T. M., Arellano, M., Coll, P. M. and Perez, P. (2003). Rga5p is a specific Rho1p GTPase-activating protein that regulates cell integrity in *Schizosaccharomyces pombe*. *Mol Microbiol* **47**, 507-18.

Calonge, T. M., Nakano, K., Arellano, M., Arai, R., Katayama, S., Toda, T., Mabuchi, I. and Perez, P. (2000). *Schizosaccharomyces pombe* rho2p GTPase regulates cell wall alpha-glucan biosynthesis through the protein kinase pck2p. *Mol Biol Cell* **11**, 4393-401.

Carnahan, R. H. and Gould, K. L. (2003). The PCH family protein, Cdc15p, recruits two F-actin nucleation pathways to coordinate cytokinetic actin ring formation in *Schizosaccharomyces pombe*. *J Cell Biol* **162**, 851-62.

Carpy, A., Krug, K., Graf, S., Koch, A., Popic, S., Hauf, S. and Macek, B. (2014). Absolute proteome and phosphoproteome dynamics during the cell cycle of *Schizosaccharomyces pombe* (Fission Yeast). *Mol Cell Proteomics* **13**, 1925-36.

Celton-Morizur, S., Bordes, N., Fraasier, V., Tran, P. T. and Paoletti, A. (2004). C-terminal anchoring of mid1p to membranes stabilizes cytokinetic ring position in early mitosis in fission yeast. *Mol Cell Biol* **24**, 10621-35.

Celton-Morizur, S., Racine, V., Sibarita, J. B. and Paoletti, A. (2006). Pom1 kinase links division plane position to cell polarity by regulating Mid1p cortical distribution. *J Cell Sci* **119**, 4710-8.

Chang, L. and Gould, K. L. (2000). Sid4p is required to localize components of the septation initiation pathway to the spindle pole body in fission yeast. *Proc Natl Acad Sci U S A* **97**, 5249-54.

Cheffings, T. H., Burroughs, N. J. and Balasubramanian, M. K. (2016). Actomyosin Ring Formation and Tension Generation in Eukaryotic Cytokinesis. *Curr Biol* **26**, R719-R737.

Cheffings, T. H., Burroughs, N. J. and Balasubramanian, M. K. (2019). Actin turnover ensures uniform tension distribution during cytokinetic actomyosin ring contraction. *Mol Biol Cell* **30**, 933-941.

Chen, C. T., Feoktistova, A., Chen, J. S., Shim, Y. S., Clifford, D. M., Gould, K. L. and McCollum, D. (2008a). The SIN kinase Sid2 regulates cytoplasmic retention of the *S. pombe* Cdc14-like phosphatase Clp1. *Curr Biol* **18**, 1594-9.

Chen, D., Wilkinson, C. R., Watt, S., Penkett, C. J., Toone, W. M., Jones, N. and Bahler, J. (2008b). Multiple pathways differentially regulate global oxidative stress responses in fission yeast. *Mol Biol Cell* **19**, 308-17.

Chen, J. S., Beckley, J. R., McDonald, N. A., Ren, L., Mangione, M., Jang, S. J., Elmore, Z. C., Rachfall, N., Feoktistova, A., Jones, C. M. et al. (2014). Identification of new players in cell division, DNA damage response, and

morphogenesis through construction of *Schizosaccharomyces pombe* deletion strains. *G3 (Bethesda)* **5**, 361-70.

Chen, J. S., Broadus, M. R., McLean, J. R., Feoktistova, A., Ren, L. and Gould, K. L. (2013). Comprehensive proteomics analysis reveals new substrates and regulators of the fission yeast *clp1/cdc14* phosphatase. *Mol Cell Proteomics* **12**, 1074-86.

Chen, Q. and Pollard, T. D. (2011). Actin filament severing by cofilin is more important for assembly than constriction of the cytokinetic contractile ring. *J Cell Biol* **195**, 485-98.

Cipak, L., Zhang, C., Kovacikova, I., Rumpf, C., Miadokova, E., Shokat, K. M. and Gregan, J. (2011). Generation of a set of conditional analog-sensitive alleles of essential protein kinases in the fission yeast *Schizosaccharomyces pombe*. *Cell Cycle* **10**, 3527-32.

Coffman, V. C., Nile, A. H., Lee, I. J., Liu, H. and Wu, J. Q. (2009). Roles of formin nodes and myosin motor activity in Mid1p-dependent contractile-ring assembly during fission yeast cytokinesis. *Mol Biol Cell* **20**, 5195-210.

Cortes, J. C., Carnero, E., Ishiguro, J., Sanchez, Y., Duran, A. and Ribas, J. C. (2005). The novel fission yeast (1,3)beta-D-glucan synthase catalytic subunit Bgs4p is essential during both cytokinesis and polarized growth. *J Cell Sci* **118**, 157-74.

Cortes, J. C., Ishiguro, J., Duran, A. and Ribas, J. C. (2002). Localization of the (1,3)beta-D-glucan synthase catalytic subunit homologue Bgs1p/Cps1p from fission yeast suggests that it is involved in septation, polarized growth, mating, spore wall formation and spore germination. *J Cell Sci* **115**, 4081-96.

Cortes, J. C., Konomi, M., Martins, I. M., Munoz, J., Moreno, M. B., Osumi, M., Duran, A. and Ribas, J. C. (2007). The (1,3)beta-D-glucan synthase subunit Bgs1p is responsible for the fission yeast primary septum formation. *Mol Microbiol* **65**, 201-17.

Cortes, J. C., Pujol, N., Sato, M., Pinar, M., Ramos, M., Moreno, B., Osumi, M., Ribas, J. C. and Perez, P. (2015). Cooperation between Paxillin-like Protein Pxl1 and Glucan Synthase Bgs1 Is Essential for Actomyosin Ring Stability and Septum Formation in Fission Yeast. *PLoS Genet* **11**, e1005358.

Cortes, J. C., Sato, M., Munoz, J., Moreno, M. B., Clemente-Ramos, J. A., Ramos, M., Okada, H., Osumi, M., Duran, A. and Ribas, J. C. (2012). Fission yeast Ags1 confers the essential septum strength needed for safe gradual cell abscission. *J Cell Biol* **198**, 637-56.

Cruz, S., Munoz, S., Manjon, E., Garcia, P. and Sanchez, Y. (2013). The fission yeast cell wall stress sensor-like proteins Mtl2 and Wsc1 act by turning on the GTPase Rho1p but act independently of the cell wall integrity pathway. *Microbiologyopen* **2**, 778-94.

Curto, M. A., Sharifmoghadam, M. R., Calpena, E., De Leon, N., Hoya, M., Doncel, C., Leatherwood, J. and Valdivieso, M. H. (2014). Membrane organization and cell fusion during mating in fission yeast requires multipass membrane protein Prm1. *Genetics* **196**, 1059-76.

Das, M., Nunez, I., Rodriguez, M., Wiley, D. J., Rodriguez, J., Sarkeshik, A., Yates, J. R., 3rd, Buchwald, P. and Verde, F. (2015). Phosphorylation-dependent inhibition of Cdc42 GEF Gef1 by 14-3-3 protein Rad24 spatially regulates Cdc42 GTPase activity and oscillatory dynamics during cell morphogenesis. *Mol Biol Cell* **26**, 3520-34.

Das, M., Wiley, D. J., Chen, X., Shah, K. and Verde, F. (2009). The conserved NDR kinase Orb6 controls polarized cell growth by spatial regulation of the small GTPase Cdc42. *Curr Biol* **19**, 1314-9.

Davidson, R., Pontasch, J. A. and Wu, J. Q. (2016). Sbg1 Is a Novel Regulator for the Localization of the beta-Glucan Synthase Bgs1 in Fission Yeast. *PLoS One* **11**, e0167043.

de Vos, A. M., Ultsch, M. and Kossiakoff, A. A. (1992). Human growth hormone and extracellular domain of its receptor: crystal structure of the complex. *Science* **255**, 306-12.

Dechant, R. and Glotzer, M. (2003). Centrosome separation and central spindle assembly act in redundant pathways that regulate microtubule density and trigger cleavage furrow formation. *Dev Cell* **4**, 333-44.

Dekker, N., Speijer, D., Grun, C. H., van den Berg, M., de Haan, A. and Hochstenbach, F. (2004). Role of the alpha-glucanase Agn1p in fission-yeast cell separation. *Mol Biol Cell* **15**, 3903-14.

Demeter, J. and Sazer, S. (1998). imp2, a new component of the actin ring in the fission yeast *Schizosaccharomyces pombe*. *J Cell Biol* **143**, 415-27.

Devrekanli, A., Foltman, M., Roncero, C., Sanchez-Diaz, A. and Labib, K. (2012). Inn1 and Cyk3 regulate chitin synthase during cytokinesis in budding yeasts. *J Cell Sci* **125**, 5453-66.

Ding, R., West, R. R., Morphey, D. M., Oakley, B. R. and McIntosh, J. R. (1997). The spindle pole body of *Schizosaccharomyces pombe* enters and leaves the nuclear envelope as the cell cycle proceeds. *Mol Biol Cell* **8**, 1461-79.

Dodgson, J., Brown, W., Rosa, C. A. and Armstrong, J. (2010). Reorganization of the growth pattern of *Schizosaccharomyces pombe* in invasive filament formation. *Eukaryot Cell* **9**, 1788-97.

Edreira, T., Celador, R., Manjon, E. and Sanchez, Y. (2020). A novel checkpoint pathway controls actomyosin ring constriction trigger in fission yeast. *Elife* **9**.

Endo, M., Shirouzu, M. and Yokoyama, S. (2003). The Cdc42 binding and scaffolding activities of the fission yeast adaptor protein Scd2. *J Biol Chem* **278**, 843-52.

Fankhauser, C., Reymond, A., Cerutti, L., Utzig, S., Hofmann, K. and Simanis, V. (1995). The *S. pombe* cdc15 gene is a key element in the reorganization of F-actin at mitosis. *Cell* **82**, 435-44.

Fankhauser, C. and Simanis, V. (1994). The cdc7 protein kinase is a dosage dependent regulator of septum formation in fission yeast. *EMBO J* **13**, 3011-9.

Feierbach, B. and Chang, F. (2001). Roles of the fission yeast formin for3p in cell polarity, actin cable formation and symmetric cell division. *Curr Biol* **11**, 1656-65.

Feoktistova, A., Morrell-Falvey, J., Chen, J. S., Singh, N. S., Balasubramanian, M. K. and Gould, K. L. (2012). The fission yeast septation initiation network (SIN) kinase, Sid2, is required for SIN asymmetry and regulates the SIN scaffold, Cdc11. *Mol Biol Cell* **23**, 1636-45.

Foltman, M., Molist, I., Arcones, I., Sacristan, C., Filali-Mouncef, Y., Roncero, C. and Sanchez-Diaz, A. (2016). Ingression Progression Complexes Control

Extracellular Matrix Remodelling during Cytokinesis in Budding Yeast. *PLoS Genet* **12**, e1005864.

Ford, J. C., al-Khodairy, F., Fotou, E., Sheldrick, K. S., Griffiths, D. J. and Carr, A. M. (1994). 14-3-3 protein homologs required for the DNA damage checkpoint in fission yeast. *Science* **265**, 533-5.

Fujita, A. and Misumi, Y. (2009). Fission yeast syt22 protein, a putative Arf guanine nucleotide exchange factor, is necessary for new end take off. *FEMS Microbiol Lett* **294**, 191-7.

Fujiwara, T., Bandi, M., Nitta, M., Ivanova, E. V., Bronson, R. T. and Pellman, D. (2005). Cytokinesis failure generating tetraploids promotes tumorigenesis in p53-null cells. *Nature* **437**, 1043-7.

Fukuda, M., Saegusa, C., Kanno, E. and Mikoshiba, K. (2001). The C2A domain of double C2 protein gamma contains a functional nuclear localization signal. *J Biol Chem* **276**, 24441-4.

Furge, K. A., Wong, K., Armstrong, J., Balasubramanian, M. and Albright, C. F. (1998). Byr4 and Cdc16 form a two-component GTPase-activating protein for the Spg1 GTPase that controls septation in fission yeast. *Curr Biol* **8**, 947-54.

Ganem, N. J., Godinho, S. A. and Pellman, D. (2009). A mechanism linking extra centrosomes to chromosomal instability. *Nature* **460**, 278-82.

Garcia, I., Jimenez, D., Martin, V., Duran, A. and Sanchez, Y. (2005). The alpha-glucanase Agn1p is required for cell separation in *Schizosaccharomyces pombe*. *Biol Cell* **97**, 569-76.

Garcia, P., Garcia, I., Marcos, F., de Garibay, G. R. and Sanchez, Y. (2009). Fission yeast rgf2p is a rho1p guanine nucleotide exchange factor required for spore wall maturation and for the maintenance of cell integrity in the absence of rgf1p. *Genetics* **181**, 1321-34.

Garcia, P., Tajadura, V., Garcia, I. and Sanchez, Y. (2006). Rgf1p is a specific Rho1-GEF that coordinates cell polarization with cell wall biogenesis in fission yeast. *Mol Biol Cell* **17**, 1620-31.

Ge, W. and Balasubramanian, M. K. (2008). Pxl1p, a paxillin-related protein, stabilizes the actomyosin ring during cytokinesis in fission yeast. *Mol Biol Cell* **19**, 1680-92.

Glotzer, M. (2017). Cytokinesis in Metazoa and Fungi. *Cold Spring Harb Perspect Biol* **9**.

Gould, K. L., Moreno, S., Owen, D. J., Sazer, S. and Nurse, P. (1991). Phosphorylation at Thr167 is required for *Schizosaccharomyces pombe* p34cdc2 function. *EMBO J* **10**, 3297-309.

Grallert, A., Patel, A., Tallada, V. A., Chan, K. Y., Bagley, S., Krapp, A., Simanis, V. and Hagan, I. M. (2013). Centrosomal MPF triggers the mitotic and morphogenetic switches of fission yeast. *Nat Cell Biol* **15**, 88-95.

Gregan, J., Zhang, C., Rumpf, C., Cipak, L., Li, Z., Uluocak, P., Nasmyth, K. and Shokat, K. M. (2007). Construction of conditional analog-sensitive kinase alleles in the fission yeast *Schizosaccharomyces pombe*. *Nat Protoc* **2**, 2996-3000.

Gu, Y. and Oliferenko, S. (2015). Comparative biology of cell division in the fission yeast clade. *Curr Opin Microbiol* **28**, 18-25.

Guertin, D. A., Chang, L., Irshad, F., Gould, K. L. and McCollum, D. (2000). The role of the sid1p kinase and cdc14p in regulating the onset of cytokinesis in fission yeast. *EMBO J* **19**, 1803-15.

Guertin, D. A. and McCollum, D. (2001). Interaction between the noncatalytic region of Sid1p kinase and Cdc14p is required for full catalytic activity and localization of Sid1p. *J Biol Chem* **276**, 28185-9.

Gupta, S., Mana-Capelli, S., McLean, J. R., Chen, C. T., Ray, S., Gould, K. L. and McCollum, D. (2013). Identification of SIN pathway targets reveals mechanisms of crosstalk between NDR kinase pathways. *Curr Biol* **23**, 333-8.

Hagan, I. and Yanagida, M. (1995). The product of the spindle formation gene *sad1+* associates with the fission yeast spindle pole body and is essential for viability. *J Cell Biol* **129**, 1033-47.

Halova, L., Cobley, D., Franz-Wachtel, M., Wang, T., Morrison, K. R., Krug, K., Nalpas, N., Macek, B., Hagan, I. M., Humphrey, S. J. et al. (2021). A TOR (target

of rapamycin) and nutritional phosphoproteome of fission yeast reveals novel targets in networks conserved in humans. *Open Biol* **11**, 200405.

Harris, M. A., Rutherford, K. M., Hayles, J., Lock, A., Bahler, J., Oliver, S. G., Mata, J. and Wood, V. (2022). Fission stories: using PomBase to understand *Schizosaccharomyces pombe* biology. *Genetics* **220**.

Hirano, T., Funahashi, S., Uemura, T. and Yanagida, M. (1986). Isolation and characterization of *Schizosaccharomyces pombe* cutmutants that block nuclear division but not cytokinesis. *EMBO J* **5**, 2973-9.

Hirata, D., Nakano, K., Fukui, M., Takenaka, H., Miyakawa, T. and Mabuchi, I. (1998). Genes that cause aberrant cell morphology by overexpression in fission yeast: a role of a small GTP-binding protein Rho2 in cell morphogenesis. *J Cell Sci* **111 (Pt 2)**, 149-59.

Hochstenbach, F., Klis, F. M., van den Ende, H., van Donselaar, E., Peters, P. J. and Klausner, R. D. (1998). Identification of a putative alpha-glucan synthase essential for cell wall construction and morphogenesis in fission yeast. *Proc Natl Acad Sci U S A* **95**, 9161-6.

Holm, L. (2022). Dali server: structural unification of protein families. *Nucleic Acids Res* **50**, W210-5.

Holmgren, A., Kuehn, M. J., Branden, C. I. and Hultgren, S. J. (1992). Conserved immunoglobulin-like features in a family of periplasmic pilus chaperones in bacteria. *EMBO J* **11**, 1617-22.

Horisberger, M., Vonlanthen, M. and Rosset, J. (1978). Localization of alpha-galactomannan and of wheat germ agglutinin receptors in *Schizosaccharomyces pombe*. *Arch Microbiol* **119**, 107-11.

Hou, M. C., Guertin, D. A. and McCollum, D. (2004). Initiation of cytokinesis is controlled through multiple modes of regulation of the Sid2p-Mob1p kinase complex. *Mol Cell Biol* **24**, 3262-76.

Hou, M. C., Salek, J. and McCollum, D. (2000). Mob1p interacts with the Sid2p kinase and is required for cytokinesis in fission yeast. *Curr Biol* **10**, 619-22.

Hoya, M., Yanguas, F., Moro, S., Prescianotto-Baschong, C., Doncel, C., de Leon, N., Curto, M. A., Spang, A. and Valdivieso, M. H. (2017). Traffic Through the

Trans-Golgi Network and the Endosomal System Requires Collaboration Between Exomer and Clathrin Adaptors in Fission Yeast. *Genetics* **205**, 673-690.

Hu, Z. and Lutkenhaus, J. (1999). Topological regulation of cell division in *Escherichia coli* involves rapid pole to pole oscillation of the division inhibitor MinC under the control of MinD and MinE. *Mol Microbiol* **34**, 82-90.

Humbel, B. M., Konomi, M., Takagi, T., Kamasawa, N., Ishijima, S. A. and Osumi, M. (2001). In situ localization of beta-glucans in the cell wall of *Schizosaccharomyces pombe*. *Yeast* **18**, 433-44.

Irino, Y., Ichinohe, M., Nakamura, Y., Nakahara, M. and Fukami, K. (2005). Phospholipase Cdelta4 associates with glutamate receptor interacting protein 1 in testis. *J Biochem* **138**, 451-6.

JC, G. C., Ramos, M., Konomi, M., Barragan, I., Moreno, M. B., Alcaide-Gavilan, M., Moreno, S., Osumi, M., Perez, P. and Ribas, J. C. (2018). Specific detection of fission yeast primary septum reveals septum and cleavage furrow ingression during early anaphase independent of mitosis completion. *PLoS Genet* **14**, e1007388.

Jochova, J., Rupes, I. and Streiblova, E. (1991). F-actin contractile rings in protoplasts of the yeast *Schizosaccharomyces*. *Cell Biol Int Rep* **15**, 607-10.

Johnson, B. F., Yoo, B. Y. and Calleja, G. B. (1973). Cell division in yeasts: movement of organelles associated with cell plate growth of *Schizosaccharomyces pombe*. *J Bacteriol* **115**, 358-66.

Jumper, J., Evans, R., Pritzel, A., Green, T., Figurnov, M., Ronneberger, O., Tunyasuvunakool, K., Bates, R., Zidek, A., Potapenko, A. et al. (2021). Highly accurate protein structure prediction with AlphaFold. *Nature* **596**, 583-589.

Kamasaki, T., Osumi, M. and Mabuchi, I. (2007). Three-dimensional arrangement of F-actin in the contractile ring of fission yeast. *J Cell Biol* **178**, 765-71.

Kang, X., Kirui, A., Muszynski, A., Widanage, M. C. D., Chen, A., Azadi, P., Wang, P., Mentink-Vigier, F. and Wang, T. (2018). Molecular architecture of fungal cell walls revealed by solid-state NMR. *Nat Commun* **9**, 2747.

Katayama, S., Hirata, D., Arellano, M., Perez, P. and Toda, T. (1999). Fission yeast alpha-glucan synthase Mok1 requires the actin cytoskeleton to localize the sites

of growth and plays an essential role in cell morphogenesis downstream of protein kinase C function. *J Cell Biol* **144**, 1173-86.

Keeney, J. B. and Boeke, J. D. (1994). Efficient targeted integration at leu1-32 and ura4-294 in *Schizosaccharomyces pombe*. *Genetics* **136**, 849-56.

Kettenbach, A. N., Deng, L., Wu, Y., Baldissard, S., Adamo, M. E., Gerber, S. A. and Moseley, J. B. (2015). Quantitative phosphoproteomics reveals pathways for coordination of cell growth and division by the conserved fission yeast kinase pom1. *Mol Cell Proteomics* **14**, 1275-87.

Kim, D. U., Hayles, J., Kim, D., Wood, V., Park, H. O., Won, M., Yoo, H. S., Duhig, T., Nam, M., Palmer, G. et al. (2010). Analysis of a genome-wide set of gene deletions in the fission yeast *Schizosaccharomyces pombe*. *Nat Biotechnol* **28**, 617-23.

Kim, H., Yang, P., Catanuto, P., Verde, F., Lai, H., Du, H., Chang, F. and Marcus, S. (2003). The kelch repeat protein, Tea1, is a potential substrate target of the p21-activated kinase, Shk1, in the fission yeast, *Schizosaccharomyces pombe*. *J Biol Chem* **278**, 30074-82.

Kitayama, C., Sugimoto, A. and Yamamoto, M. (1997). Type II myosin heavy chain encoded by the myo2 gene composes the contractile ring during cytokinesis in *Schizosaccharomyces pombe*. *J Cell Biol* **137**, 1309-19.

Kobayashi, A., Kanaba, T., Satoh, R., Fujiwara, T., Ito, Y., Sugiura, R. and Mishima, M. (2013). Structure of the second RRM domain of Nrd1, a fission yeast MAPK target RNA binding protein, and implication for its RNA recognition and regulation. *Biochem Biophys Res Commun* **437**, 12-7.

Koch, A., Krug, K., Pengelley, S., Macek, B. and Hauf, S. (2011). Mitotic substrates of the kinase aurora with roles in chromatin regulation identified through quantitative phosphoproteomics of fission yeast. *Sci Signal* **4**, rs6.

Kokkoris, K., Gallo Castro, D. and Martin, S. G. (2014). The Tea4-PP1 landmark promotes local growth by dual Cdc42 GEF recruitment and GAP exclusion. *J Cell Sci* **127**, 2005-16.

Kovar, D. R., Wu, J. Q. and Pollard, T. D. (2005). Profilin-mediated competition between capping protein and formin Cdc12p during cytokinesis in fission yeast. *Mol Biol Cell* **16**, 2313-24.

Krajcovic, M., Johnson, N. B., Sun, Q., Normand, G., Hoover, N., Yao, E., Richardson, A. L., King, R. W., Cibas, E. S., Schnitt, S. J. et al. (2011). A non-genetic route to aneuploidy in human cancers. *Nat Cell Biol* **13**, 324-30.

Krapp, A., Collin, P., Cano Del Rosario, E. and Simanis, V. (2008). Homeostasis between the GTPase Spg1p and its GAP in the regulation of cytokinesis in *S. pombe*. *J Cell Sci* **121**, 601-8.

Krapp, A., Schmidt, S., Cano, E. and Simanis, V. (2001). *S. pombe* cdc11p, together with sid4p, provides an anchor for septation initiation network proteins on the spindle pole body. *Curr Biol* **11**, 1559-68.

Kume, K., Hashimoto, T., Suzuki, M., Mizunuma, M., Toda, T. and Hirata, D. (2017). Identification of three signaling molecules required for calcineurin-dependent monopolar growth induced by the DNA replication checkpoint in fission yeast. *Biochem Biophys Res Commun* **491**, 883-889.

Kume, K., Koyano, T., Kanai, M., Toda, T. and Hirata, D. (2011). Calcineurin ensures a link between the DNA replication checkpoint and microtubule-dependent polarized growth. *Nat Cell Biol* **13**, 234-42.

Laporte, D., Coffman, V. C., Lee, I. J. and Wu, J. Q. (2011). Assembly and architecture of precursor nodes during fission yeast cytokinesis. *J Cell Biol* **192**, 1005-21.

Lee, M. E., Rusin, S. F., Jenkins, N., Kettenbach, A. N. and Moseley, J. B. (2018). Mechanisms Connecting the Conserved Protein Kinases Ssp1, Kin1, and Pom1 in Fission Yeast Cell Polarity and Division. *Curr Biol* **28**, 84-92 e4.

Lentze, N. and Auerbach, D. (2008). Membrane-based yeast two-hybrid system to detect protein interactions. *Curr Protoc Protein Sci* **Chapter 19**, Unit 19 17.

Li, J., Van Vranken, J. G., Pontano Vaites, L., Schweppe, D. K., Huttlin, E. L., Etienne, C., Nandhikonda, P., Viner, R., Robitaille, A. M., Thompson, A. H. et al. (2020). TMTpro reagents: a set of isobaric labeling mass tags enables simultaneous proteome-wide measurements across 16 samples. *Nat Methods* **17**, 399-404.

Liu, J., Tang, X., Wang, H., Oliferenko, S. and Balasubramanian, M. K. (2002). The localization of the integral membrane protein Cps1p to the cell division site

is dependent on the actomyosin ring and the septation-inducing network in *Schizosaccharomyces pombe*. *Mol Biol Cell* **13**, 989-1000.

Liu, J., Wang, H., McCollum, D. and Balasubramanian, M. K. (1999). Drc1p/Cps1p, a 1,3-beta-glucan synthase subunit, is essential for division septum assembly in *Schizosaccharomyces pombe*. *Genetics* **153**, 1193-203.

Lock, A., Rutherford, K., Harris, M. A., Hayles, J., Oliver, S. G., Bahler, J. and Wood, V. (2019). PomBase 2018: user-driven reimplementations of the fission yeast database provides rapid and intuitive access to diverse, interconnected information. *Nucleic Acids Res* **47**, D821-D827.

Loewith, R., Hubberstey, A. and Young, D. (2000). Skh1, the MEK component of the mkh1 signaling pathway in *Schizosaccharomyces pombe*. *J Cell Sci* **113 (Pt 1)**, 153-60.

Longo, L. V. G., Goodyear, E. G., Zhang, S., Kudryashova, E. and Wu, J. Q. (2022). Involvement of Smi1 in cell wall integrity and glucan synthase Bgs4 localization during fission yeast cytokinesis. *Mol Biol Cell* **33**, ar17.

Lopez-Lluch, G., Bird, M. M., Canas, B., Godovac-Zimmerman, J., Ridley, A., Segal, A. W. and Dekker, L. V. (2001). Protein kinase C-delta C2-like domain is a binding site for actin and enables actin redistribution in neutrophils. *Biochem J* **357**, 39-47.

Lucena, R., Dephoure, N., Gygi, S. P., Kellogg, D. R., Tallada, V. A., Daga, R. R. and Jimenez, J. (2015). Nucleocytoplasmic transport in the midzone membrane domain controls yeast mitotic spindle disassembly. *J Cell Biol* **209**, 387-402.

Ma, Y., Sugiura, R., Koike, A., Ebina, H., Sio, S. O. and Kuno, T. (2011). Transient receptor potential (TRP) and Cch1-Yam8 channels play key roles in the regulation of cytoplasmic Ca²⁺ in fission yeast. *PLoS One* **6**, e22421.

Madrid, M., Soto, T., Khong, H. K., Franco, A., Vicente, J., Perez, P., Gacto, M. and Cansado, J. (2006). Stress-induced response, localization, and regulation of the Pmk1 cell integrity pathway in *Schizosaccharomyces pombe*. *J Biol Chem* **281**, 2033-43.

Madrid, M., Vazquez-Marin, B., Soto, T., Franco, A., Gomez-Gil, E., Vicente-Soler, J., Gacto, M., Perez, P. and Cansado, J. (2017). Differential functional

regulation of protein kinase C (PKC) orthologs in fission yeast. *J Biol Chem* **292**, 11374-11387.

Magliozzi, J. O., Sears, J., Cressey, L., Brady, M., Opalko, H. E., Kettenbach, A. N. and Moseley, J. B. (2020). Fission yeast Pak1 phosphorylates anillin-like Mid1 for spatial control of cytokinesis. *J Cell Biol* **219**.

Mah, A. S., Elia, A. E., Devgan, G., Ptacek, J., Schutkowski, M., Snyder, M., Yaffe, M. B. and Deshaies, R. J. (2005). Substrate specificity analysis of protein kinase complex Dbf2-Mob1 by peptide library and proteome array screening. *BMC Biochem* **6**, 22.

Mak, T., Jones, A. W. and Nurse, P. (2021). The TOR-dependent phosphoproteome and regulation of cellular protein synthesis. *EMBO J* **40**, e107911.

Malla, M., Pollard, T. D. and Chen, Q. (2022). Counting actin in contractile rings reveals novel contributions of cofilin and type II myosins to fission yeast cytokinesis. *Mol Biol Cell* **33**, ar51.

Mangione, M. C. and Gould, K. L. (2019). Molecular form and function of the cytokinetic ring. *J Cell Sci* **132**.

Marcus, S., Polverino, A., Chang, E., Robbins, D., Cobb, M. H. and Wigler, M. H. (1995). Shk1, a homolog of the *Saccharomyces cerevisiae* Ste20 and mammalian p65PAK protein kinases, is a component of a Ras/Cdc42 signaling module in the fission yeast *Schizosaccharomyces pombe*. *Proc Natl Acad Sci U S A* **92**, 6180-4.

Martin, S. G., McDonald, W. H., Yates, J. R., 3rd and Chang, F. (2005). Tea4p links microtubule plus ends with the formin for3p in the establishment of cell polarity. *Dev Cell* **8**, 479-91.

Martin, V., Garcia, B., Carnero, E., Duran, A. and Sanchez, Y. (2003). Bgs3p, a putative 1,3-beta-glucan synthase subunit, is required for cell wall assembly in *Schizosaccharomyces pombe*. *Eukaryot Cell* **2**, 159-69.

Martin-Cuadrado, A. B., Duenas, E., Sipiczki, M., Vazquez de Aldana, C. R. and del Rey, F. (2003). The endo-beta-1,3-glucanase eng1p is required for dissolution of the primary septum during cell separation in *Schizosaccharomyces pombe*. *J Cell Sci* **116**, 1689-98.

- Martin-Garcia, R., Duran, A. and Valdivieso, M. H.** (2003). In *Schizosaccharomyces pombe* chs2p has no chitin synthase activity but is related to septum formation. *FEBS Lett* **549**, 176-80.
- Martin-Garcia, R. and Valdivieso, M. H.** (2006). The fission yeast Chs2 protein interacts with the type-II myosin Myo3p and is required for the integrity of the actomyosin ring. *J Cell Sci* **119**, 2768-79.
- Mata, J. and Nurse, P.** (1997). tea1 and the microtubular cytoskeleton are important for generating global spatial order within the fission yeast cell. *Cell* **89**, 939-49.
- Matsuo, Y., Tanaka, K., Nakagawa, T., Matsuda, H. and Kawamukai, M.** (2004). Genetic analysis of chs1+ and chs2+ encoding chitin synthases from *Schizosaccharomyces pombe*. *Biosci Biotechnol Biochem* **68**, 1489-99.
- May, K. M., Watts, F. Z., Jones, N. and Hyams, J. S.** (1997). Type II myosin involved in cytokinesis in the fission yeast, *Schizosaccharomyces pombe*. *Cell Motil Cytoskeleton* **38**, 385-96.
- McCusker, D., Denison, C., Anderson, S., Egelhofer, T. A., Yates, J. R., 3rd, Gygi, S. P. and Kellogg, D. R.** (2007). Cdk1 coordinates cell-surface growth with the cell cycle. *Nat Cell Biol* **9**, 506-15.
- McDargh, Z., Zhu, T., Zhu, H. and O'Shaughnessy, B.** (2023). Actin turnover protects the cytokinetic contractile ring from structural instability. *J Cell Sci* **136**.
- McDonald, N. A., Takizawa, Y., Feoktistova, A., Xu, P., Ohi, M. D., Vander Kooi, C. W. and Gould, K. L.** (2016). The Tubulation Activity of a Fission Yeast F-BAR Protein Is Dispensable for Its Function in Cytokinesis. *Cell Rep* **14**, 534-546.
- Meggio, F., Marin, O. and Pinna, L. A.** (1994). Substrate specificity of protein kinase CK2. *Cell Mol Biol Res* **40**, 401-9.
- Mehta, S. and Gould, K. L.** (2006). Identification of functional domains within the septation initiation network kinase, Cdc7. *J Biol Chem* **281**, 9935-41.
- Meitinger, F., Petrova, B., Lombardi, I. M., Bertazzi, D. T., Hub, B., Zentgraf, H. and Pereira, G.** (2010). Targeted localization of Inn1, Cyk3 and Chs2 by the mitotic-exit network regulates cytokinesis in budding yeast. *J Cell Sci* **123**, 1851-61.

- Meuillet, E. J., Mahadevan, D., Berggren, M., Coon, A. and Powis, G.** (2004). Thioredoxin-1 binds to the C2 domain of PTEN inhibiting PTEN's lipid phosphatase activity and membrane binding: a mechanism for the functional loss of PTEN's tumor suppressor activity. *Arch Biochem Biophys* **429**, 123-33.
- Miller, P. J. and Johnson, D. I.** (1994). Cdc42p GTPase is involved in controlling polarized cell growth in *Schizosaccharomyces pombe*. *Mol Cell Biol* **14**, 1075-83.
- Minet, M., Nurse, P., Thuriaux, P. and Mitchison, J. M.** (1979). Uncontrolled septation in a cell division cycle mutant of the fission yeast *Schizosaccharomyces pombe*. *J Bacteriol* **137**, 440-6.
- Mirdita, M., Schutze, K., Moriwaki, Y., Heo, L., Ovchinnikov, S. and Steinegger, M.** (2022). ColabFold: making protein folding accessible to all. *Nat Methods* **19**, 679-682.
- Mishra, M., Karagiannis, J., Trautmann, S., Wang, H., McCollum, D. and Balasubramanian, M. K.** (2004). The Clp1p/Flp1p phosphatase ensures completion of cytokinesis in response to minor perturbation of the cell division machinery in *Schizosaccharomyces pombe*. *J Cell Sci* **117**, 3897-910.
- Mitchison, J. M.** (1957). The growth of single cells. I. *Schizosaccharomyces pombe*. *Exp Cell Res* **13**, 244-62.
- Mitchison, J. M. and Nurse, P.** (1985). Growth in cell length in the fission yeast *Schizosaccharomyces pombe*. *Journal of Cell Science* **75**, 357-376.
- Moorhouse, K. S., Gudejko, H. F., McDougall, A. and Burgess, D. R.** (2015). Influence of cell polarity on early development of the sea urchin embryo. *Dev Dyn* **244**, 1469-84.
- Moreno, S., Klar, A. and Nurse, P.** (1991). Molecular genetic analysis of fission yeast *Schizosaccharomyces pombe*. *Methods Enzymol* **194**, 795-823.
- Morrell, J. L., Tomlin, G. C., Rajagopalan, S., Venkatram, S., Feoktistova, A. S., Tasto, J. J., Mehta, S., Jennings, J. L., Link, A., Balasubramanian, M. K. et al.** (2004). Sid4p-Cdc11p assembles the septation initiation network and its regulators at the *S. pombe* SPB. *Curr Biol* **14**, 579-84.

Morrell-Falvey, J. L., Ren, L., Feoktistova, A., Haese, G. D. and Gould, K. L. (2005). Cell wall remodeling at the fission yeast cell division site requires the Rho-GEF Rgf3p. *J Cell Sci* **118**, 5563-73.

Mortimer, D., Fothergill, T., Pujic, Z., Richards, L. J. and Goodhill, G. J. (2008). Growth cone chemotaxis. *Trends Neurosci* **31**, 90-8.

Motegi, F., Mishra, M., Balasubramanian, M. K. and Mabuchi, I. (2004). Myosin-II reorganization during mitosis is controlled temporally by its dephosphorylation and spatially by Mid1 in fission yeast. *J Cell Biol* **165**, 685-95.

Motegi, F., Nakano, K., Kitayama, C., Yamamoto, M. and Mabuchi, I. (1997). Identification of Myo3, a second type-II myosin heavy chain in the fission yeast *Schizosaccharomyces pombe*. *FEBS Lett* **420**, 161-6.

Mulvihill, D. P., Edwards, S. R. and Hyams, J. S. (2006). A critical role for the type V myosin, Myo52, in septum deposition and cell fission during cytokinesis in *Schizosaccharomyces pombe*. *Cell Motil Cytoskeleton* **63**, 149-61.

Munoz, J., Cortes, J. C., Sipiczki, M., Ramos, M., Clemente-Ramos, J. A., Moreno, M. B., Martins, I. M., Perez, P. and Ribas, J. C. (2013). Extracellular cell wall beta(1,3)glucan is required to couple septation to actomyosin ring contraction. *J Cell Biol* **203**, 265-82.

Mutoh, T., Nakano, K. and Mabuchi, I. (2005). Rho1-GEFs Rgf1 and Rgf2 are involved in formation of cell wall and septum, while Rgf3 is involved in cytokinesis in fission yeast. *Genes Cells* **10**, 1189-202.

Nabeshima, K., Nakagawa, T., Straight, A. F., Murray, A., Chikashige, Y., Yamashita, Y. M., Hiraoka, Y. and Yanagida, M. (1998). Dynamics of centromeres during metaphase-anaphase transition in fission yeast: Dis1 is implicated in force balance in metaphase bipolar spindle. *Mol Biol Cell* **9**, 3211-25.

Nakano, K., Arai, R. and Mabuchi, I. (1997). The small GTP-binding protein Rho1 is a multifunctional protein that regulates actin localization, cell polarity, and septum formation in the fission yeast *Schizosaccharomyces pombe*. *Genes Cells* **2**, 679-94.

Nakano, K., Mutoh, T. and Mabuchi, I. (2001). Characterization of GTPase-activating proteins for the function of the Rho-family small GTPases in the fission yeast *Schizosaccharomyces pombe*. *Genes Cells* **6**, 1031-42.

Naqvi, N. I., Wong, K. C., Tang, X. and Balasubramanian, M. K. (2000). Type II myosin regulatory light chain relieves auto-inhibition of myosin-heavy-chain function. *Nat Cell Biol* **2**, 855-8.

Nigg, E. A. (1993). Cellular substrates of p34(cdc2) and its companion cyclin-dependent kinases. *Trends Cell Biol* **3**, 296-301.

Nishihama, R., Schreiter, J. H., Onishi, M., Vallen, E. A., Hanna, J., Moravcevic, K., Lippincott, M. F., Han, H., Lemmon, M. A., Pringle, J. R. et al. (2009). Role of Inn1 and its interactions with Hof1 and Cyk3 in promoting cleavage furrow and septum formation in *S. cerevisiae*. *J Cell Biol* **185**, 995-1012.

Nurse, P., Thuriaux, P. and Nasmyth, K. (1976). Genetic control of the cell division cycle in the fission yeast *Schizosaccharomyces pombe*. *Mol Gen Genet* **146**, 167-78.

Ohkura, H., Hagan, I. M. and Glover, D. M. (1995). The conserved *Schizosaccharomyces pombe* kinase plo1, required to form a bipolar spindle, the actin ring, and septum, can drive septum formation in G1 and G2 cells. *Genes Dev* **9**, 1059-73.

Ottillie, S., Miller, P. J., Johnson, D. I., Creasy, C. L., Sells, M. A., Bagrodia, S., Forsburg, S. L. and Chernoff, J. (1995). Fission yeast pak1+ encodes a protein kinase that interacts with Cdc42p and is involved in the control of cell polarity and mating. *EMBO J* **14**, 5908-19.

Padmanabhan, A., Bakka, K., Sevugan, M., Naqvi, N. I., D'Souza, V., Tang, X., Mishra, M. and Balasubramanian, M. K. (2011). IQGAP-related Rng2p organizes cortical nodes and ensures position of cell division in fission yeast. *Curr Biol* **21**, 467-72.

Padte, N. N., Martin, S. G., Howard, M. and Chang, F. (2006). The cell-end factor pom1p inhibits mid1p in specification of the cell division plane in fission yeast. *Curr Biol* **16**, 2480-7.

Palani, S., Chew, T. G., Ramanujam, S., Kamnev, A., Harne, S., Chapa, Y. L. B., Hogg, R., Sevugan, M., Mishra, M., Gayathri, P. et al. (2017). Motor Activity

Dependent and Independent Functions of Myosin II Contribute to Actomyosin Ring Assembly and Contraction in *Schizosaccharomyces pombe*. *Curr Biol* **27**, 751-757.

Palani, S., Srinivasan, R., Zambon, P., Kamnev, A., Gayathri, P. and Balasubramanian, M. K. (2018). Steric hindrance in the upper 50 kDa domain of the motor Myo2p leads to cytokinesis defects in fission yeast. *J Cell Sci* **131**.

Pelham, R. J. and Chang, F. (2002). Actin dynamics in the contractile ring during cytokinesis in fission yeast. *Nature* **419**, 82-6.

Pham, K., Shimoni, R., Charnley, M., Ludford-Menting, M. J., Hawkins, E. D., Ramsbottom, K., Oliaro, J., Izon, D., Ting, S. B., Reynolds, J. et al. (2015). Asymmetric cell division during T cell development controls downstream fate. *J Cell Biol* **210**, 933-50.

Pinar, M., Coll, P. M., Rincon, S. A. and Perez, P. (2008). *Schizosaccharomyces pombe* Pxl1 is a paxillin homologue that modulates Rho1 activity and participates in cytokinesis. *Mol Biol Cell* **19**, 1727-38.

Pohlmann, J. and Fleig, U. (2010). Asp1, a conserved 1/3 inositol polyphosphate kinase, regulates the dimorphic switch in *Schizosaccharomyces pombe*. *Mol Cell Biol* **30**, 4535-47.

Pollard, L. W., Onishi, M., Pringle, J. R. and Lord, M. (2012). Fission yeast Cyk3p is a transglutaminase-like protein that participates in cytokinesis and cell morphogenesis. *Mol Biol Cell* **23**, 2433-44.

Prevorovsky, M., Stanurova, J., Puta, F. and Folk, P. (2009). High environmental iron concentrations stimulate adhesion and invasive growth of *Schizosaccharomyces pombe*. *FEMS Microbiol Lett* **293**, 130-4.

Proctor, S. A., Minc, N., Boudaoud, A. and Chang, F. (2012). Contributions of turgor pressure, the contractile ring, and septum assembly to forces in cytokinesis in fission yeast. *Curr Biol* **22**, 1601-8.

Ramos, M., Cortes, J. C. G., Sato, M., Rincon, S. A., Moreno, M. B., Clemente-Ramos, J. A., Osumi, M., Perez, P. and Ribas, J. C. (2019). Two *S. pombe* septation phases differ in ingression rate, septum structure, and response to F-actin loss. *J Cell Biol* **218**, 4171-4194.

Ren, L., Willet, A. H., Roberts-Galbraith, R. H., McDonald, N. A., Feoktistova, A., Chen, J. S., Huang, H., Guillen, R., Boone, C., Sidhu, S. S. et al. (2015). The Cdc15 and Imp2 SH3 domains cooperatively scaffold a network of proteins that redundantly ensure efficient cell division in fission yeast. *Mol Biol Cell* **26**, 256-69.

Rethinaswamy, A., Birnbaum, M. J. and Glover, C. V. (1998). Temperature-sensitive mutations of the CKA1 gene reveal a role for casein kinase II in maintenance of cell polarity in *Saccharomyces cerevisiae*. *J Biol Chem* **273**, 5869-77.

Revilla-Guarinos, M. T., Martin-Garcia, R., Villar-Tajadura, M. A., Estravis, M., Coll, P. M. and Perez, P. (2016). Rga6 is a Fission Yeast Rho GAP Involved in Cdc42 Regulation of Polarized Growth. *Mol Biol Cell* **27**, 1524-35.

Ribas, J. C., Diaz, M., Duran, A. and Perez, P. (1991). Isolation and characterization of *Schizosaccharomyces pombe* mutants defective in cell wall (1-3)beta-D-glucan. *J Bacteriol* **173**, 3456-62.

Rincon, S. A., Estravis, M., Dingli, F., Loew, D., Tran, P. T. and Paoletti, A. (2017). SIN-Dependent Dissociation of the SAD Kinase Cdr2 from the Cell Cortex Resets the Division Plane. *Curr Biol* **27**, 534-542.

Rincon, S. A., Ye, Y., Villar-Tajadura, M. A., Santos, B., Martin, S. G. and Perez, P. (2009). Pob1 participates in the Cdc42 regulation of fission yeast actin cytoskeleton. *Mol Biol Cell* **20**, 4390-9.

Roberts-Galbraith, R. H., Chen, J. S., Wang, J. and Gould, K. L. (2009). The SH3 domains of two PCH family members cooperate in assembly of the *Schizosaccharomyces pombe* contractile ring. *J Cell Biol* **184**, 113-27.

Roberts-Galbraith, R. H., Ohi, M. D., Ballif, B. A., Chen, J. S., McLeod, I., McDonald, W. H., Gygi, S. P., Yates, J. R., 3rd and Gould, K. L. (2010). Dephosphorylation of F-BAR protein Cdc15 modulates its conformation and stimulates its scaffolding activity at the cell division site. *Mol Cell* **39**, 86-99.

Robertson, A. M. and Hagan, I. M. (2008). Stress-regulated kinase pathways in the recovery of tip growth and microtubule dynamics following osmotic stress in *S. pombe*. *J Cell Sci* **121**, 4055-68.

Roncero, C., Sanchez-Diaz, A. and Valdivieso, M. H. (2016). 9 Chitin Synthesis and Fungal Cell Morphogenesis, pp. 167-190: Springer International Publishing.

Rosenberg, J. A., Tomlin, G. C., McDonald, W. H., Snyderman, B. E., Muller, E. G., Yates, J. R., 3rd and Gould, K. L. (2006). Ppc89 links multiple proteins, including the septation initiation network, to the core of the fission yeast spindle-pole body. *Mol Biol Cell* **17**, 3793-805.

Rupes, I., Jia, Z. and Young, P. G. (1999). Ssp1 promotes actin depolymerization and is involved in stress response and new end take-off control in fission yeast. *Mol Biol Cell* **10**, 1495-510.

Saka, Y., Fantes, P. and Yanagida, M. (1994). Coupling of DNA replication and mitosis by fission yeast rad4/cut5. *J Cell Sci Suppl* **18**, 57-61.

Saksela, K. and Permi, P. (2012). SH3 domain ligand binding: What's the consensus and where's the specificity? *FEBS Lett* **586**, 2609-14.

Salimova, E., Sohrmann, M., Fournier, N. and Simanis, V. (2000). The *S. pombe* orthologue of the *S. cerevisiae* mob1 gene is essential and functions in signalling the onset of septum formation. *J Cell Sci* **113 (Pt 10)**, 1695-704.

Samejima, I., Matsumoto, T., Nakaseko, Y., Beach, D. and Yanagida, M. (1993). Identification of seven new cut genes involved in *Schizosaccharomyces pombe* mitosis. *J Cell Sci* **105 (Pt 1)**, 135-43.

Samson, C., Petitalot, A., Celli, F., Herrada, I., Ropars, V., Le Du, M. H., Nhiri, N., Jacquet, E., Arteni, A. A., Buendia, B. et al. (2018). Structural analysis of the ternary complex between lamin A/C, BAF and emerin identifies an interface disrupted in autosomal recessive progeroid diseases. *Nucleic Acids Res* **46**, 10460-10473.

Sanchez-Diaz, A., Marchesi, V., Murray, S., Jones, R., Pereira, G., Edmondson, R., Allen, T. and Labib, K. (2008). Inn1 couples contraction of the actomyosin ring to membrane ingression during cytokinesis in budding yeast. *Nat Cell Biol* **10**, 395-406.

Sanchez-Mir, L., Soto, T., Franco, A., Madrid, M., Viana, R. A., Vicente, J., Gacto, M., Perez, P. and Cansado, J. (2014). Rho1 GTPase and PKC ortholog Pck1

are upstream activators of the cell integrity MAPK pathway in fission yeast. *PLoS One* **9**, e88020.

Satoh, R., Morita, T., Takada, H., Kita, A., Ishiwata, S., Doi, A., Hagihara, K., Taga, A., Matsumura, Y., Tohda, H. et al. (2009). Role of the RNA-binding protein Nrd1 and Pmk1 mitogen-activated protein kinase in the regulation of myosin mRNA stability in fission yeast. *Mol Biol Cell* **20**, 2473-85.

Sayers, L. G., Katayama, S., Nakano, K., Mellor, H., Mabuchi, I., Toda, T. and Parker, P. J. (2000). Rho-dependence of *Schizosaccharomyces pombe* Pck2. *Genes Cells* **5**, 17-27.

Sazer, S., Lynch, M. and Needleman, D. (2014). Deciphering the evolutionary history of open and closed mitosis. *Curr Biol* **24**, R1099-103.

Sburlati, A. and Cabib, E. (1986). Chitin synthetase 2, a presumptive participant in septum formation in *Saccharomyces cerevisiae*. *J Biol Chem* **261**, 15147-52.

Schindelin, J., Arganda-Carreras, I., Frise, E., Kaynig, V., Longair, M., Pietzsch, T., Preibisch, S., Rueden, C., Saalfeld, S., Schmid, B. et al. (2012). Fiji: an open-source platform for biological-image analysis. *Nat Methods* **9**, 676-82.

Schmidt, M., Bowers, B., Varma, A., Roh, D. H. and Cabib, E. (2002). In budding yeast, contraction of the actomyosin ring and formation of the primary septum at cytokinesis depend on each other. *J Cell Sci* **115**, 293-302.

Schmidt, S., Sohrmann, M., Hofmann, K., Woollard, A. and Simanis, V. (1997). The Spg1p GTPase is an essential, dosage-dependent inducer of septum formation in *Schizosaccharomyces pombe*. *Genes Dev* **11**, 1519-34.

Schneider, C. A., Rasband, W. S. and Eliceiri, K. W. (2012). NIH Image to ImageJ: 25 years of image analysis. *Nat Methods* **9**, 671-5.

Sengar, A. S., Markley, N. A., Marini, N. J. and Young, D. (1997). Mkh1, a MEK kinase required for cell wall integrity and proper response to osmotic and temperature stress in *Schizosaccharomyces pombe*. *Mol Cell Biol* **17**, 3508-19.

Sethi, K., Palani, S., Cortes, J. C., Sato, M., Sevugan, M., Ramos, M., Vijaykumar, S., Osumi, M., Naqvi, N. I., Ribas, J. C. et al. (2016). A New Membrane Protein Sbg1 Links the Contractile Ring Apparatus and Septum Synthesis Machinery in Fission Yeast. *PLoS Genet* **12**, e1006383.

Shaner, N. C., Lambert, G. G., Chammas, A., Ni, Y., Cranfill, P. J., Baird, M. A., Sell, B. R., Allen, J. R., Day, R. N., Israelsson, M. et al. (2013). A bright monomeric green fluorescent protein derived from *Branchiostoma lanceolatum*. *Nat Methods* **10**, 407-9.

Shao, X., Li, C., Fernandez, I., Zhang, X., Sudhof, T. C. and Rizo, J. (1997). Synaptotagmin-syntaxin interaction: the C2 domain as a Ca²⁺-dependent electrostatic switch. *Neuron* **18**, 133-42.

Shaw, J. A., Mol, P. C., Bowers, B., Silverman, S. J., Valdivieso, M. H., Duran, A. and Cabib, E. (1991). The function of chitin synthases 2 and 3 in the *Saccharomyces cerevisiae* cell cycle. *J Cell Biol* **114**, 111-23.

Shimada, Y., Gulli, M. P. and Peter, M. (2000). Nuclear sequestration of the exchange factor Cdc24 by Far1 regulates cell polarity during yeast mating. *Nat Cell Biol* **2**, 117-24.

Sietsma, J. H. and Wessels, J. G. (1990). The occurrence of glucosaminoglycan in the wall of *Schizosaccharomyces pombe*. *J Gen Microbiol* **136**, 2261-5.

Silverman, S. J., Sburlati, A., Slater, M. L. and Cabib, E. (1988). Chitin synthase 2 is essential for septum formation and cell division in *Saccharomyces cerevisiae*. *Proc Natl Acad Sci U S A* **85**, 4735-9.

Simanis, V. and Nurse, P. (1986). The cell cycle control gene *cdc2+* of fission yeast encodes a protein kinase potentially regulated by phosphorylation. *Cell* **45**, 261-8.

Sipiczki, M., Takeo, K. and Grallert, A. (1998). Growth polarity transitions in a dimorphic fission yeast. *Microbiology* **144 (Pt 12)**, 3475-85.

Slonim, L. N., Pinkner, J. S., Branden, C. I. and Hultgren, S. J. (1992). Interactive surface in the PapD chaperone cleft is conserved in pilus chaperone superfamily and essential in subunit recognition and assembly. *EMBO J* **11**, 4747-56.

Smallwood, N. D., Hausman, B. S., Wang, X. and Liedtke, C. M. (2005). Involvement of NH₂ terminus of PKC- δ in binding to F-actin during activation of Calu-3 airway epithelial NKCC1. *Am J Physiol Cell Physiol* **288**, C906-12.

Snell, V. and Nurse, P. (1994). Genetic analysis of cell morphogenesis in fission yeast--a role for casein kinase II in the establishment of polarized growth. *EMBO J* **13**, 2066-74.

Snider, C. E., Willet, A. H., Brown, H. T., Chen, J. S., Evers, J. M. and Gould, K. L. (2020). Fission yeast Opy1 is an endogenous PI(4,5)P(2) sensor that binds to the phosphatidylinositol 4-phosphate 5-kinase Its3. *J Cell Sci* **133**.

Sohrmann, M., Fankhauser, C., Brodbeck, C. and Simanis, V. (1996). The *dmf1/mid1* gene is essential for correct positioning of the division septum in fission yeast. *Genes Dev* **10**, 2707-19.

Soto, T., Villar-Tajadura, M. A., Madrid, M., Vicente, J., Gacto, M., Perez, P. and Cansado, J. (2010). Rga4 modulates the activity of the fission yeast cell integrity MAPK pathway by acting as a Rho2 GTPase-activating protein. *J Biol Chem* **285**, 11516-25.

Streiblova, E. and Wolf, A. (1972). Cell wall growth during the cell cycle of *Schizosaccharomyces pombe*. *Z Allg Mikrobiol* **12**, 673-84.

Sudbery, P. E. (2011). Growth of *Candida albicans* hyphae. *Nat Rev Microbiol* **9**, 737-48.

Sugiura, R., Kita, A., Shimizu, Y., Shuntoh, H., Sio, S. O. and Kuno, T. (2003). Feedback regulation of MAPK signalling by an RNA-binding protein. *Nature* **424**, 961-5.

Sugiura, R., Toda, T., Dhut, S., Shuntoh, H. and Kuno, T. (1999). The MAPK kinase Pek1 acts as a phosphorylation-dependent molecular switch. *Nature* **399**, 479-83.

Sutton, R. B., Davletov, B. A., Berghuis, A. M., Sudhof, T. C. and Sprang, S. R. (1995). Structure of the first C2 domain of synaptotagmin I: a novel Ca²⁺/phospholipid-binding fold. *Cell* **80**, 929-38.

Sutton, R. B. and Sprang, S. R. (1998). Structure of the protein kinase C β phospholipid-binding C2 domain complexed with Ca²⁺. *Structure* **6**, 1395-405.

Swaffer, M. P., Jones, A. W., Flynn, H. R., Snijders, A. P. and Nurse, P. (2016). CDK Substrate Phosphorylation and Ordering the Cell Cycle. *Cell* **167**, 1750-1761 e16.

Swaffer, M. P., Jones, A. W., Flynn, H. R., Snijders, A. P. and Nurse, P. (2018). Quantitative Phosphoproteomics Reveals the Signaling Dynamics of Cell-Cycle Kinases in the Fission Yeast *Schizosaccharomyces pombe*. *Cell Rep* **24**, 503-514.

Tajadura, V., Garcia, B., Garcia, I., Garcia, P. and Sanchez, Y. (2004). *Schizosaccharomyces pombe* Rgf3p is a specific Rho1 GEF that regulates cell wall beta-glucan biosynthesis through the GTPase Rho1p. *J Cell Sci* **117**, 6163-74.

Takada, H., Nishimura, M., Asayama, Y., Mannse, Y., Ishiwata, S., Kita, A., Doi, A., Nishida, A., Kai, N., Moriuchi, S. et al. (2007). Atf1 is a target of the mitogen-activated protein kinase Pmk1 and regulates cell integrity in fission yeast. *Mol Biol Cell* **18**, 4794-802.

Tanaka, K. and Kanbe, T. (1986). Mitosis in the fission yeast *Schizosaccharomyces pombe* as revealed by freeze-substitution electron microscopy. *J Cell Sci* **80**, 253-68.

Tay, Y. D., Leda, M., Spanos, C., Rappsilber, J., Goryachev, A. B. and Sawin, K. E. (2019). Fission Yeast NDR/LATS Kinase Orb6 Regulates Exocytosis via Phosphorylation of the Exocyst Complex. *Cell Rep* **26**, 1654-1667 e7.

Toda, T., Dhut, S., Superti-Furga, G., Gotoh, Y., Nishida, E., Sugiura, R. and Kuno, T. (1996). The fission yeast *pmk1+* gene encodes a novel mitogen-activated protein kinase homolog which regulates cell integrity and functions coordinately with the protein kinase C pathway. *Mol Cell Biol* **16**, 6752-64.

Tran, P. T., Marsh, L., Doye, V., Inoue, S. and Chang, F. (2001). A mechanism for nuclear positioning in fission yeast based on microtubule pushing. *J Cell Biol* **153**, 397-411.

Ueda, S. M. and Masahiro. (2018). Mutual inhibition between PTEN and PIP3 generates bistability for polarity in motile cells. *Nature Communications* **9**.

Uehara, R., Goshima, G., Mabuchi, I., Vale, R. D., Spudich, J. A. and Griffis, E. R. (2010). Determinants of myosin II cortical localization during cytokinesis. *Curr Biol* **20**, 1080-5.

Varadi, M., Anyango, S., Deshpande, M., Nair, S., Natassia, C., Yordanova, G., Yuan, D., Stroe, O., Wood, G., Laydon, A. et al. (2022). AlphaFold Protein

Structure Database: massively expanding the structural coverage of protein-sequence space with high-accuracy models. *Nucleic Acids Res* **50**, D439-D444.

Vavylonis, D., Wu, J. Q., Hao, S., O'Shaughnessy, B. and Pollard, T. D. (2008). Assembly mechanism of the contractile ring for cytokinesis by fission yeast. *Science* **319**, 97-100.

Villar-Tajadura, M. A., Coll, P. M., Madrid, M., Cansado, J., Santos, B. and Perez, P. (2008). Rga2 is a Rho2 GAP that regulates morphogenesis and cell integrity in *S. pombe*. *Mol Microbiol* **70**, 867-81.

Wach, A., Brachat, A., Pohlmann, R. and Philippsen, P. (1994). New heterologous modules for classical or PCR-based gene disruptions in *Saccharomyces cerevisiae*. *Yeast* **10**, 1793-808.

Werner, M., Munro, E. and Glotzer, M. (2007). Astral signals spatially bias cortical myosin recruitment to break symmetry and promote cytokinesis. *Curr Biol* **17**, 1286-97.

Willet, A. H., Bohnert, K. A. and Gould, K. L. (2018). Cdk1-dependent phosphoinhibition of a formin-F-BAR interaction opposes cytokinetic contractile ring formation. *Mol Biol Cell* **29**, 713-721.

Willet, A. H., DeWitt, A. K., Beckley, J. R., Clifford, D. M. and Gould, K. L. (2019). NDR Kinase Sid2 Drives Anillin-like Mid1 from the Membrane to Promote Cytokinesis and Medial Division Site Placement. *Curr Biol* **29**, 1055-1063 e2.

Willet, A. H., McDonald, N. A., Bohnert, K. A., Baird, M. A., Allen, J. R., Davidson, M. W. and Gould, K. L. (2015). The F-BAR Cdc15 promotes contractile ring formation through the direct recruitment of the formin Cdc12. *J Cell Biol* **208**, 391-9.

Win, T. Z., Gachet, Y., Mulvihill, D. P., May, K. M. and Hyams, J. S. (2001). Two type V myosins with non-overlapping functions in the fission yeast *Schizosaccharomyces pombe*: Myo52 is concerned with growth polarity and cytokinesis, Myo51 is a component of the cytokinetic actin ring. *J Cell Sci* **114**, 69-79.

Wloka, C. and Bi, E. (2012). Mechanisms of cytokinesis in budding yeast. *Cytoskeleton (Hoboken)* **69**, 710-26.

Wu, J. Q., Kuhn, J. R., Kovar, D. R. and Pollard, T. D. (2003). Spatial and temporal pathway for assembly and constriction of the contractile ring in fission yeast cytokinesis. *Dev Cell* **5**, 723-34.

Wu, J. Q., Sirotkin, V., Kovar, D. R., Lord, M., Beltzner, C. C., Kuhn, J. R. and Pollard, T. D. (2006). Assembly of the cytokinetic contractile ring from a broad band of nodes in fission yeast. *J Cell Biol* **174**, 391-402.

Yaffe, M. B., Rittinger, K., Volinia, S., Caron, P. R., Aitken, A., Leffers, H., Gamblin, S. J., Smerdon, S. J. and Cantley, L. C. (1997). The structural basis for 14-3-3:phosphopeptide binding specificity. *Cell* **91**, 961-71.

Yoon, H. J., Feoktistova, A., Chen, J. S., Jennings, J. L., Link, A. J. and Gould, K. L. (2006). Role of Hcn1 and its phosphorylation in fission yeast anaphase-promoting complex/cyclosome function. *J Biol Chem* **281**, 32284-93.

Yu, Z. Q., Liu, X. M., Zhao, D., Xu, D. D. and Du, L. L. (2021). Visual detection of binary, ternary and quaternary protein interactions in fission yeast using a Pil1 co-tethering assay. *J Cell Sci* **134**.

Yumura, S., Ueda, M., Sako, Y., Kitanishi-Yumura, T. and Yanagida, T. (2008). Multiple mechanisms for accumulation of myosin II filaments at the equator during cytokinesis. *Traffic* **9**, 2089-99.

Zaitsevskaya-Carter, T. and Cooper, J. A. (1997). Spm1, a stress-activated MAP kinase that regulates morphogenesis in *S.pombe*. *EMBO J* **16**, 1318-31.

Zhou, M. and Wang, Y. L. (2008). Distinct pathways for the early recruitment of myosin II and actin to the cytokinetic furrow. *Mol Biol Cell* **19**, 318-26.